A SEISMIC HAZARD ASSESSMENT AND MICROZONATION OF BUNDABERG

By

Michael Lloyd Turnbull BAppSc(Distinctions) GAIP JP(Com.Dec.)

A thesis submitted in fulfilment of the requirements for the Degree of Master of Applied Science

(Seismology)

Central Queensland University

Faculty of Engineering and Physical Systems

ABSTRACT

A Seismic Hazard Assessment and Microzonation of Bundaberg

by

Michael Lloyd Turnbull BAppSc(Distinctions) GAIP JP(Com.Dec.)

This thesis investigates the statistical seismic hazard that exists within the Bundaberg area and derives microzonation information for Bundaberg City, suitable for conjoint use with AS1170.4 – 1993, and its future replacements, in determining Earthquake Loading for design and construction engineering. A brief history of significant seismic events that have occurred in the Bundaberg area is provided, including presentation of an isoseismal map for the 1997 Bundaberg earthquake, and the regional geography is outlined. The effect of ground motion amplification and how it increases the seismic risk at sites within the Bundaberg City area is examined. The use of spectral ratios of ambient seismic noise, calculated from seismograms of microtremors, in characterising local site response to ground motion is discussed in detail. Specifically, horizontal to vertical spectral ratios (HVSR), otherwise referred to as Nakamura Spectra, are used to determine the local site responses of engineering interest (microzonation), for a 1 km grid of the Bundaberg City area. A methodology and associated computer software is developed to calculate Nakamura Spectra and to carry out the microzonation analysis. The results are presented in map form, suitable for viewing on a Geographical Information System (GIS). The Nakamura Spectra are also used to estimate the known depths of sedimentary deposits in the Bundaberg area. The estimated depths show a positive correlation with known depths thus verifying the applicability of the Nakamura Spectra for the purposes of microzonation.

DEDICATION

I was the first member of my family to gain a University education. My parents could not afford to educate me past year 10 but they both instilled in me an ethic for work, a thirst for knowledge and a drive for achievement that money cannot buy and rote learning cannot accomplish.

This work is dedicated to my parents:

Robert James Turnbull, and

Daphne Jane Elizabeth Turnbull (Ne Griffith).

TABLE OF CONTENTS

LIST OF FIGURES

LIST OF TABLES

ACKNOWLEDGMENTS

I acknowledge the contributions that many people have made towards the process and research, which eventuated in this publication being completed. In doing so I am mindful that so many people were consulted and offered help in the research that the danger in listing names is that some valued and much appreciated contributor may be inadvertently missed out. If such is the case it is not intentional and I apologise most sincerely.

The staff members at the Physics Department, and later the Faculty of Engineering and Physical Systems, of CQU were supportive throughout my study. **Bruce Boreham** was my principal supervisor for the first two years of my Masters program. Bruce was also my research mentor and provided assistance in getting a laptop computer with which to operate the Kelunji data logger. It was Bruce's enthusiasm for seismic research that got me started on this project. **Craig Bugden** provided invaluable advice on the operation and maintenance of Kelunji data recorders. He was also an excellent geology practical demonstrator. **Jenny Hafner** provided much need moral support and encouragement. **Byron Mckavanah** was my geology lecturer. Like Jenny he provided me with encouragement to continue in the masters program when I needed it most. **Ken Kwong** kindly agreed to replace Bruce as my principal supervisor when Bruce left. Ken's advice as to the extent of my research was timely. His recommendation to the Academic Board in support of my application for sabbatical was greatly appreciated. The Faculty of Engineering and Physical Systems made available to me all of the seismic equipment that was no longer being used for research when the Physics Department was subsumed by the faculty. This equipment was important to the research carried out for this project and will allow me to conduct significant research in the future.

XingHuo Yu kindly agreed to be one of my associate supervisors to monitor the progress my research on behalf of my faculty. The **Faculty of Informatics and Communications** provided funding for a trip to the Townsville Cities Project Workshop and sponsored my application for sabbatical. Without the sabbatical leave I would not have been able to continue with my Masters course. Day to day work commitments would have forced me to cancel the course.

I am indebted to the staff at **QUAKES** for their collegial support during my visits to that organization. **Steven Jaumé** provided companionship at *Cities Project* workshops and was amazed at the fact that two weeks after receiving my first set of seismographic equipment I still did not know what type of seismic sensor I had. **Russell Cuthbertson** provided me with important instructions on how to set the Kelunji configuration to improve the sensitivity of my seismographic equipment. It was at Russell's suggestion that I made approaches to **Peter Mora** to spend some of my sabbatical at QUAKES. **Mike Winter** allowed me free access to all of his C source code. **Col Lynham** gave me some valuable pointers in reading regional seismograms.

I am indebted to the staff at the Geohazards section of **AGSO** for their collegial support during my visit to that organization. In particular, **Kevin McCue** was my much valued and appreciated expert supervisor. He provided opinion on my work and bridged the supervisory gap when Bruce left the employ of the university. Kevin proof read all of the drafts of the thesis and encouraged me to *keep writing* when it was simply impossible for me to see where it would all end. Without Kevin's encouragement and help I doubt that I would have finished the project.

I am grateful for the assistance given to me by the **Bundaberg City Council**, especially the staff of the GIS section of the Drafting Department.

Vaughan Wesson kindly provided me with details of the Kelunji Classic data-file format, and other insights into the workings of the Seismac software. Without that information I would never have been able to begin the development of the microzonation analysis software and the other small pieces of software that were written to assist data analysis. I am also indebted to **Adam Pascale** and other staff members at the **Seismological Research Centre** for providing me with information, including the specifications for the Kelunji Classoc Seismograph and the Sprengnether S6000 sensor.

Pam Turnbull put up with her husband's mood swings, keyed in data and assisted with the preliminary spreadsheeting analysis. **Melodie Turnbull** converted many of the seismograms into FFT spectra for her dad; kindly allowed him to help her with her mathematics and physics studies, and rewarded him by getting an OP1 in her tertiary entrance score.

Alex Grady offered advice on matters geological and helped identify rock samples. He also proofread my drafts and provided valued comments on my geological commentary sections.

John Latter made himself available to discuss volcanology and suggested suitable literature for researching the volcanology of the Bundaberg area.

Bill Souter from the Queensland Department of Natural Resources and **Warwick Wood** of GeoEng helped by supplying test borehole data for the Bundaberg region and allowed me to view the draft report for the Bundaberg Underwater Investigation Project 1989/99.

Ian Ferris from C.M.Testing Bundaberg enthused me with his knowledge of the under-belly of Bundaberg city from the perspective of a geo-technician. Ian provided me with shallow borehole data that allowed me to estimate the shear wave velocity of the Bundaberg sediments.

My good friend **Jeff Farrow** proof read the final draft and ensured that my citations and references matched up correctly.

DECLARATION

This thesis contains no material that has previously been submitted for a degree or diploma to any other university or institution of tertiary education. I carried out the work described herein, except where otherwise acknowledged, during the period of my candidature.

M.L. Turnbull

October 2000, April 2001

CHAPTER 1 INTRODUCTION

Bundaberg's Seismicity in the World perspective.

The Australian continent is situated within the Australian/Indian tectonic plate. This plate is bordered, to the north by the Eurasian and Pacific plates, to the south by the Antarctic plate, to the east by the Pacific plate and to the west by the African plate. The eastern segment of the Australian/Pacific boundary extends from the Australia/Antarctic boundary in the south, through the New Zealand islands, then trends to the northeast through the New Hebrides group, and swings westward along the north coast of New Guinea. The nearest plate boundary to Bundaberg is in the New Hebrides islands, some 1200 km away to the northeast. It is therefore clear that Bundaberg is an intraplate zone, the seismicity of which cannot be attributed to plate boundary mechanisms.

The geological mechanisms causing earthquakes along and adjacent to plate boundaries have been studied extensively over the last 200 years, and are generally well understood. On a world scale most earthquakes occur along the plate boundaries. It is these plate boundary earthquakes that present the greatest danger to life and property and are the most spectacular; and, perhaps because of this, attract more study than do less impressive earthquakes.

In contrast, the number of earthquakes occurring within plates at considerable distance from boundaries is relatively small in the world perspective. These intraplate events are generally of lower intensity and are less noticed by the general population than plate boundary earthquakes are. Perhaps because of this, the detailed geological mechanisms that cause intraplate earthquakes have not been intensively studied, and are not well understood.

Australia, being wholly an intraplate continent, has relatively low seismicity in world terms.

Figure 1.1 is a map showing the location of earthquakes of magnitude 4.0 or greater that have been recorded in Australia from 1884 to 1994.

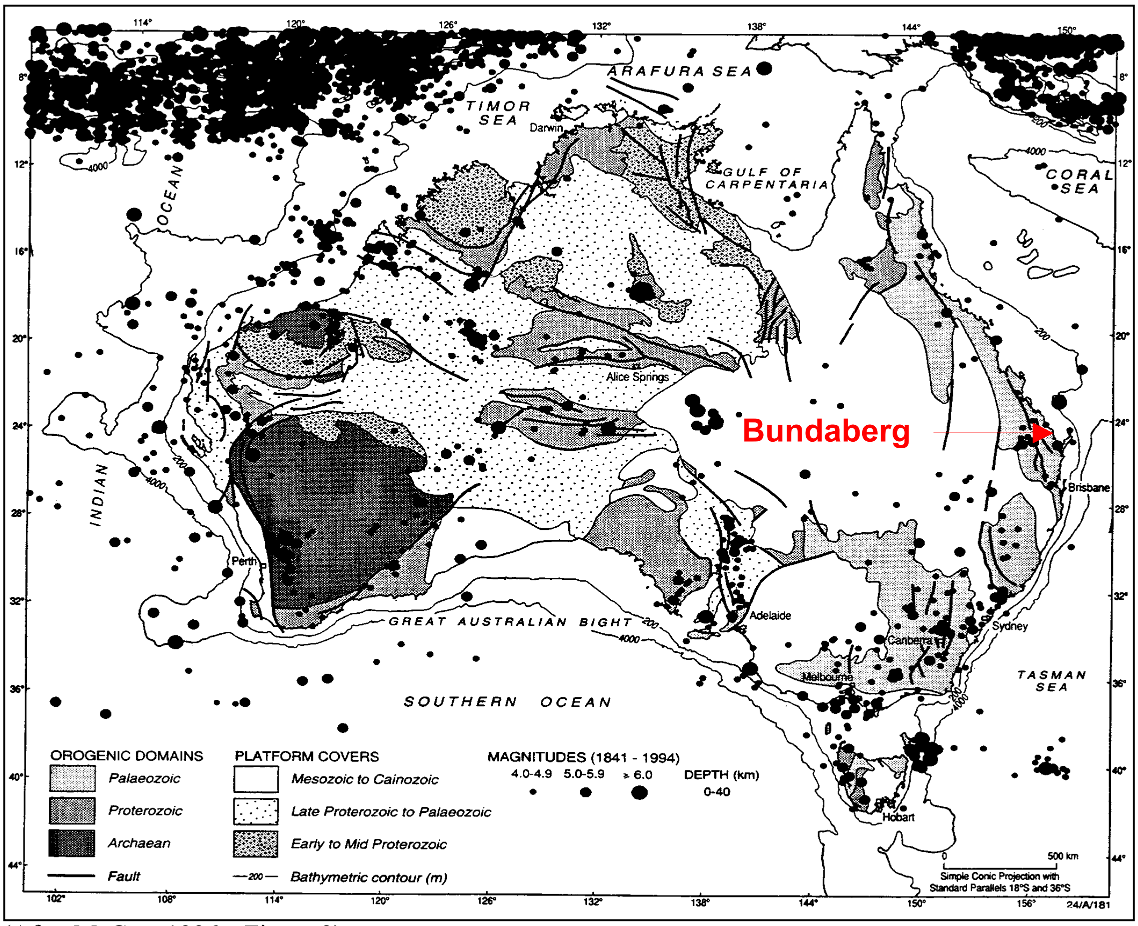

(After McCue, 1996a, Figure 2)

Figure 1.1 **Australian earthquakes M ≥ 4 , 1884 to 1994**

By 1883 seismic instruments capable of recording magnitude 6 events anywhere along the east coast of Australia had been installed near Launceston, Tasmania (Doyle & Underwood, 1965). From 1883 through to 1918 great reliance was placed on felt reports of earthquakes. In 1883 an earthquake, allocated a magnitude of 5.6 based on the many felt reports, was recorded near Gayndah, Queensland (QUAKES, 2000). Reliable seismic instrumentation, certainly capable of recording magnitude 6 events anywhere in Australia, was operating in Melbourne, Perth and Sydney by 1906 (Doyle & Underwood, 1965). By 1953 instruments capable of recording magnitude 4 events anywhere in Queensland were in operation in Brisbane (Doyle & Underwood, 1965). Given the deployment of instrumentation and coverage from felt reports, the author considers that the historical record, within Queensland, for earthquakes of magnitude 4 and above is complete from about 1960 and the record for magnitude 5.5 events is complete from circa 1883.

Figure 1.1 indicates that considerable seismic activity has been recorded in the Bundaberg area over the past century.

The Australian Earthquake Building Codes

Prior to 1993 the Australian building code relating to earthquake loading, AS 2121-1979 (SAA, 1979), was based on a system of seismic zoning. The zones were intended to encompass places with similar earthquake hazard, characterised by expected return time of particular measures of ground shaking, taking into account all known Australian earthquakes from 1897 through to 1976. The primary measures of ground shaking used were the peak ground particle velocity and the Modified Mercalli intensity, which were allocated an empirical relationship to one another. Four zones of design interest were defined, ranging in severity from Zone 2, Zone 1, Zone A to Zone Zero (Zone 2 having the highest seismic hazard). It was acknowledged in the code that the zone boundary placement was simplified, and that the precision of their placement was considered low. All locations that were not included within either Zone 2, 1 or A were included in Zone Zero, within which there was considered to be negligible earthquake hazard for building design purposes. Within Queensland only two non-zero zones were recognised in AS 2121-1979 (See Figure 9.1), one small area at the southern end of the Northern Territory border, and a larger area on the east coast extending from about Gladstone in the north down to about Gympie in the south, and west to about Theodore. Both these were Zone A, the lowest rating of earthquake design interest.

Subsequent to the release of AS 2121-1979 several notable earthquakes occurred in Australia that prompted concern that the standard needed reviewing.

On 22 January 1988 three earthquakes of magnitudes 6.3, 6.4 and 6.7 occurred at Tennant Creek within a 12-hour period. These earthquakes caused significant damage to a buried natural gas pipeline and above ground structures in Tennant Creek, and resulted in a 35 km long, 2 m high fault scarp (Jones et al, 1992).

On 28 December 1989 an earthquake of magnitude 5.6 occurred on the western outskirts of Newcastle. This event resulted in 13 deaths (the first recorded deaths directly attributable to earthquake in Australia), and caused millions of dollars worth of damage to property and physical infrastructure (Lewis, 1999).

In AS 2121-1979 the regions around Newcastle and Tenant Creek were within Zone Zero. That is, at that time the hazard from ground shaking in Newcastle and Tennant Creek had been rated as negligible, based on the best advice available up to 1979. Subsequent to the Newcastle event, and in light of knowledge gained since 1979, the earthquake loading standard was reviewed and replaced by AS 1170.4-1993 (SAA, 1993a & b), which provided considerable more detail for designers. It is noted, however, that little more is known now about the causes of intraplate earthquakes than was known in 1979.

In AS 1170.4-1993 Bundaberg is located at the centre of (in terms of Australian seismicity) a relatively high-hazard local zone – in fact, it is given the same hazard rating as the zone at which Newcastle is centred (See Figure 9.2). The standard allocates a uniform hazard for all of the Bundaberg City area. As a result of the research carried out for this thesis the relative hazard within the Bundaberg City area can be specified on a much finer resolution than that presented in the standard. As part of this thesis, the author has presented a methodology for characterising this information in a manner that can be used to supplement the standard (See Chapter 10).

Overall research goal

The overall goal of this research project is to carry out a seismic hazard assessment and microzonation of Bundaberg City. The assessment treats only the direct physical aspects of earthquake risk. It does not extend into the social, commercial and economic aspects that additionally qualify the *vulnerability* component of earthquake risk; nor does it attempt to address risk mitigation.

The importance of relative risk assessment

Everingham et al (1982, p 7) and Rynn et al (1987, p 5) divided the definition of seismic risk into two aspects:

> *"The relative risk is the comparative earthquake hazard from one site to another. The probabilistic risk is the odds of earthquake occurrence within a given time interval and region."*

The above definitions of risk are now considered outdated terminology. They are mentioned here because they are frequently found in the literature prior to about 1990. In recent literature a distinction between *risk* and *hazard* has evolved. McCue (1996a, p 6) defines seismic risk as:

> *"The probability of damage."*

and seismic hazard as:

> *"The probability of an earthquake occurring within a given time interval and region."*

The term *risk* is closely related to the term *hazard*. Given any two sites (locale, structure or object of interest) that are subject to the same degree of hazard from some potentially damaging mechanism (e.g. earthquakes), it is common for one of those sites to be more or less *vulnerable* to damage than the other site. This relative vulnerability may be due to structural differences such as design and/or material composition, or it may be due to characteristic differences in the earth foundation at that locale. Thus we may say that *risk is hazard modified by vulnerability*.

RISK = HAZARD × VULNERABILITY

The current author agrees with McCue's definition of seismic hazard, and applies the following definition to seismic risk:

> *The relative likelihood that damage will occur, as a direct consequence of a seismic event, at a given site as compared with an adjacent site.*

It is not possible to define earthquake risk in absolute terms. To do so for any particular site would require absolute knowledge of the earthquake hazard for that site, absolute knowledge of the ground to structure movement transfer characteristics, and absolute knowledge of structural response under all modes of movement. As none of these contributing factors can be defined in absolute terms neither can their combined effect. On the other hand it is a comparatively simple task to quantify the risk in relative terms.

Knowledge of the relative likelihood that damage will occur as a direct consequence of a seismic event (within a given area as compared with an adjacent area) provides important policy planning information for governments at all levels – particularly for local government bodies and disaster action organisations. Such knowledge provides a basis for effective town planning. It facilitates sensible placement of future utility service structures and hospitals. It enables disaster plans to be put in place that have a higher chance of success than might otherwise be the case. Even if the absolute risk could be assessed it would be of no more practical advantage to general society than a relative risk assessment.

Regional perspective

Prior to carrying out an earthquake hazard assessment for Bundaberg City it was necessary to gain a working knowledge of the region’s geology and its seismic history, and to determine what earthquake hazard was present. These topics, especially the seismic history and hazard, enable any resultant risk assessment to be interpreted in local context. Based on research carried out by the author it is apparent that, in a global context, Bundaberg is situated within a relatively low seismic hazard region. However, in an Australian context Bundaberg is situated within a relatively high seismic hazard region. During the course of the research the author has spoken with and communicated with numerous people who live within the Bundaberg area. There is a general perception among many of the local population, who have settled in the area over the past few decades, that Bundaberg has no significant hazard from earthquakes. This is contrasted with the perceptions of the long-term population, whose families have been in the area for two or three generations, who are very aware of persistent and continuing seismicity in the area.

During the term of the research a small earthquake occurred close to Bundaberg. Several people within a 50 km radius of Bundaberg City reported effects of this event. From these reports the author was able to draw an isoseismal map of the event and make comparisons with an earlier event (1918), which occurred in approximately the same location. The author was able to demonstrate a strong correlation between the extent of the felt effects of this event, the regional topography and the historical seismicity of the region (Turnbull, 2000).

Knowledge of the regional seismic history allowed the determination of earthquake hazard probabilities to be more closely associated with the Bundaberg area in particular than with the South-East Queensland region in general. This hazard association is of specific import when interpreting relative risk assessment in the Bundaberg area.

Theoretical perspective

Research of the literature indicates that, although there has been considerable activity into earthquake hazard and risk determination, there has been little actual theoretical underpinning of the statistical methods used to analyse historical data to produce the resultant forecasts of recurrence periods. In general the current body of knowledge consists of data derived from empirical application of statistical methods that have been shown by retrospective comparison to be appropriate to the analysis of extreme events, and of conclusions based on analysis of that data.

The hazard analysis carried out in this thesis is based on an empirical application of a particular branch of extreme-value statistics. This statistical approach to extreme events was first developed by Emile Gumbel (1958) and later applied to earthquake hazard analysis by Lomnitz in several publications (1974, 1976a, 1976b) and also by Burton (1979). Whilst there is no *a prori* theoretical rationale for using these statistics to analyse earthquake hazard, they have been used successfully to analyse floods and atmospheric weather phenomena. Such applications have the advantage that their applicability can be verified within the lifetime of the observer. Application of *any* approach to earthquake hazard analysis is subject to the qualification that the results can only be verified over geological time scales.

Summary of research achievements presented in this Thesis

This thesis will,

- establish the statistical seismic hazard that exists in the Bundaberg area, based on the past recorded earthquake history;

- demonstrate the use of the statistical results in forecasting future seismic events in terms of the probability of their occurrence within given time scales;
- present a methodology and associated computer software for characterising ground motion amplification – a major contributing factor to increased site vulnerability;
- present a methodology and associated computer software for carrying out a microzonation risk analysis within a specified area;
- conduct a microzonation risk analysis of Bundaberg City, and,
- validate the microzonation results by using the input data to estimate known sedimentary depths within the microzonation area.

CHAPTER 2 GEOLOGY OF THE BUNDABERG AREA

Introduction

Although the geographical site on which Bundaberg is located is on a coastal plain of the Maryborough Basin transected by the Burnett River, this was not always so. During the Devonian and Carboniferous periods the coastline was at least 100 km inland from Bundaberg. The sedimentary Maryborough Formation, which conformably underlies the Burrum Coal Measures, was probably deposited during the Aptian age of the Cretaceous period in a geologically dynamic shallow marine environment (Ellis & Whitaker, 1976, p25). The thick Burrum Coal Measures were later deposited during the late Aptian in a relatively short period, suggesting rapid subsidence in a shallow swampy environment (Ellis & Whitaker, 1976, p28). The thin sediments of the Elliott Formation, the foundation on which Bundaberg stands, were deposited, possibly during the late Oligocene to early Miocene, on a fluviatile peneplain that extended over a wide area (Ellis & Whitaker, 1976, p34). Active volcanism was occurring 1.8 Ma within the immediate Bundaberg area (Sloping Hummock) and as recently as 0.4 Ma further inland in the present Proston area. Although previous reports have suggested that the Sloping Hummock was an onshore volcano, there is new evidence (GeoEng, 1999) that supports the view that it was an offshore volcano, and that the general area around Bundaberg has only fully emerged within the last 2 million years during the Pleistocene and early Holocene epochs. This demonstrates that the area has been tectonically active for at least the past 2 million years, which is an important consideration with respect to the current seismicity of the area.

Onshore Structural Elements and Solid Geology

The positioning of the geological elements referred to in this chapter are shown in Figure 2.1, and are further depicted in cross-sections in Figures 2.2 and 2.3.

The three main onshore geological structural elements in the immediate Bundaberg area are the Coastal Block, the Rosedale Block and the Maryborough Basin. Each of these major blocks exhibits a different history of tectonic and depositional activity. The Coastal Block, to the west, is separated from the

Rosedale Block by the Electra Fault Zone. The Bullyard Fault Zone generally defines the eastern margin of the Rosedale Block, with the Maryborough Basin to the east, south of Baffle Creek. Magmatic intrusion and volcanic extrusion have featured in the geological development of the area

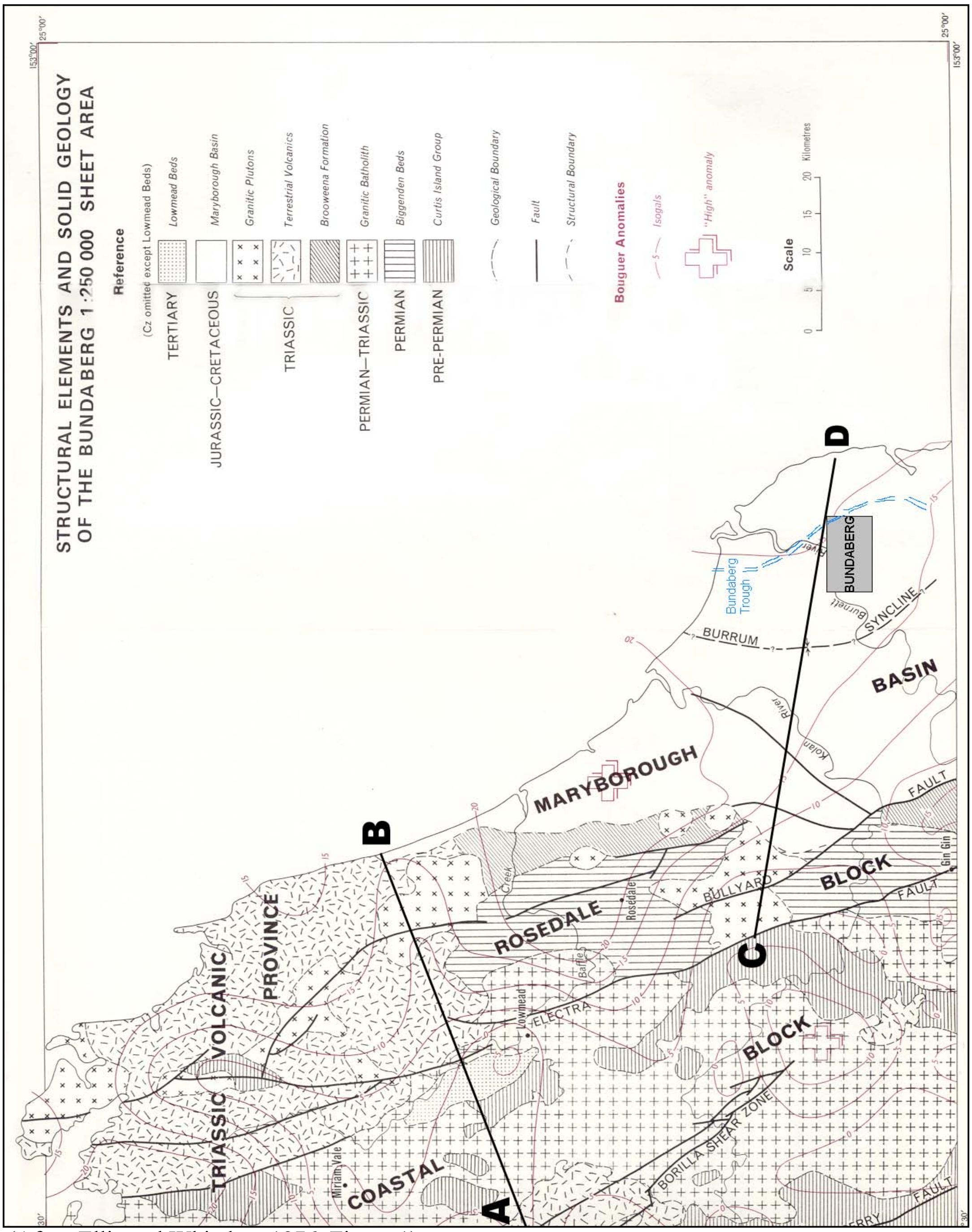

(After: Ellis and Whitaker, 1976, Figure 1)

Figure 2.1 **Structural Elements and Solid Geology of the Bundaberg Area**

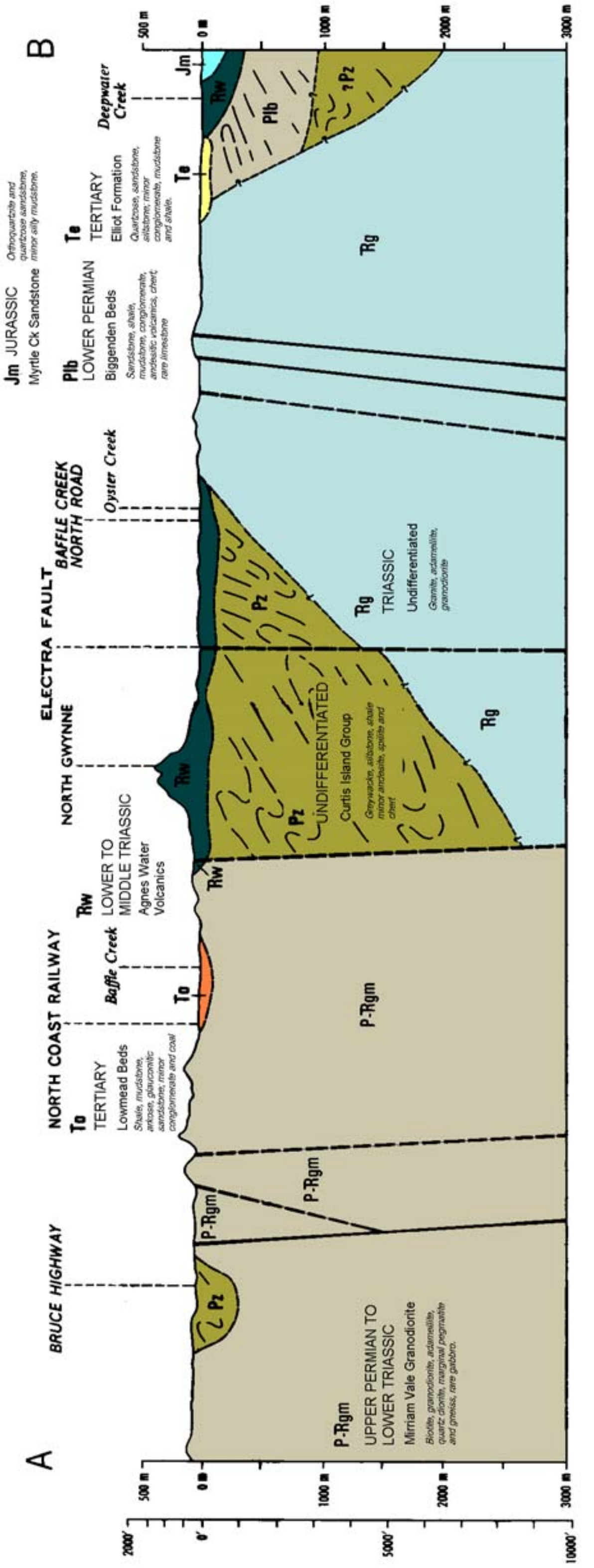

(After Geological Survey of Queensland, 1974)

Figure 2.2 **<u>A-B Cross-section from Figure 2.1</u>**

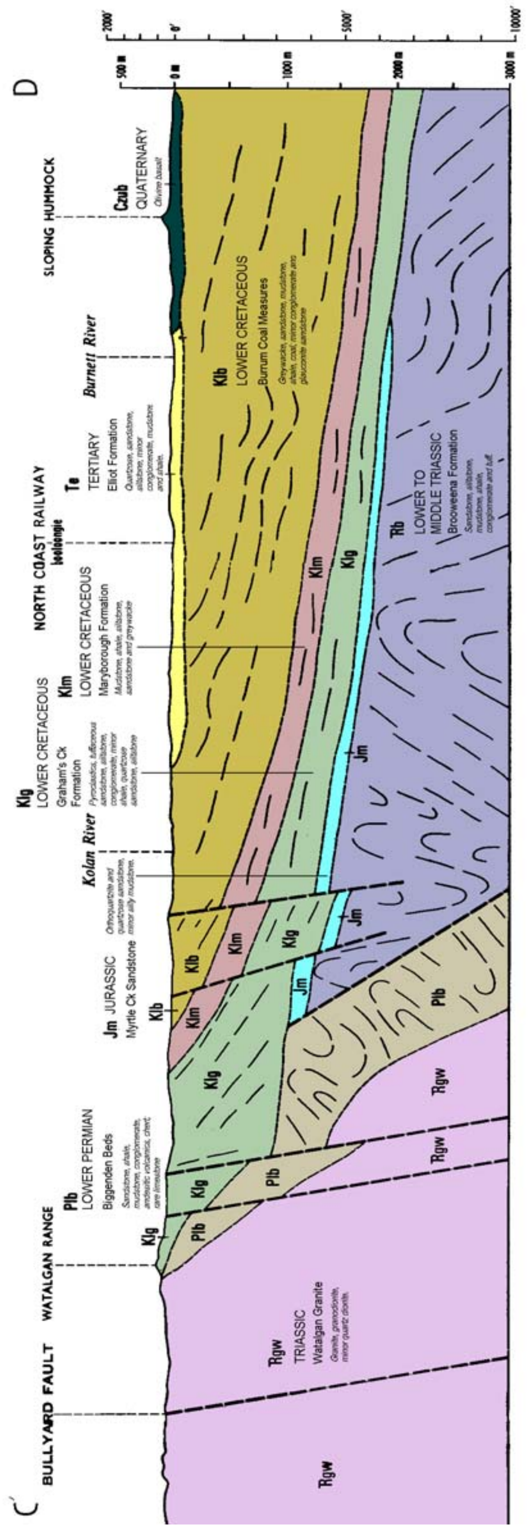

(After Geological Survey of Queensland, 1974)

Figure 2.3 C-D Cross-section from Figure 2.1

The Coastal Block is composed of mainly metamorphosed marine sediments of pre-Permian age and volcanics of the Curtis Island Group, whose age is uncertain but may be from Devonian to Carboniferous. The Miriam Vale Granodiorites extensively intruded the volcanics during the Late Permian to Triassic. The Electra Fault Zone, which generally defines the eastern margin of the block, was active from at least the Triassic to the early Tertiary. (c.f. Ellis & Whitaker, 1976)

The Rosedale Block is made up of Early Permian marine sediments and Biggenden Beds volcanics to the west, overlain or faulted against Early to Middle Triassic sediments of the Brooweena Formation to the east. The western margin of the Biggenden Beds has been intruded by sections of Miriam Vale Granodiorites. To the north an extensive province of Middle Triassic volcanics, that predate Triassic plutons intruded into the Brooweena Formation, overlies the Rosedale Block and the Coastal Block. (c.f. Ellis & Whitaker, 1976)

The Maryborough Basin consists of a sequence of at least 5 strata of freshwater and marine sediments and volcanics. The basin basement is generally defined by the lower to Middle Triassic Brooweena Formation that is overlain by a sequence of three thin units (c.f. Figure 2.3). This sequence of strata onlap or are faulted against the Rosedale Group to the west. The basement sequence consists of three relatively thin layers.

The Jurassic fluvial Myrtle Creek Sandstones are laid down over the Brooweena Formation and faulted against the Biggenden Beds to the west. Above the Myrtle Creek Sandstones is the Graham's Creek Formation, consisting of Cretaceous volcanics and sediments. This formation thickens and surfaces to the west of the basin between the Watalgan Range and the Kolan River, where it onlaps the Triassic Watalgan Granites in which is located a section of the Bullyard Fault complex. Over the Graham's Creek strata are lain the Early Cretaceous shallow water marine sediments of the Maryborough Formation.

The balance of the Maryborough Basin is made up of the relatively thick layer of continental sediments comprising the Burrum Coal Measures and terminates with the thin sections of the fluvially deposited Early Eocene Fairymead Beds. Late Oligocene to early Miocene Elliott Formation, and Pleistocene to

Holocene volcanics of the Sloping Hummock Landform and marine margin sediments in the Moore Park Landform (c.f. Robinson, 1979) unconformably overlay the Mesozoic sequences in the Bundaberg region.

Geological History

The pre-Cainozoic geological history presented here is mainly composed of information sourced from Ellis & Whitaker (1976), and Johnson (1989). The Cainozoic history comes mainly from Robertson (1979), and GeoEng (1999). However all four references contain historical commentary which spans pre-Cainozoic periods. Locational references are in relation to the region depicted in Figure 2.1.

In the Devonian and Carboniferous the Curtis Island Group was deposited in the western half of the region. This group was strongly deformed prior to the end of the Permian but it is not known how many episodes of folding and metamorphism took place nor over what periods. Late Carboniferous and Middle to Late Permian deformation may be indicated by possible correlated rocks found elsewhere.

During the Permian the sediments and volcanics of the Biggenden Beds were deposited on the Curtis Island Group. These are present in the Rosedale Block and are thought to be of Early Permian age but observations from other equivalent beds may indicate a date from Late Carboniferous to Late Permian. These beds were strongly deformed prior to the end of the Permian, probably contemporaneously with the Curtis Island Group. Major fault zones such as the Electra Fault may have been initiated during this time.

Subsequent to deformation, during the Late Permian to Middle Triassic, the Miriam Vale Granodiorites were intruded into the Curtis Island Group and the Biggenden Beds, probably as a sequence of individual plutons. During the Early to Middle Triassic the Brooweena Formation sediments were deposited in the east against the margin of the deformed and uplifted Biggenden Beds. The Broweena sediments were later deformed during the Triassic, and at some time large volumes of volcanics were extruded over them to the north and west.

The major fault systems that trend generally north to south were apparently active during the Triassic, more so towards the end of the period. Ellis and Whitaker (1976) suggest that the faults may reflect late Paleozoic compressional structures.

From the Early Jurassic onwards, erosional deposition into the Maryborough Basin took place, starting with the Myrtle Creek Sandstones. The provenance for this deposition came from the uplifted region to the west. From the observed (and inferred?) distribution of these sandstones, Ellis and Whitaker (1976) propose a possible later history of downfaulting on the Bullyard Fault System. Subsequent deposition of the Graham's Creek Formation during the Neocomian may have taken its provenance from an eastern source (Ellis & Whitaker, 1976), implying the presence of an uplifted landform to the east of the basin at that time.

The shallow marine sediments of the Maryborough Formation onlap the Graham's Creek Formation, are of Aptian age, and are overlain by the Burrum Coal Measures, which are of Albian age. The presence of the coal measures implies a shallow freshwater environment during that period, although there is some evidence of minor marine incursions (Ellis & Whitaker, 1976). Palynological evidence (fossilised plant spores) indicates that the coal measures were laid down in a relatively short period of time in conditions of rapid subsidence.

During the latter part of the Cretaceous strong folding took place in the western margin of the basin. At about this time the basin was downfaulted against the Rosedale Block along the line of the Bullyard Fault system. An early Tertiary, possibly Eocene, timing is inferred from erosion of the base levels. Contemporaneously with the Bullyard Fault activity the Electra Fault System was reactivated in the vicinity of Lowmead. There is evidence of several small graben having formed in the Lowmead area and north of Gin Gin due to this activity. This activity may be related to tensional stress resulting from the opening of the Coral Sea Basin and the spreading of the Tasman Sea floor.

Ellis & Whitaker propose (1976) and Robertson accepts (1979) that the Elliott Formation, which overlies the Fairymead Beds within the Bundaberg Trough, was deposited under fluvial conditions on a widespread, easterly dipping peneplain. The northeast and eastern limits of the Elliott Formation may coincide with the axis of the Bunker High that separates the Maryborough Basin from the Capricorn Basin (Robertson, 1979). Periodic torrential deposition and other evidence from the sorting distribution of the Elliott sediments indicate that the source area was to the northwest and that there were periods of adjustment to the gradient of the plain possibly related to differential subsidence of the Queensland Plateau and movements in the Capricorn Basin during the Late Eocene to Early Miocene (Robertson, 1979) or readjustment along the Electra and Bullyard fault lines (Ellis & Whitaker, 1976). The present flow of the Kolan, Burnett and Elliott Rivers is from the west and southwest Therefore, if we are to accept the evidence that the provenance for the Elliott Formation came mainly from the northwest, the Kolan, Burnett or Elliott Rivers could not have transported it.

Robertson (1979) refers to a feature known informally as the *Bundaberg Trough*. The presence of the so-called Bundaberg Trough has been inferred from contours of the top surface of the Burrum Coal Measures and distribution of the Fairymead Beds (Robertson, 1979). Tectonic instability during the Late Cretaceous to Early Tertiary has been proposed to account for the creation of the Bundaberg Trough (Robertson, 1979); however, recent geophysical investigations carried out for the Queensland Department of Natural Resources (GeoEng, 1999) present strong evidence that the trough is in fact the previous course of the Gregory River which had cut its bed from the southwest, through the Burrum Coal Measures, during the early Tertiary, probably Palaeocene to early Miocene. The term *proto-Gregory* has been informally applied to this feature. Uplifting in the upper reaches of the proto-Gregory or subsidence of the lower reaches (during the Eocene?) may be invoked as contributing agents that caused the diversion of the Gregory. A fault that strikes northwest to southeast, with the downthrow side to the northeast, has been identified in the Childers area (GeoEng, 1999). It appears that the Gregory River has changed its course to the southeast, along this fault.

A Landsat image (from Landsat scene TM 90/77 dated 25 June 1997) presented in the Bundaberg Groundwater Investigation Draft Report (GeoEng, 1999) shows strong visual evidence of a possible groundwater discharge into Hervey Bay north of Theodolite Creek, in the Kinkuna National Park. This evidence supports the hypothesised existence of an underground channel, coming from the northwest, which overlies the proto-Gregory and underlies the present Burnett and Elliott Rivers. This hypothetical channel could be invoked as the transport agent for the early deposition of the Elliott Formation.

Robertson (1979) considers that the Burnett and Elliott Rivers cut their beds during the Early Pleistocene, when the sea level off Bundaberg was about 40 m lower than at present.

By the Miocene the whole area had become emergent. During the Pleistocene and the Holocene subaerial volcanism, attributed by Robertson (1979) to *crustal readjustment*, extruded basalt at several locations in the area. During the Holocene coastal and estuarine sediments were deposited along the eastern margin of the basin.

Recent Volcanism

During the Late Mesozoic and early Tertiary, seafloor spreading in the Tasman and Coral seas is considered to have been associated with a temporary extensional plate boundary (Johnson, 1989). This boundary is considered to have closed during the Palaeogene (Early to Middle Tertiary). From the Late Palaeocene through to the early Holocene several short periods of volcanism occurred in the Bundaberg area (c.f. Figure 2.4). Lavas can be identified in the Bundaberg, Hill End, Gin Gin, Berrembea, Childers, Tararan, Mundubbera, Coalstoun Lakes, Proston, Boyne and Bunnya regions.

The oldest volcanic activity from the Late Palaeocene is in the area represented by the Pemberton Grange Basalts at the base of the Bundaberg Trough (Johnson, 1989). Lateritised basalt exposed to the east and south of Gin Gin between the Electra and Bullyard faults may be of the same age (Robertson, 1979). Volcanic rocks at the northern end of Fraser Island and at Waddy Point are Oligocene to early Miocene in age. Nepheline-rich extrusions during the late Miocene to late Pliocene were controlled in general by the Electra and Bullyard faults. The extrusion at Hill End seems to be an exception. Anorthoclase from the Tararan vent has been isotopically dated to 3.0 – 2.7 Ma and a rock sample from Hill End indicated an age of 5.1 Ma.

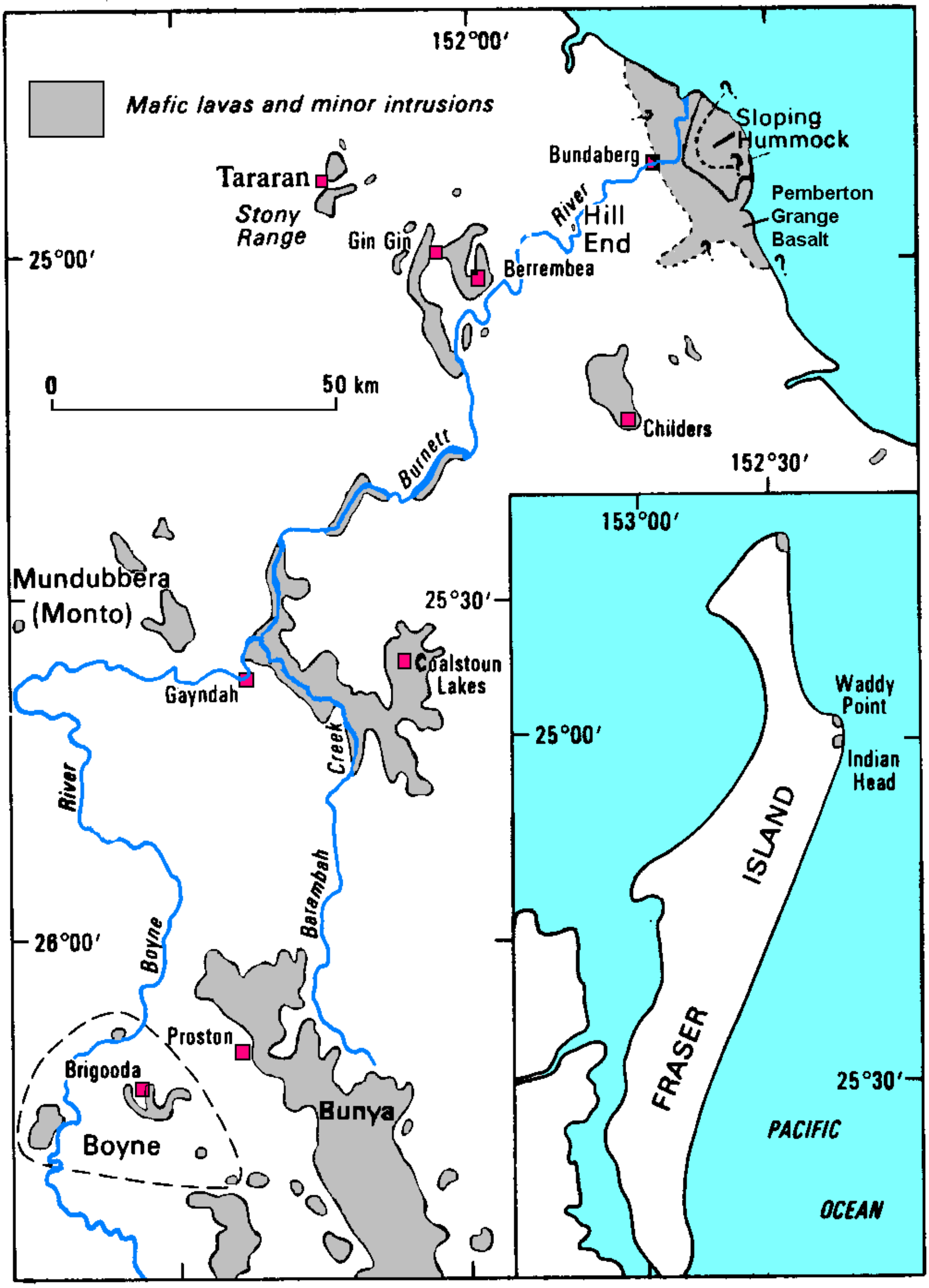

(After Johnson, 1989, Figure 3.4.4)

Figure 2.4 **Distribution of volcanic rocks in the Bundaberg area**

There are three Pleistocene to Holocene eruptions recorded; one near Bundaberg (Sloping Hummock), one at Berrembea and another at Coalstoun Lakes. The Hummock Basalt has been dated at 1.1 – 0.9 Ma (Johnson, 1989). A tentative age of Late Pleistocene was assigned to the Berrembea flows by Robertson (in Johnson, 1989). The isotopic age for the Barambah Basalt centred on Coalstoun Lakes is 0.6 Ma (Johnson, 1989).

In the Brigooda Basalt group of the Boyne province southwest of Proston deposits with anorthoclase isotopically dated to 0.45 ± 0.04 and 0.381 ± 0.025 Ma have been recorded (Johnson, 1989).

Summary

The geology of the Bundaberg area has been active from the Late Palaeozoic through to the Quaternary. From the Mesozoic to Early Tertiary the geological development was controlled to a large degree by the tectonic influence of a temporary extensional plate boundary at the site of the Tasman and Coral Seas spreading. Major north to south fault zones, the Electra and the Bullyard systems, have played an important role in development of the coastal plain and have been associated with Late Miocene to Late Pliocene volcanism from Bundaberg to as far west as Gin Gin and Tararan. The Electra and Bullyard fault systems possibly formed axes for subsidence of the Maryborough Basin, starting during the Jurassic.

Volcanic activity has featured prominently since the late Palaeocene and has continued in the area to as recent as 380,000 years ago. The area exhibits a relatively high earthquake hazard, in comparison to the majority of the Australian continental landform, indicating that geological processes are still active in the area. However, no reliable evidence of faulting due to recent volcanic activity and large historic earthquakes has been recorded in the Bundaberg area.

CHAPTER 3 SEISMIC HISTORY OF THE BUNDABERG REGION

Introduction

Melchers (1994), commenting on the characteristics of intraplate earthquakes in general, suggests that significant events may occur in regional clusters and that there appears to be a pattern in the development of significant earthquake activity over time, suggesting a relationship with an overall tectonic stress-state. The tendency of Australian intraplate earthquakes to cluster has also been noted or implied by other investigators (Spassov et al (1997), Gaull et al (1990)). Inspection of a map of Australian earthquake epicentres (See Figure 1.1) indicates that such a cluster has developed in the southeastern region of Queensland.

Recent research carried out by McFadden et al (2000) demonstrates beyond a reasonable statistical doubt that seismicity in Australia is not uniformly distributed.

McCue et al (1998) suggested a seismicity model for Australia that includes an identifiable high seismicity region in southeast Queensland. This region includes the greater metropolitan area of Brisbane and several regional cities, including the Gold Coast, Toowoomba, Maryborough, Gladstone and Bundaberg, and extends through to northern New South Wales. It coincides with most of Queensland's population and is the location of the major proportion of the State's economic industry.

Seismic Activity in Southeast Queensland

Comprehensive research carried out by Rynn (1986) confirmed that a significant risk exists in Queensland in general, and the northern part of southeast Queensland in particular. There is ample historical and contemporary evidence of continuing significant seismic activity in the Bundaberg area.

	Events of Magnitude ≥ 3					
	Since 1866			Since 1980		
	Count	QLD%	SEQ%	Count	QLD%	SEQ%
All Qld	359	100%		145	100%	
S.E. Qld.	154	42.9%	100%	82	56.6%	100%
Bundaberg area	49	13.6%	31.8%	14	9.7%	17.1%

(Source: QUAKES Earthquake database)

Table 3.1 **Significant Recorded Events in Queensland**

Table 3.1 indicates the percentage of significant earthquakes, of magnitude 3.0 or greater, that have been recorded in the southeast Queensland region since 1866, and since 1980. The statistics shown in the table include the main shocks and the aftershocks associated with those events. The data show that the southeast Queensland region, which comprises about 10% of the total area of Queensland, is the source of about 50% of all seismic events in Queensland, of magnitude 3 or above. The statistics also show that about 10% of all significant Queensland seismic events (or about 20% of the south-east region events) occur within the 3° grid centred approximately on Bundaberg (Latitude –23.5° to –26.5°, Longitude 151° to 154°).

The Queensland Earthquake Database (QED), maintained by the Queensland University Advanced Centre for Earthquake Studies (QUAKES), contains 2103 events recorded in the southeast region in the period 1872 to 1997. Of those events 1982 are less than magnitude 2; 98.9% of which have been recorded since 1976. Of those micro-earthquakes recorded since 1976, 337 were located at the Boondooma Dam, near Proston. Of all of the low magnitude events recorded for Queensland, 598, or 30% were recorded in the southeast region.

The propensity of micro-earthquakes in the database subsequent to 1976 is probably an artefact due to the installation of seismographs, particularly in the southeast Queensland region, since 1976. Prior to that time detection of low magnitude events was not reliable, especially outside of the southeast region. Examination of the distribution of micro-earthquakes detected since 1980 indicates that, even at the time of writing (March 2000), detection of low magnitude events in southeast Queensland is only taking place in the close proximity of seismographic equipment. Most micro-earthquakes occurring in southeast Queensland are not being detected.

Significant Seismic Events

The largest earthquake ever recorded along the east coast of mainland Australia had a magnitude ML6.0 (Everingham et al, 1982) or ML6.3 (QED). It occurred on 6 June 1918 (Everingham et al, 1982). The epicentre was initially located out at sea approximately 200 km northeast of Bundaberg at 24° S, 154° E (Pigot, 1918). Seismic recordings of the event were made by five Australian stations (Riverview, Sydney, Melbourne, Adelaide and Perth), and three overseas stations (Batavia (Djakarta), Helwan (Egypt) and Tortosa (Spain)) (Turner, 1923). Based on the information obtained from the eight stations that recorded the event, the International Seismological Summary (ISS) for 1918 (Turner, 1923) placed the epicentre at 23.3° S, 150.6° E, 10 km south of Rockhampton! Rynn discounts the ISS location as being impossible, based on macroseismic data (Rynn, 1985-86), and places the most likely epicentre at 23.5° S, 152.5° E, about 120 km NNE of Bundaberg and 120 km east of Gladstone. Despite this locational discrepancy in the literature there is considerable evidence that the event was felt over a large area of Queensland. The initial event and its aftershocks were reported being felt as far west as Roma, as far south as Grafton and as far north as Mackay, over a long period of time (aftershocks were being reported up to 34 days after the initial event) (Rynn, 1985-86). Figure 3.1 presents the isoseismal map drawn by Rynn (in Everingham et al, 1982), which would favour the Riverview location.

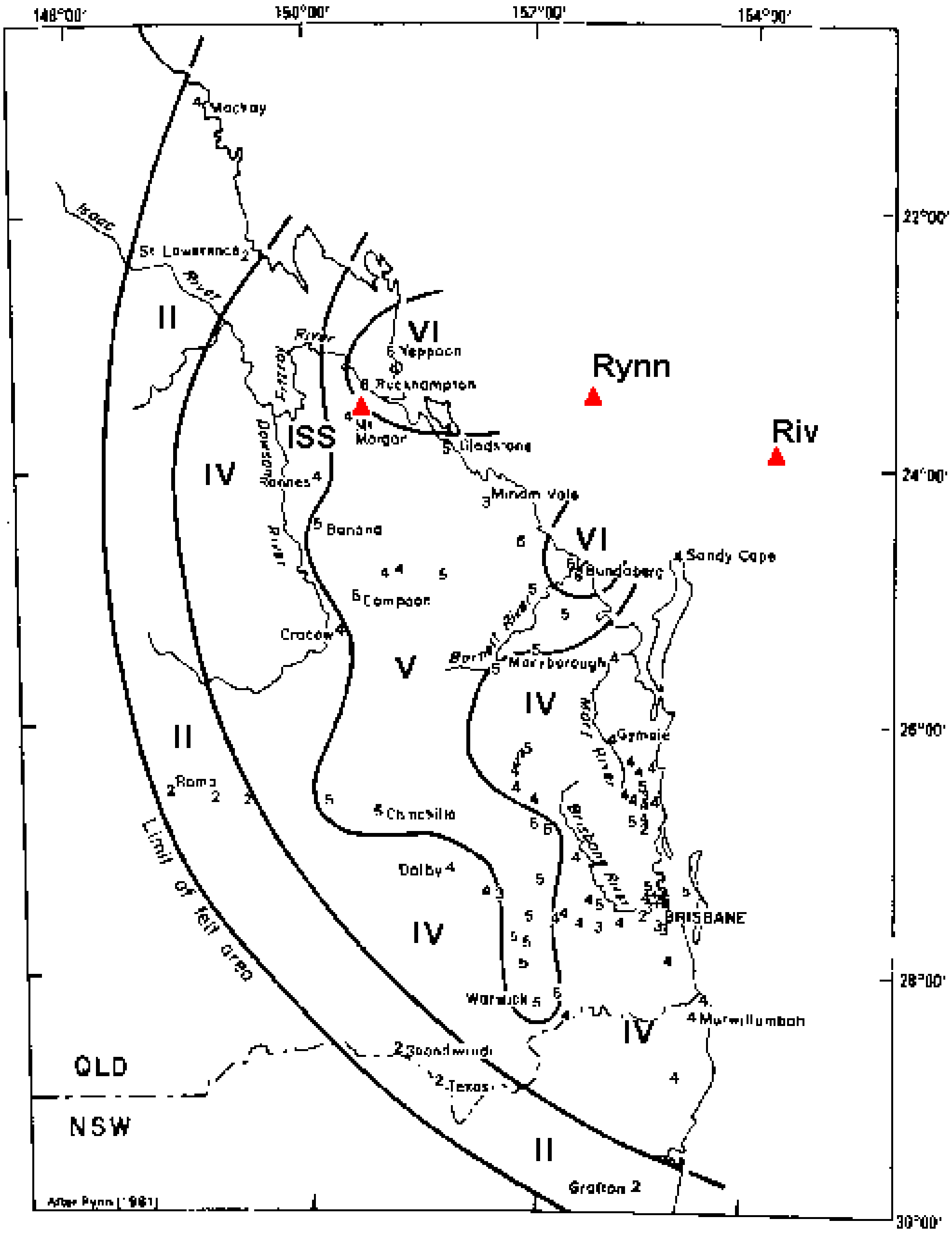

(After Everingham 1982)

Figure 3.1 **Isoseismal map of 1918 Bundaberg Earthquake.**

Hedley (1925) described the 1918 event as, "The greatest earthquake to shake Queensland, since European colonisation ...". The QED records that the 1918 event exhibited six aftershocks in a space of 2 hours, ranging in magnitude from MP5.1 to MP5.6. Rynn et at (1987) provides isoseismal maps for two of the aftershocks (9 minutes, and 1 hour 6 minutes after the initial event), estimated as having magnitudes of 5.5 and 5.7 respectively. The MP magnitude is obtained from the observed relationship between historical events that have been both instrumentally recorded and for which sufficient felt reports have been obtained to establish a reliable radius of perceptibility (c.f. Figure 4.2). For events that have reliable felt reports, but no instrumental recording, the MP magnitude can be determined from the reported radius of perceptibility.

On 12 April 1935 an earthquake, allocated a magnitude of ML6.1 in the QED, occurred near Gayndah. This event was recorded on instruments at Riverview College (Sydney), Sydney, Melbourne and Adelaide Observatories, Perth (Western Australia) and the Dominion Observatory (New Zealand) (Bryan &Whitehouse, 1938, pp107 & 108). From numerous felt reports Bryan and Whitehouse were able to draw a detailed isoseismal map (Figure 3.2) that indicates the earthquake was felt from Gladstone to Toowoomba, and as far west as Miles. Bryan and Whitehouse allocated an epicentral intensity of MM VII for the event (See Figure 3.2). They placed the epicentre at approximately 10 miles (16 km), northeast of the town of Gandah.

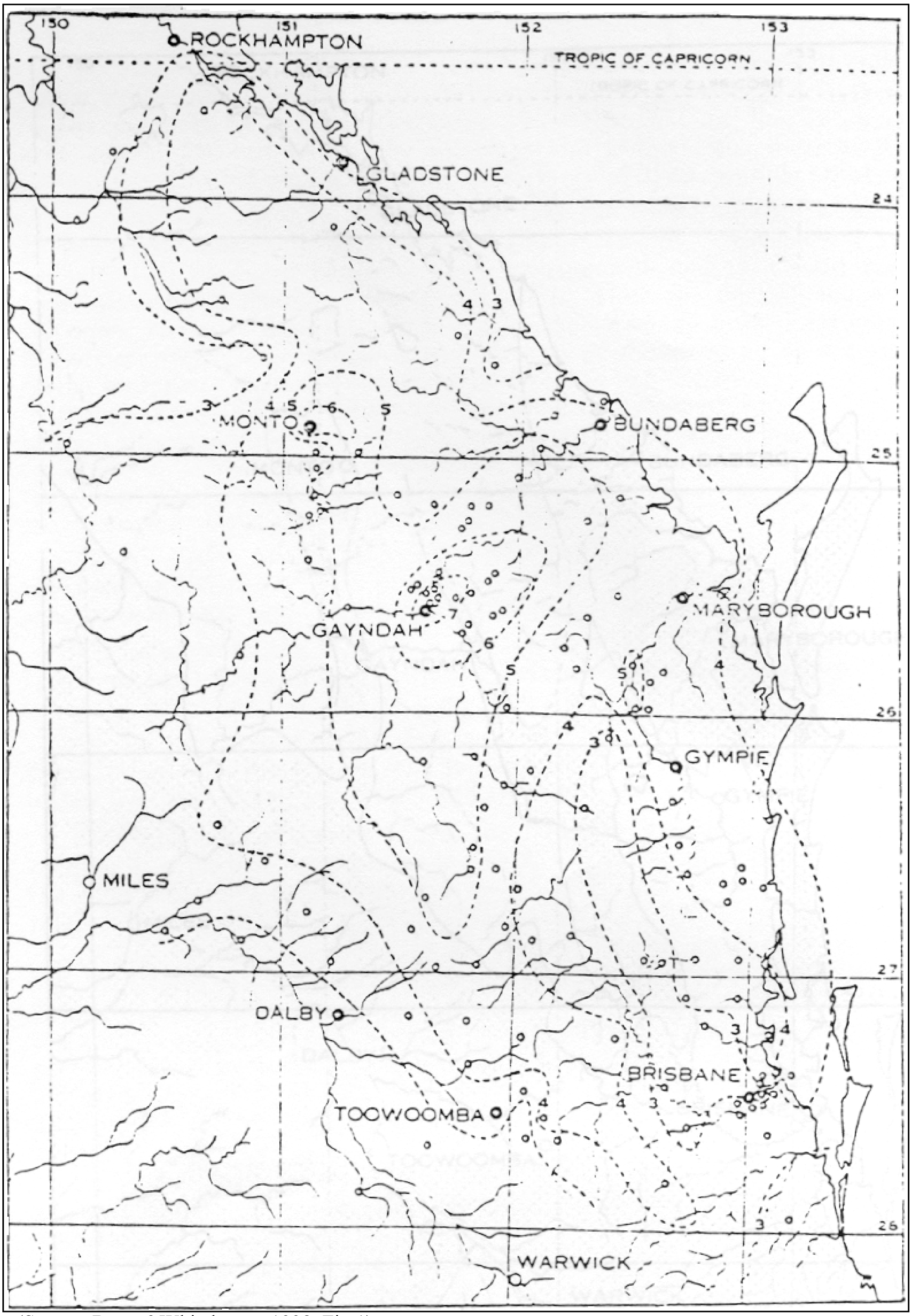

(Source: Bryan&Whitehouse, 1938, Fig 1)

Figure 3.2 **Isoseismal map of 1935 Gayndah Earthquake.**

The most recent significant event in the Bundaberg area occurred at 3:55am local time, on 29 May 1997. It was allocated a magnitude of 3.5 in the AGSO Earthquake Database and 3.0 in the QED. It was located at latitude 24.253ºS, longitude 153.25ºE, out at sea approximately 120km north-east of Bundaberg. Effects of the earthquake were reported from as far north as Moore Park, south to Burrum Heads, and west to Gin Gin. The author has drawn an isoseismal map of the event based on felt reports (See Figure 4.1).

Table 3.2 shows the 14 earthquakes listed in the QED of magnitude 3 or above which have occurred from 1980 to 1997, in the 3° grid centred approximately on Bundaberg (Latitude –23.5° to –26.5°, Longitude 151° to 154°).

LOCAL DATE	LOCAL TIME	Longitude	Latitude	Place	Magnitude
25-Mar-80	10:26:50.34	152.895	-23.794	BUNDABERG	MD 3.8
31-Jan-83	07:18:49.01	151.356	-25.914	BOONDOOMA	MD 3.4
30-Oct-84	16:29:48.16	151.965	-26.313	MURGON	ML 3.9
27-Jan-85	14:03:46.10	152.292	-24.507	BUNDABERG	ML 3.1
08-Feb-85	18:23:41.86	153.623	-25.119	OFF INDIAN HEAD	ML 4.6
28-Jul-85	13:13:25.61	151.711	-24.336	MIRIAM VALE	ML 3
02-Dec-85	16:19:00.93	151.725	-25.392	BIGGENDEN	ML 3.2
31-Oct-87	16:02:50.16	152.841	-23.828	LADY ELLIOTT ISLAND	ML 3.5
27-Dec-87	17:16:43.92	153.673	-24.111	OFF FRASER ISLAND	ML 3.2
21-May-88	12:23:20.83	151.741	-23.87	GLADSTONE	ML 3.3
30-Oct-88	06:52:43.17	151.291	-24.913	MONTO	ML 3.2
25-Nov-93	14:06:40.98	152.632	-23.922	LADY ELLIOTT ISLAND	ML 3.7
01-Sep-96	18:01:00.00	151.444	-26.112	BOWEN BASIN	ML 3.8
29-May-97	03:55:49.62	152.816	-24.449	OFFSHORE FROM BUNDABERG	ML 3

(Source, QUAKES Queensland Earthquake Database)

Table 3.2 <u>Recent Significant Earthquakes in the Bundaberg District</u>

The record of significant earthquakes catalogued from 1980 to 1997, in the 3° grid centred approximately on Bundaberg is considered to be complete for events of magnitude 3 and above. During the same period 643 events of magnitude less than 3.0, including 575 of magnitude less than 2, were recorded in the QED for the same 3° segment. Of the lower magnitude events 336, or 58%, were located at the Boondooma dam near Proston. It is likely that many, maybe most, of the micro-earthquakes recorded at the Boondooma Dam site are reservoir induced rather than tectonic in nature. However, there are numerous other reservoirs in the Bundaberg area that can potentially induce seismic activity, including the Fred Haige Dam 10 km north of Gin Gin, and the recently completed Walla Weir, 30 km southwest of Bundaberg. Since it is highly unlikely that 58% of all southeast Queensland's small events are occurring at the one site, it is probable that numerous small events are occurring in the Bundaberg district, but not being detected, because of inadequate coverage of the region with seismic instrumentation.

Summary

About 20% of southeast Queensland's significant seismic events recorded in the period from 1980 to 1997, occurred within a 3° grid centred on Bundaberg. This figure is based on seismic events of magnitude 3.0 or greater, during the period for which the record is considered complete.

It is highly probable that the majority of small events, of magnitude ≤ 2, which occur in the southeast Queensland region, are not being detected. The fact that 58% of all such small events in the Bundaberg area have been detected at the same site (where a seismograph is located near-by) supports this conjecture.

The largest earthquake recorded on the east coast of mainland Australia occurred in 1918 and was located within 150 km of Bundaberg. An earthquake of similar magnitude occurred in 1935 near the town of Gayndah. Both of these events were larger than the magnitude 5.5 event that caused the death of 13 people in Newcastle in 1989.

Since 1980 there have been 14 earthquakes, of magnitude 3 or greater, within the 3° grid centred on Bundaberg. The most recent was in 1997, about 120 km from Bundaberg.

CHAPTER 4 AN ISOSEISMAL MAP OF THE BUNDABERG 1997 EARTHQUAKE

Introduction

At 3:55am local time, on 29 May 1997, an earthquake occurred at latitude 24.253ºS, longitude 153.25ºE, out at sea approximately 120 km northeast of Bundaberg. It was allocated a magnitude of 3 by the Queensland University Advanced Centre for Earthquake Studies (QUAKES), and 3.5 by the Australian Geological Survey Organisation (AGSO). Effects of the earthquake were reported from as far north as Moore Park, south to Burrum Heads, and west to Gin Gin.

The reports of felt effects collected by the author have been analysed and a Modified Mercalli intensity value has been allocated to each (New Zealand Version, 1995, after Eiby, 1996, as described by McCue, 1996a, p8). It was found that the credibility of the reports varied from sound to dubious.

From the MM intensities an isoseismal map has been compiled (See Figure 4.1). This map indicates a general trend for the effects of the earthquake to be more noticeable in a line from the epicentre through Bundaberg in a southwest direction, following the Burnett River basin.

Putting the Bundaberg 1997 earthquake into perspective.

A magnitude 3.5 earthquake is not an insignificant event. Such an earthquake releases as much energy as about 73 tons of TNT. A magnitude 3.0 earthquake is equivalent to about 29 tons of TNT, and a magnitude 4.0 event is equivalent to about a 1 Kton of TNT (a small atomic bomb) (Louie, 2001).

The 27 December 1989 Newcastle earthquake had a magnitude of 5.5 ML (M^{C}Cue, 1996a). Thirteen deaths occurred from that event, 160 people were injured and a damage bill of about $4000Million Australian, including an insured loss of about $1000Million, was incurred (Lewis, online 1999). The Kobe earthquake on 16 January 1995 had a magnitude of 6.9 Mw (USGS National Earthquake Information Center: Earthquake search results, online 17 April 2000).

The felt effect reports

Tables 4.1 summarises the reports of felt effects received by the author from members of the public in the Bundaberg area, following the 1997 earthquake. In this table the locations of the witnesses at the time of the effect have not been included. The locations are presented in Table 4.2.

SUMMARY OF THE REPORTS
A spanner crab fisherman, fishing in vicinity of Lady Elliott Island early hours of Thursday 29/05/97. Never noticed any thing unusual except that the crab catch was very unusually low. Put pots in about 5.30am. First pull at 6.30am. Got 2 strings with about 40kg & then nothing until about 2pm and that is very unusual.
Witness2 got up at 2am on Thursday morning to go to loo & couldn't get back to sleep. Felt a thump like an underground explosion and suspected at the time that it was an EQ. No noise, no sway, just a sharp thump. Witness2 lives in a ground level flat on a concrete slab.
Wife woke up just before 4am on Thursday 29th and thought she had felt something. Had in her mind that it might have been a tremor. Went back to sleep.
Deep rumbling like a jet plane in trouble at about 5 to 4 on Wednesday morning (?). In the distance at first coming closer then a lull and then travelling away. Deep rolling sound. for 30s to a minute. Bedroom window faces north.
Witness5 woke up sometime between 1 and 3am (witness was unsure of exact time) on Thursday morning when she heard a big bang like thunder. She went into the lounge room and the counter on the video machine was "spinning around" and she couldn't reset it with the buttons. She had to pull the plug out of the wall to stop it. Witness5 said the event scared her badly.
When Witness6 woke up on Thursday morning she noticed that several pictures on the wall had been displaced about an inch off the normal position. This was unusual, as the pictures did not normally move at all.
Witness7 has respiratory problem & was up on Thursday morning between 0330 and 0400. His cat started running around and going "funny". This was very strange as the cat always stays inside at night and is always quiet. He let it outside. Heard rumbling like deep thunder but did not feel anything. When it was light he noticed the cat was on the deck of a 32 ft boat he is building in the back yard and would not come down. This was strange as the cat is a very amiable animal but never goes up the ladder to the deck whenever he is working on the boat. The cat appeared to not want to walk on the ground. Witness7 says that the most noticeable thing was the antics of the cat rather than the rumbling sound.
Witness8 lives in an old wooden house with a small dog for company. About 9:30 Sunday night Witness8 heard several sounds in corner of house like someone knocking on a door. The dog noticed it too. About 11:30 to 12 midnight Monday a similar thing happened. On Tuesday night (Wednesday morning) about 2:30am the same thing occurred. On Thursday morning at about 4am the dog started racing in and out of the front room from the back door to the front. The dog didn't seem to be able to locate the direction of whatever disturbance was causing his actions. Witness8 is inclined to think there was a build up of tremors culminating in the EQ. He says the house is built on two layers of old swamp ground that he observed when the sewage was being installed. One layer about 5ft down and another layer about 8 to 9 ft down. He says that this would make the house very sensitive to ground movement. Witness8 says he has worked with Indigo Jones for years researching long-range weather predictions using the electromagnetic disturbances that the earth is influenced by. He says that he and Indigo Jones measured the intensity of the electromagnetic fields by using their bodies as detector instruments in conjunction with regular readings they received from laboratories in Zurich, America and another here in Australia. He said the labs supplied them with readings of air to ground measurements in Gauss. He said that, although the labs said the measurement fluctuations were caused by sunspot activity, he was of the opinion that the sunspot activity was actually caused by the fluctuations of the electromagnetic radiation that emanated from further out in the solar system. He said that at present the radiation was coming from somewhere near Orion and he predicted that "within the next month or so" we could expect another rather large EQ in this region. He partly based this prediction on the fact that we were so close to the plate boundary to the east and "the other one out near Gayndah".
On Thursday morning Witness9 was in a real deep sleep and awoke at sound of a "tremendous explosion". Sat up in bed and shouted out, thinking it was something to do with the electricity. She had a night-light and an electric heater on and she checked them; but they were ok. Witness9 is sure that she did not feel anything, only heard the explosion. Lives in a single level brick house on a concrete slab. Witness9 has experienced 3 tremors before. One in Birmingham England, one in Newcastle (NSW) and one outside Newcastle (NSW).
Witness10 heading out of Burnett Heads at 0630 on Thursday morning 290597 on a bearing of about 5 degrees. Sea glassy with about a 1m swell. At a position of about 10 miles north of Bundaberg there was a sudden change in the sea surface as if going across a boat's wake. Crests were about 2m apart and about 4 to 6 inches high and superimposed on the sea swell. The wind had not changed and no crafts were moving within sight. The crests were coming in from the right hand side of the bow from the northeast. The boat continued travelling for about 2 to 3 miles at 20 knots before the sea went back to normal. The event was unusual enough for Witness10 and the boat owner [name suppressed] to discuss it at the time and wonder what was causing the strange ripples.
Witness11 woke up in the early hours of Thursday morning when she felt the sheets moving on her legs. She had felt the same thing from tremors before in Frankston, Victoria, south of Melbourne.
At about 4am on Thursday 29th May Witness12 was awoken by a loud bang. He thought his son had kicked the wall. It sounded like someone blowing a boulder up with dynamite (witness worked on a building site where workers next door were blasting boulders). Witness12 lives in an old Queenslander building [at Burrum Heads].

(Source: Author's personal records)

Table 4.1 <u>Summary of felt reports.</u>

Witness13 was visiting son in Rockhampton. On Wednesday night, in the early hours of Thursday morning, the sliding doors in the wardrobe started rattling like mad. They are quite big doors. Witness thought he heard "something". Later, maybe 4 to 5 minutes later, they rattled again.
Witness14 works as a nurse at the Bundaberg base Hospital. On Thursday morning at around about 4am she was tending patients on the 2nd floor. She heard a tremendous explosion. Went to the window and looked outside; but could see nothing unusual. Thought nothing more of it until she read about the earthquake in the News Mail later [on Saturday].
Witness15 comes from NZ and has experienced EQs before. In the early am of Thursday 29th Witness2's dogs started howling (not barking). At the same time the neighbour's geese started up an unusually sounding call and started running about.

(Source: Author's personal records)

Table 4.1 **Summary of felt reports (continued).**

Analysis of felt reports

Felt reports were obtained by mail, from personal and phone interview, and from media reports. Table 4.2 lists the Modified Mercalli intensities allocated, based on the felt reports. Where reports indicated the event was heard but not felt, it was assigned an intensity of MM II. Where the event was felt and recognized as an earthquake, or a physical effect was observed, it was assigned MM IV. Where only animal behavior was observed it was assigned MM I. No intensity was allocated where animal behavior was not directly observed.

Location	Latitude	Longitude	Heard	Felt	Physical Effect	Animal Behavior	MM
Heaps St., Bundaberg	-24º 54'	152º 22'		✔			IV
Crofton St., Bundaberg	-24º 52'	152º 21'		✔			IV
Thomsen St., Bundaberg	-24º 53'	152º 19'		✔			IV
Bangalo St., Moore Park	-24º 43'	152º 15'			✔		IV
Burnett Heads river mouth					✔		IV
B'berg News Mail Sat May 31			✔	✔			III
B'berg Base Hospital	-24º 52'	152º 19'	✔				II
Whittred St., Bundaberg	-24º 51'	152º 22'	✔				II
Gahans Rd., Bundaberg	-24º 51'	152º 23'	✔				II
Memory Bd. Innis Park	-24º 52'	152º 29'	✔				II
Kinch St., Burnett Hds	-24º 47'	152º 25'	✔			✔	II
Hoffman St., Burrum Hds	-25º 11'	152º 37'	✔				II
Newhaven Ct., B'berg	-24º 53'	152º 18'				✔	I
Kolan South	-24º 55'	152º 13'				✔	I
Gin Gin	-24º 58'	151º 57'				✔	I

Table 4.2 **Analysis of felt effects.**

Isoseismal map

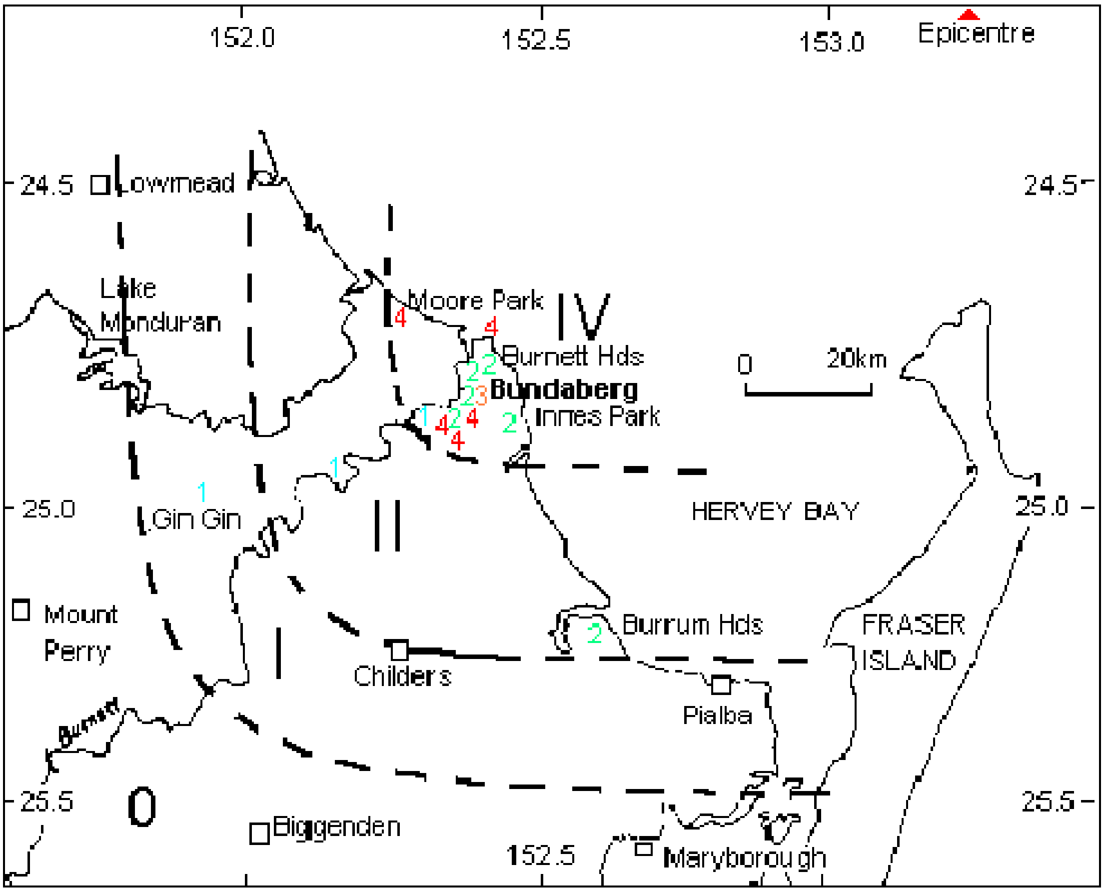

Figure 4.1 **Isoseismal map of Bundaberg 1997 earthquake**

Implications for Bundaberg

Greenhalgh et al (1988) analysed 100 Australian earthquakes for which reliable instrumental magnitudes and felt reports were available. They determined that, for Australian earthquakes covering the magnitude range M_L 1.5 to M_L 7.2, the expected radius of perception (R_P), in kilometres, for an earthquake of any given local magnitude (M_L) can be calculated using Eq 4.1, which produces real solutions for $\log_{10}R_P$, for $M_L \geq 1.215$ (See Appendix C). A graph of the relationship fitted to historical events of about magnitude 2.5 up to about magnitude 7.2 (see Figure 4.2) can be used to estimate R_P for any magnitude within the range M_L 2.5 to M_L 7.2.

$$M_L = 0.33(\log_{10} R_P)^2 + 0.74(\log_{10} R_P) + 1.63 \quad \ldots \quad \text{Eq 4.1}$$

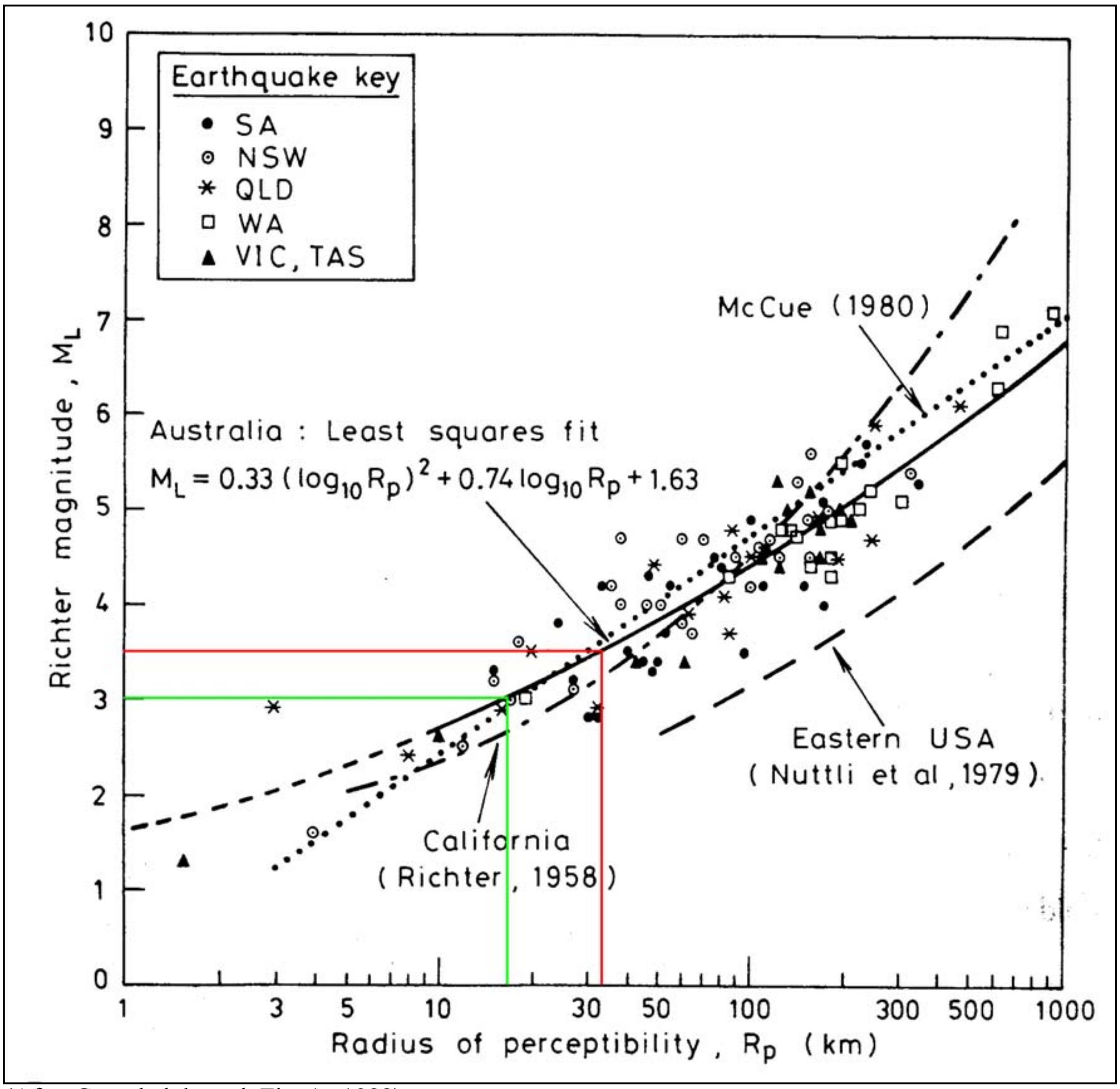

(After Greenhalgh et al, Fig. 1., 1988)

Figure 4.2 **Radius of Perception of Australian Earthquakes** **(See text for significance)**

McCue (personal communications July 2000) uses a linear relation as given in Eq 4.2.

$$M_L \approx 1.01 \ln(R_P) + 0.13 \quad \ldots \quad \text{Eq 4.2}$$

McCue's relationship is also represented in Figure 4.2. In Figure 4.2 the green and red lines indicate the radius of perception of events of magnitudes 3 and 3.5 respectively, based on Greenhalgh's relationship. It can be seen the McCue's relationship provides similar results for those magnitudes.

Both Greenhalgh's and McCue's relationships indicate that an earthquake of magnitude 3.0 has an expected radius of perception of about 17 km, and an earthquake of magnitude 3.5 has an expected radius of perception of about 28 km to 35 km. Under the usual circumstances an earthquake of magnitude 3.5 should not be felt as far away as 120 km!

Subsequent to the 1997 Bundaberg event the author had communications with the manager of the Lady Elliott Island Resort (60 km north-west of the epicentre) and a Queensland National Parks and Wildlife ranger stationed at Waddy Point on Fraser Island (70 km south of the epicentre). Both of these people were at the indicated locations at the time of the earthquake and said that they had not felt any effects and were, in fact, unaware that an earthquake had occurred until contacted by the author. The manager of the Lady Elliot Island Resort indicated that numerous guests were in residence at the resort at the time, and that he had received no reports from any of them.

That the earthquake was felt in Bundaberg, over 120 km from the epicentre, but was not felt at locations closer to the epicentre, indicates that unusual conditions exist in the Bundaberg City area. Because of these unusual conditions the degree of ground motion induced at Bundaberg, by the seismic waves generated at the epicentre of the earthquake 120 km away, was accentuated to a larger than normal extent. Amplification of the ground motion must have occurred in the Bundaberg area.

The propensity for a site to amplify seismic ground motion increases the seismic hazard expected at that site; and consequently increases the seismic risk to structural damage at that site. The occurrence of ground motion amplification was identified as an important contributing factor to structural damage resulting from the Newcastle earthquake in 1989 (Sommerville et al, 1993).

The microzonation sections of this thesis are concerned with assessing the extent of ground motion amplification within the Bundaberg City area.

CHAPTER 5 EARTHQUAKE HAZARD IN THE BUNDABERG AREA, ESTIMATED USING GUMBEL TYPE I STATISTICS.

Introduction.

The criteria that are required of any statistical analysis model applied to earthquake hazard estimation are that:

- it is able to emulate the known historical data, and
- it can produce suitable formulation from which the probability of future events of interest can be inferred within a specified certainty.

As long as these criteria are met the choice of model is open, and the model can be deemed suitable for the purpose.

The verification of earthquake hazard estimations produced by any suitable model can only be accomplished on time-scales typified by the recurrence periods of the events of interest. For large magnitude events on the Australian continent this could be hundreds or thousands of years, or more. Consequently all hazard estimations derived from historical data collected over periods considerably shorter than the estimated return times have to be interpreted with care.

In a comprehensive treatment of earthquake hazard estimation, Lomnitz (1974) details a method for using the Gumbel Type I extreme event probability distribution (Gumbel, 1954 & 1958) to estimate design earthquake recurrence times using observed annual extreme magnitudes. The statistical model uses the properties of extreme values derived by Gumbel in the 1940s and first published as a paper (Gumbel, 1954) and then as a book (Gumbel, 1958), The model's applicability to seismology was further explained by Benjamin and Cornell (1970), and Yegulalp (1974). It has been used with success to analyse the recurrences of other natural phenomena such as floods (Gumbel, 1958; Haan, 1977; Bobée, 1995), rainfall precipitation forecasts (Hammill, 1996 & 1997) and cobble size in gravel deposits (Gumbel, 1958). In 1945 Nordquist used Gumbel Type I statistics to analyse maximum earthquake events on a world scale, and also for sections of southern California and an area around Los Angeles. McCue and Boreham have used the technique in the Rockhampton area (McCue, 1996b).

In this paper the Gumbel Type I extreme value method has been used to analyse earthquake data for events recorded in the region between latitudes 23.5º to 26.5º South, and longitudes 151º to 154º East, between the years 1977 to 1997. This data has been extracted from the Queensland University Advanced Centre for Earthquake Studies (QUAKES) Queensland Earthquakes database (QUAKES, 2000), herein referred to as the QED. This area of interest is the 3° grid centred approximately on Bundaberg, and will be referred to as the Bundaberg area.

The Gumbel Type I Extreme Event Probability Distribution

The Gumbel Type I cumulative frequency probability distribution function for extreme value y is

$$G(y) = \exp(-\alpha e^{-\beta y}) \ : \ (y \geq 0) \qquad \ldots \quad \text{Eq 5.1}$$

where α and β are parameters to be determined.

Lomnitz (1974) shows that, if a homogeneous earthquake process with a cumulative magnitude distribution

$$F(x) = 1 - e^{-\beta x} \ : \ (x \geq 0) \qquad \ldots \quad \text{Eq 5.2}$$

is assumed, where β is the inverse of the average magnitude of earthquakes in the region under consideration; and α is the average number of earthquakes per year above magnitude 0.0; then y, the maximum annual earthquake magnitude, will be distributed as in Eq 5.1.

The values of α and β are estimated by considering the largest yearly earthquake magnitudes $y_1, y_2, y_3, \ldots, y_n$ in a sample of n consecutive years. The magnitudes are ranked in ascending order such that $y_1 \leq y_2 \leq y_3 \leq \ldots y_n$, and then the plotting positions of cumulative frequency probability G(y) are calculated using

$$G(y_j) = j / (n + 1) : (j = 1, 2, 3, \ldots, n) \quad \ldots \quad \text{Eq 5.3}$$

The values of α and β are then estimated from a least-square fit to the reduced variate linear equation

$$-\ln[-\ln(G(y_j))] = \beta y_j - \ln(\alpha) \quad \ldots \quad \text{Eq 5.4}$$

or, equivalently

$$\ln[-\ln(G(y_j))] = \ln(\alpha) - \beta y_j \quad \ldots \quad \text{Eq 5.5}$$

which was derived from Eq 5.1.

Estimation of α and β

Year	Maximum Magnitude	Rank (j)	Plotting Position $G_1(y_j) = j / (N + 1)$	Reduced variate $\ln(-\ln G_1(y_j))$
1995	1.7 M_L	1	0.0455	1.1285
1982	2.4 M_L	2	0.0909	0.8746
1989	2.4 M_L	3	0.1364	0.6894
1994	2.4 M_L	4	0.1818	0.5334
1992	2.6 M_L	5	0.2273	0.3931
1986	2.8 M_L	6	0.2727	0.2618
1990	2.8 M_L	7	0.3182	0.1355
1981	2.9 M_L	8	0.3636	0.0115
1991	2.9 M_L	9	0.4091	-0.1123
1997	3.0 M_L	10	0.4545	-0.2377
1977	3.1 MD	11	0.5000	-0.3665
1988	3.3 M_L	12	0.5455	-0.5007
1983	3.4 MD	13	0.5909	-0.6423
1979	3.5 MD	14	0.6364	-0.7941
1987	3.5 M_L	15	0.6818	-0.9597
1993	3.7 M_L	16	0.7273	-1.1443
1980	3.8 MD	17	0.7727	-1.3555
1996	3.8 M_L	18	0.8182	-1.6061
1984	3.9 M_L	19	0.8636	-1.9200
1985	4.6 M_L	20	0.9091	-2.3506
1978	4.8 M_L	21	0.9545	-3.0679

(Source: QUAKES Queensland Earthquake Database)

Table 5.1 **Maximum Magnitude events in the Bundaberg area, 1977 to 1997.**

The annual maximum magnitude seismic events recorded within the 3° grid centred on Bundaberg, from the year 1977 to 1997, are shown in Table 5.1. During that period there is a continuous record of maximum events in each year.

The events are arranged in ranked order, and values of G(y_j), the cumulative frequency probability, are calculated using Eq 5.3. The Extreme Event Type I reduced variate is then calculated as per Eq 5.5. The data obtained from this process are shown in Table 5.1.

Figure 5.1 uses the linear relationship in Eq 5.5 to display the reduced variate versus the maximum magnitudes, and to compute α and β using linear regression of the data.

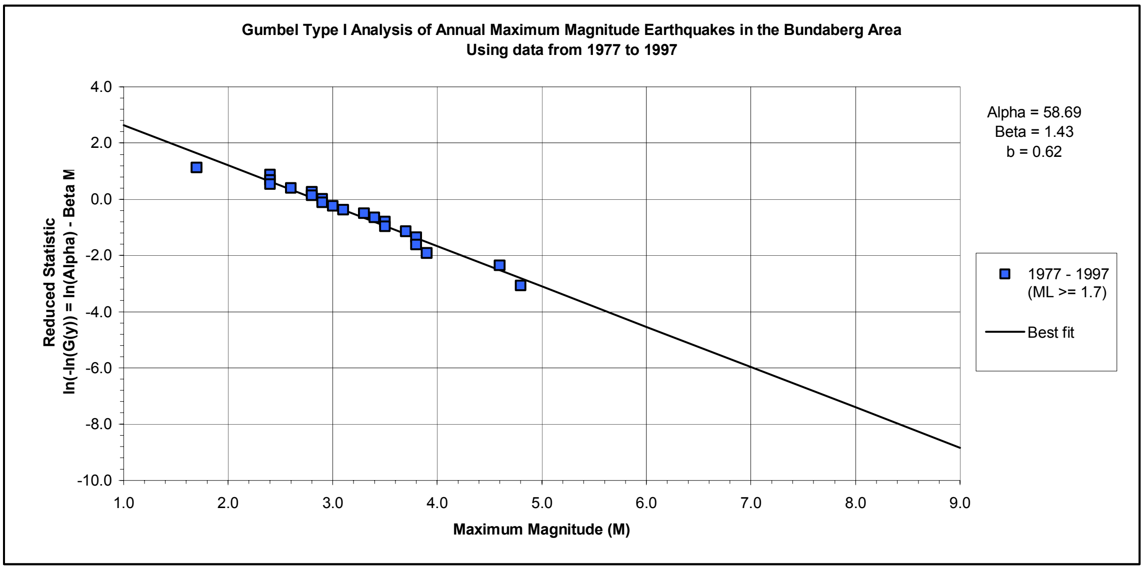

Figure 5.1 **Estimation of α and β using data from 1977 to 1997**

Table 5.2 indicates the statistics derived from the linear regression, and their physical interpretation. It is noted that the linear regression provides a correlation coefficient of 0.97 between the annual maximum magnitudes and the reduced statistic, indicating a very high goodness of fit to Eq 5.5.

Statistic	Value	Interpretation
Slope (-β)	-1.4346	
β	1.4346	The inverse of the average magnitude of earthquakes in the area of interest.
Intercept (ln(α))	4.0723	
α	58.69	Average number of earthquakes per year above magnitude 0.

Table 5.2 **Determination of α and β for 1977 to 1997 Analysis.**

The parameter β is related to the Richter/Guttenberg *b* value (c.f. Appendix F) by the Eq 5.6 (Lomnitz & Singh, 1976):

$$b = \beta \log_{10} e \qquad \ldots \qquad \text{Eq 5.6}$$

This results in a *b* value of about 0.62 in the magnitude range $2.0 \le M_L \le 4.8$ over the 20-year sample period for the Bundaberg area, which is low, implying a moderate to high stress drop for the region (c.f. Appendix F).

Extrapolation of Results

The historical data from 1977 to 1997 was used in the above analysis because it represented a continuous and complete set of annual maximum magnitude events. The maximum annual magnitudes ranged from M_L 1.7 to M_L4.8. As will be demonstrated below, the analysis results can be used to determine a variety of statistics, including the average recurrence periods of annual maximum magnitude earthquakes. For instance, the results indicate that the mean recurrence period for an earthquake of magnitude 4.0 is 5.3 years. It is tempting to use the results to extrapolate for statistics relating to potentially more damaging events of, say, magnitude 6 or 7. However, since the data used to perform the analysis did not contain any maximum events of those magnitudes, extrapolation to events with magnitudes larger than about M_L 5 becomes unreliable.

To extend the usefulness of the analysis it is possible to add earlier data that contains higher magnitude maximum events, in a piece-wise manner.

When the extended range data is combined with the original range data, only the data relating to the maximum magnitude for which the extended data set is considered complete is used. The author considers that the historical data set from 1883 to 1997 is complete for events of magnitude > 5.5 (c.f. Chapter 1).

Table 5.3 shows the additional data that has been extracted from the historical record from 1882 to 1997. Only the data for extreme events of magnitude > 5.0 are shown.

Year	Maximum Magnitude	Rank (j)	Plotting Position $G_1(y_j) = j / (N + 1)$	Reduced variate $\ln(-\ln G_1(y_j))$
1883	MP5.9	124	0.976377953	-3.7336
1935	M_L 6.1	125	0.984251969	-4.1431
1918	M_L 6.3	126	0.992125984	-4.8402

(Source: QUAKES Queensland Earthquake Database)

Table 5.3 **Additional Maximum Magnitude events in the Bundaberg area, extracted from the 1882 to 1997 data set.**

Figure 5.2 displays the piece-wise combined data sets from the two complete series 1977 to 1997, and 1882 to 1997. Comparison with Figure 5.1 will show that the additional data has caused some reduction in the *b* value (0.62 to 0.59) and has enhanced the ability of the results to produce confident statistics to M_L6.0.

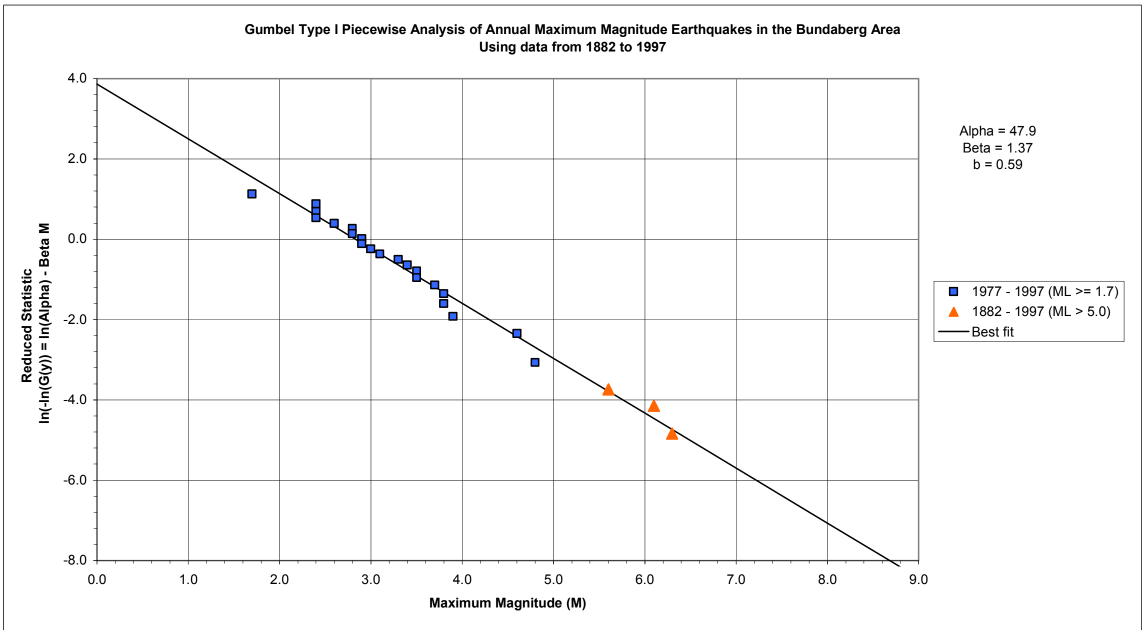

Figure 5.2 **Estimation of α and β using data from 1882 to 1997**

Statistic	Value	Interpretation
Slope (-β)	-1.36678	
β	1.37	The inverse of the average magnitude of earthquakes in the area of interest.
Intercept (ln(α))	3.86833	
α	47.86	Average number of earthquakes per year above magnitude 0.

Table 5.4 **Determination of α and β for 1882 to 1997 Piece-wise Analysis.**

Table 5.4 indicates the statistics derived from the linear regression, and their physical interpretation. It is noted that the linear regression provides a correlation coefficient of 0.99 between the annual maximum magnitudes and the reduced statistic, indicating a very high goodness of fit to Eq 5.5.

Estimating Seismic Hazard

Lomnitz (1974) provides a number of equations that use α and β to determine statistical quantities frequently used in analysis of what he refers to as earthquake *risk*. Everingham et al (1982) and Rynn et al (1987) define *seismic risk* as "… the odds of earthquake occurrence within a given time interval and region". McCue (1996a) defines *seismic risk* as "The probability of damage", and *seismic hazard* as "… the probability of earthquake occurrence within a given time interval and region." The equations provided by Lomnitz can be used to estimate the seismic hazard of a region, as defined by McCue.

Earthquake hazard is referred to a design magnitude. A design magnitude is the magnitude that an earthquake of interest is likely to equal or exceed. An earthquake that fits this design criterion is referred to as a design earthquake of magnitude *y*. For earthquake engineering purposes the design magnitude is commonly chosen as that magnitude, above which the probability of an earthquake occurring during a given time period is considered to be negligibly small, depending on what is considered to be an *acceptable* risk. In order to be able to make such engineering decisions, statistics providing the average recurrence period for earthquakes of any given magnitude, and the probabilities of single and multiple earthquake occurrences over any given period, need to be available.

The average recurrence period

The average recurrence period T_y, of an earthquake of magnitude y, is given by

$$T_y = 1 / N_y \qquad \ldots \qquad \text{Eq 5.7}$$

where N_y, the number of expected earthquakes per year exceeding magnitude y is given by

$$N_y = \alpha e^{-\beta y} \qquad \ldots \qquad \text{Eq 5.8}$$

giving

$$T_y = (\alpha e^{-\beta y})^{-1} \qquad \ldots \qquad \text{Eq 5.9}$$

Table 5.5 displays the determination of average recurrence periods for specified design earthquakes within the Bundaberg area, based on extrapolation of the Gumbel Type I analysis of maximum magnitude events recorded from 1882 to 1997.

Also noted in Table 5.5 are the most recent events that fit the design magnitudes M_L 1 to M_L 7. For those events that have been observed there is a good relationship between the estimated recurrence period and recorded history of those events.

Design Magnitude (ML)	Average Recurrence Period (years)	Average Recurrence Period (months)	Average Recurrence Period (days)	Most recent event	Time lapse prior to 31/12/97 (days)
1	0.07	0.84	26	25/12/97	6
2	0.26	3.12	95	15/10/97	77
3	1.22	14.64	446	28/05/97	178
4	5.01	60.12	1830	08/02/85	4711
5	20.51	246.12	7491	24/06/52	16386
6	84.02	1008.24	30688	12/04/35	22578
7	344.15	4129.8	125700	None observed	

Table 5.5 **Average Design Earthquake Recurrence Periods**

Confidence of recurrence period

The probability P{t ≥ T} that the recurrence period of a design earthquake of magnitude y exceeds an arbitrary recurrence period of T years is given by (c.f. Lomnitz, 1974)

$$P\{t \geq T\} = \exp(-T / T_y) \qquad \ldots \qquad \text{Eq 5.10}$$

Equation 5.10 is a fundamental relationship derivable from the Poisson model. Its use here is a consequence of the fact that the Gumbel extreme value method is based on a lognormal relationship, of which the Poisson model is an example. Therefore a Poisson model can be reasonably assumed to apply. Therefore, the probability of the recurrence period being less than an arbitrary time T is given by

$$P\{t \leq T\} = 1 - \exp(-T / T_y) \qquad \ldots \quad \text{Eq 5.11}$$

from which it can be deduced that the period T within which at least one earthquake of magnitude *y* will occur with probability P is given by

$$T = -T_y \ln(1 - P) \qquad \ldots \quad \text{Eq 5.12}$$

Eq 5.12 can be used to calculate the expected period within which at least one earthquake of any given magnitude will occur with any stated probability. For instance, the recurrence period for at least one earthquake of magnitude *y* within a probability of 89% is given by

$$T_{89} = -T_y \ln(1 - 0.89) \qquad \ldots \quad \text{Eq 5.13}$$

For an earthquake of magnitude M_L6, which has an average recurrence period of 84.02 years, the 89% probability recurrence period is calculated, using Eq 5.13, at being 185.46 years. The 89% probability has been chosen because it is at that level of probability that the calculated return periods conform to the observed recurrence periods.

An intuitive interpretation of the 89% probability recurrence period results is that, within the Bundaberg area, there is an 89% probability that, in any given 185 year period, at least one earthquake of magnitude M_L6 or greater will occur. As a corollary, within any given 185 year period there is an 11% probability that an earthquake of magnitude M_L6 or more will not occur.

Table 5.6 shows that all of the most recent annual maximum magnitude earthquakes observed within the Bundaberg area up to the end of 1997 have occurred within the 89% probability recurrence period.

Design Magnitude (ML)	89% Confidence Recurrence Period (years)	89% Confidence Recurrence Period (months)	89% Confidence Recurrence Period (days)	Most recent event	Time lapse prior to 31/12/97 (days)
1	0.15	1.8	55	25/12/97	6
2	0.57	6.8	208	15/10/97	77
3	2.69	32.3	983	28/05/97	178
4	11.06	132.7	4040	08/02/85	4711
5	45.27	543.2	16535	24/06/52	16386
6	185.46	2225.5	67739	12/04/35	22578
7	759.63	9115.6	277455	None observed	

Table 5.6 **Design Earthquake Recurrence Periods for 89% Confidence.**

From Eq 5.12, if the confidence recurrence period (T) is equal to the average recurrence period it can be calculated that the probability of at least one earthquake of any given magnitude recurring during the average recurrence period for that magnitude event is 63.2%

An intuitive interpretation of this result is that, within the Bundaberg area, there is a 63.2% probability that, in any given 84 year period, at least one earthquake of magnitude M_L6 or greater will occur. As a corollary, within any given 84 year period there is a 36.8% probability that an earthquake of magnitude M_L 6 or more will not occur.

Probabilities of Multiple Events

The Poisson properties of the underlying earthquake process can be used to calculate the statistical probabilities of the occurrence of multiple earthquake of a given magnitude within the average recurrence period for that magnitude event. Table 5.7 shows these probabilities.

Number of events (n)	Probability of exactly n events occurring within the average recurrence period	Probability of n or less events occurring within the average recurrence period	Probability of at least (n + 1) events occurring within the average recurrence period
0	0.3679	0.3679	0.6321
1	0.3679	0.7358	0.2642
2	0.1839	0.9197	0.0803
3	0.0613	0.9810	0.0190
4	0.0153	0.9963	0.0037
5	0.0031	0.9994	0.0006
6	0.0005	0.9999	0.0001
7	0.0001	1.0000	0.0000
8	0.0000	1.0000	0.0000

Table 5.7 **Probabilities of the Occurrence of Multiple Events**

As can be seen from Table 5.7, the probability of at least one earthquake occurring within its average recurrence period is 63.2%; which agrees with the same determination made using Eq 5.12.

Earthquake hazard

Earthquake hazard $H_D(y)$ is the probability of recurrence of an earthquake of magnitude y within a period of D years, and is given by

$$H_D(y) = 1 - \exp(-\alpha D e^{-\beta y}) \quad \ldots \quad \text{Eq 5.14}$$

Figure 5.3 shows the 20-year earthquake hazard for the Bundaberg area, based on the analysis carried out in this paper.

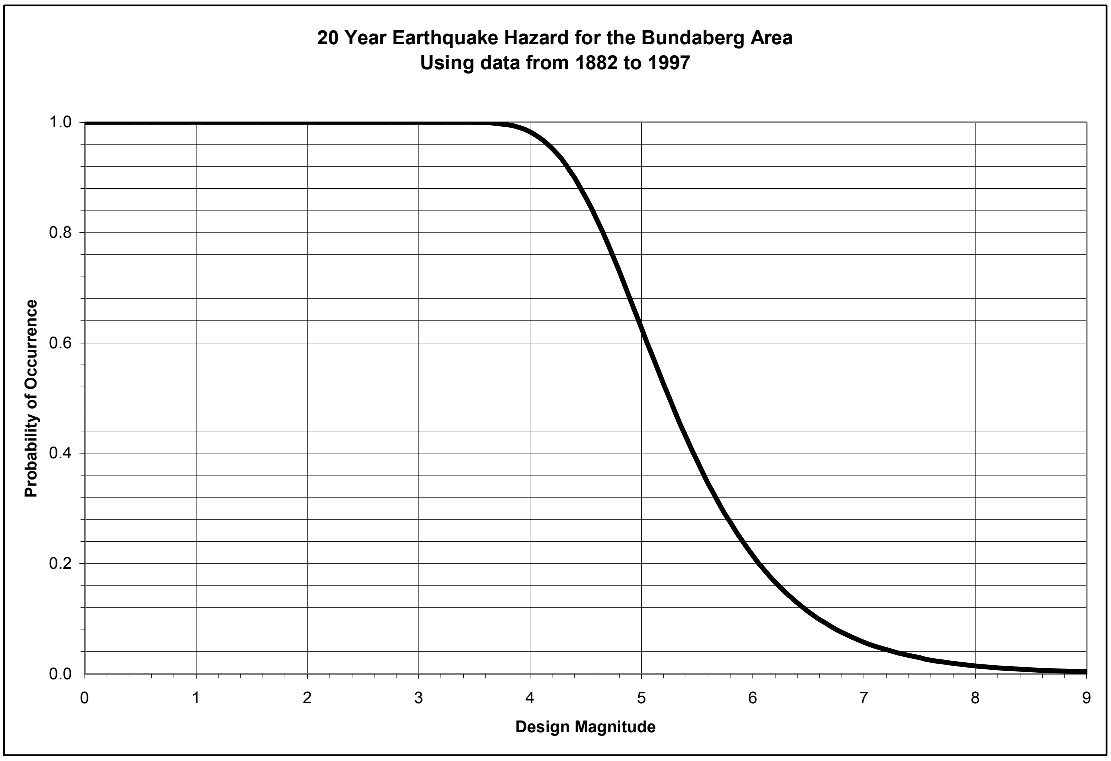

Figure 5.3 **<u>20-year Earthquake Hazard for the Bundaberg Area.</u>**

It should be noted that, in interpreting the hazard probabilities, there is a non-zero probability of no event occurring over any given period of time, and the probability of any particular event occurring never reaches 1.0 (The probability of any particular event is never absolutely certain). The probability of an earthquake of magnitude 3.5 occurring in the Bundaberg area within any 20-year period, according to this analysis, is about 0.999. That is, it is almost certain that at least one such event will occur within that period of time.

Summary and Conclusions

The record of maximum magnitude earthquakes in the Bundaberg area from 1977 to 1997, as recorded in the QUAKES Queensland Earthquake database, is considered by the author to be complete and continuous for earthquakes of magnitude ≥ 2.4. The same record, in the period from 1882 to 1997 is considered complete for earthquakes of magnitude ≥ 5.0. Gumbel Type I extreme event statistics has been applied to analyse those maximum magnitude data with a satisfactory degree of correlation (0.99). The results of that analysis has enabled the earthquake hazard that exists in the Bundaberg area to be quantified in terms of recurrence periods and probabilities of occurrence of earthquakes of any given magnitude.

There is a 63% probability that, in any given 84 year period, at least one earthquake of magnitude M_L 6 or greater will occur within the Bundaberg area. There is a 26% probability that, in any given 84 year period, at least two earthquake of magnitude M_L 6 or greater will occur within the Bundaberg area. Two earthquakes of magnitude about M_L 6 have occurred in the Bundaberg area within the 69 years prior to 1997; the “Queensland”, or “Bundaberg” earthquake of 1918 (M_L 6.3), and the “Gayndah” earthquake of 1935 (M_L 6.1).

CHAPTER 6 CHARACTERISATION OF GROUND MOTION AMPLIFICATION

Introduction

It has already been stated that the effects of a magnitude 3.5 earthquake, such as the one that occurred on 29 May 1997 northeast of Bundaberg, should not, under normal circumstances, be felt by people sited more than about 30 km from the epicentre. In fact it has been documented in this thesis that the 1997 earthquake was not felt at distances of 60 km (Lady Elliott Island) and 70 km ((Fraser Island), but that it was felt by up to 14 people as far away as Bundaberg City and Burrum Heads – over 120 km from the epicentre. It would appear then that the foundations at Bundaberg and Burrum Heads are somehow different to those at Lady Elliot Island and Fraser Island. The foundations at Bundaberg and Burrum Heads are more conducive to accentuating ground movement than at the other two places. This observation could be explained by ground motion amplification.

The presence of ground motion amplification during earthquakes has been noted at a number of places around the world by numerous investigators. Some of the more notable instances of site amplification are: the San Fransisco Bay area (c.f., Borcherdt, 1970; Boatwright et al, 1991; Borcherdt and Glassmoyer, 1992); the vast destruction caused during the Mexico City 1995 earthquake (c.f., Anderson et al, 1986; Singh et al, 1988); the Loma Prieta 1989 event (c.f., Hough et al, 1990; Hanks & Krawinkler, 1991); the Armenia 1988 earthquake (c.f., Borcherdt et al, 1989); and Newcastle (Sommerville et al, 1993). This brief listing is by no means complete. The significance of ground motion amplification to the potential for an earthquake to cause damage was noted as early as 1898 (Milne, 1898). Considerable emphasis has been placed on characterising, quantifying and cataloguing the phenomena over recent decades, particularly in urbanised areas.

What is *Ground Motion Amplification*

The seismic energy released during an earthquake is radiated from the hypocentre as a combination of shear and longitudinal waves. Some of the waves propagate within fractions of a wavelength of the crustal surface as *surface* waves and some propagate through the body of the crust and lower strata as *body* waves. Due to refraction and reflection within the earth, and the spherical nature of the earth, the body waves generally re-emerge as surface waves at some distance from the epicentre. It is the surface waves that contribute to ground motion. As the surface waves pass through the surface materials they cause those materials to move both horizontally and vertically.

Ground motion amplification, at a particular site of interest, can be regarded as being the ratio of the ground motion at that site to the ground motion (caused by the same wave) at some nearby reference site. The reference site may be, for instance, a nearby outcrop of basement rock or the bottom of a borehole drilled down to bedrock. In other words, *ground motion amplification* is a measure of the exceedence of motion produced by a wave at a surface site, over the motion produced by the same wave in bedrock in the vicinity of the surface site.

In some cases the ground motion at the site of interest will be less than that at the reference site. In that case there is attenuation rather than amplification. The amplification must, for fundamental physical reasons, be restricted to limited frequency ranges. Amplification to all modes of movement could not occur over the whole frequency range, as this would contravene the law of conservation of energy. Consequently a combination of amplification and attenuation usually occurs in different frequency ranges. In general, however, there is more than one mode of motion available. In those situations it is possible for energy from one mode to be converted to energy in another mode. For instance, if energy were converted from the vertical mode to the horizontal mode, then this would result in amplification of the horizontal motion.

Horizontal and vertical ground motion

Of the two categories of surface waves produced by an earthquake (longitudinal and shear) it is the shear wave component that produces the more damaging ground movement. Two types of shear surface waves are propagated; those that produce predominantly horizontal ground movement (Love waves), and those that produce both horizontal and vertical ground movement (Rayleigh waves). A Rayleigh wave passing through a physical medium will cause the particles in the medium to perform elliptical motion in the vertical plane, in the direction of propagation. This elliptical motion will contain horizontal motion (in the line of propagation), and vertical motion (normal to the line of propagation). The elliptical path traced by the particles of the medium is called the *particle orbit*. In an isotropic medium the particle orbit will be circular. This would produce a horizontal to vertical ratio of movement of unity (i.e. H / V = 1). That is, the *ellipticity* of the wave will be unity (c.f. Figure 6.1). This situation is closely approximated by solid basement rock. Because of the stiffness of the rock the localised effect of gravity is negligible and one would expect bedrock, through which a Rayleigh wave is passing, to produce a horizontal to vertical movement ratio of unity.

Materials that tend to produce horizontal to vertical movement ratios greater than unity are said to amplify the horizontal ground movement. In other words, *horizontal ground motion amplification* is a measure of the exceedence of horizontal motion produced by a wave at the surface, over the vertical motion produced by the same wave at that site. If it can be shown that the surface vertical motion is characteristic of the underlying bedrock movement then horizontal ground movement amplification is a measure of ground motion amplification.

Although a discussion of Rayleigh wave particle motion has been used to explain the concept of horizontal ground motion amplification, such amplification occurs for all surface wave types.

Rayleigh wave particle orbits

Konno and Ohmachi (1998) demonstrate that the particle orbits produced by Rayleigh waves can be classified in three types, depending on whether the velocity contrast between the surface layer and the basement substrate of a simplified strata model is low (Type 1), moderately high (Type 2) or very high (Type 3).

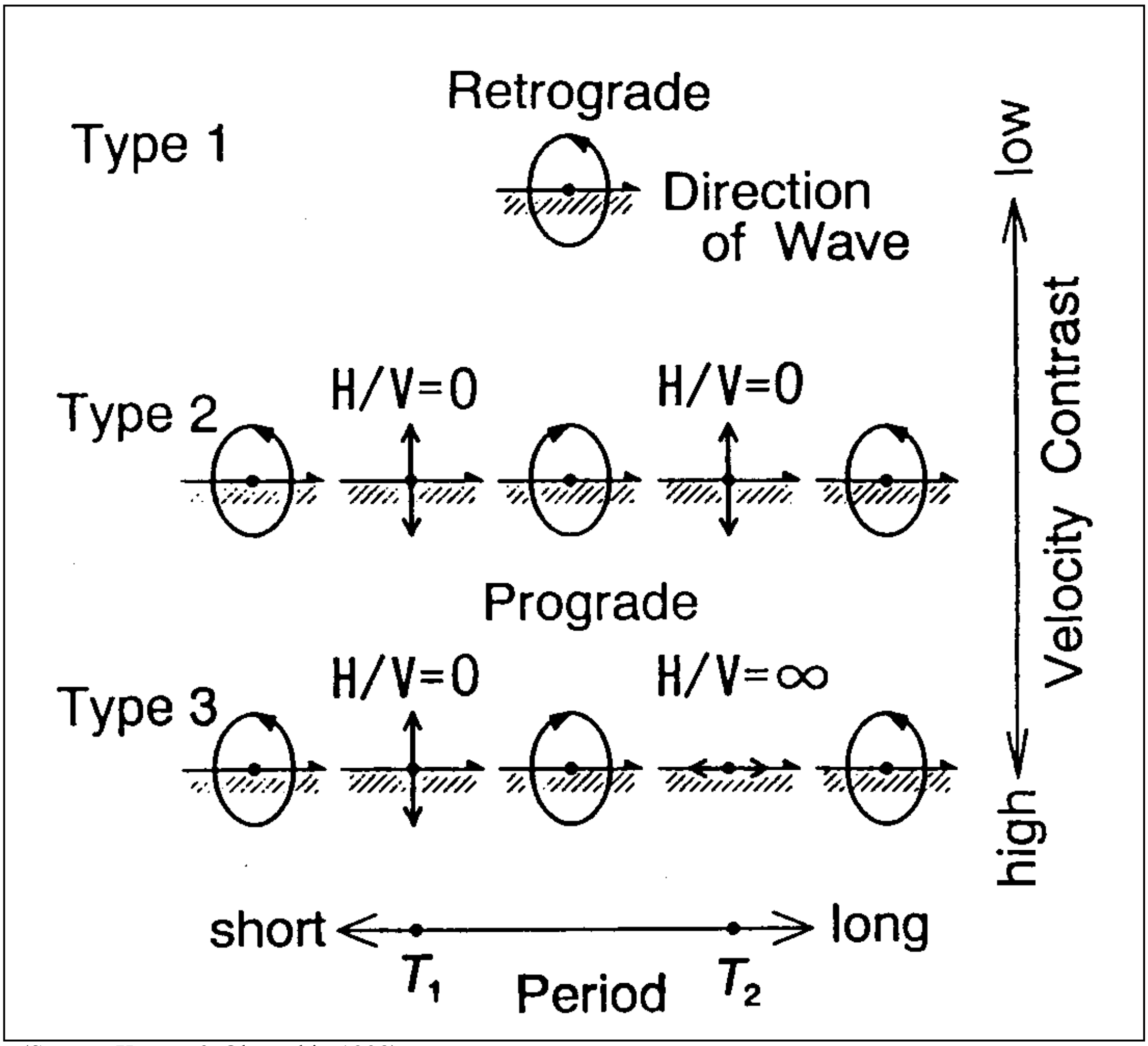

(Source: Konno & Ohmachi , 1998)

Figure 6.1 **Particle orbit of three types of fundamental-mode Raleigh waves for simplified surface/substrate model.**

For Type 1 motion the particle motion is always retrograde. The direction of the particles at the top of the orbit is always opposite to the direction of propagation of the wave. This condition is satisfied when the ratio of the shear wave velocities is low ($V_{substrate}/V_{surface} \leq 2.5$).

For the conditions $V_{substrate}/V_{surface} \approx 2.5$ Type 2 movement conditions exist. Under these conditions, depending on the period of the wave, the particle orbit will be retrograde, prograde or vertical only. At periods where the motion is purely vertical the horizontal ground amplification will be zero.

Type 3 movement exists where $V_{substrate}/V_{surface} \geq 2.5$. In this case the particle motion will be retrograde, prograde, purely vertical or purely horizontal, depending on the wave period. At periods where the motion is purely horizontal the horizontal ground amplification will be infinite.

Thus it can be seen that the combinations of horizontal and vertical motion which may be stimulated by a compound surface wave at a site with other than simple geology will be far from simple. It can also be seen that the surface vertical motion will not, in general, be characteristic of the motion in the underlying substrate.

Amplification spectra

In general the ground motion amplification exhibited at a site varies with the frequency content of the wave that is producing the motion; or, equivalently, with the period content of the wave. For this reason the ground amplification for a site is usually characterized graphically by means of an amplification *spectrum*. In amplification spectra the measure of amplification is displayed on the vertical axis, and the frequency or period is displayed on the horizontal axis. It is common to use logarithmic scales for both axes.

The measure of gain or amplification may vary over a wide range and the use of a logarithmic scale allows a common vertical axis scale to be used thus facilitating visual comparison of a full set of graphs without the need to change scales between individual graphs.

In cases where a wide frequency range extending over several orders of magnitude is being displayed, or if the period is being used instead of frequency, it is convenient to make use of the regular non-linearity of a logarithmic scale to give a neat and uncluttered appearance. In cases where the frequency range is restricted to one or two orders of magnitude a logarithmic scale adds no real benefit. In those cases a linear scale is more appropriate. Throughout the remainder of this thesis ground amplification spectra will, in general, be displayed using a linear frequency scale.

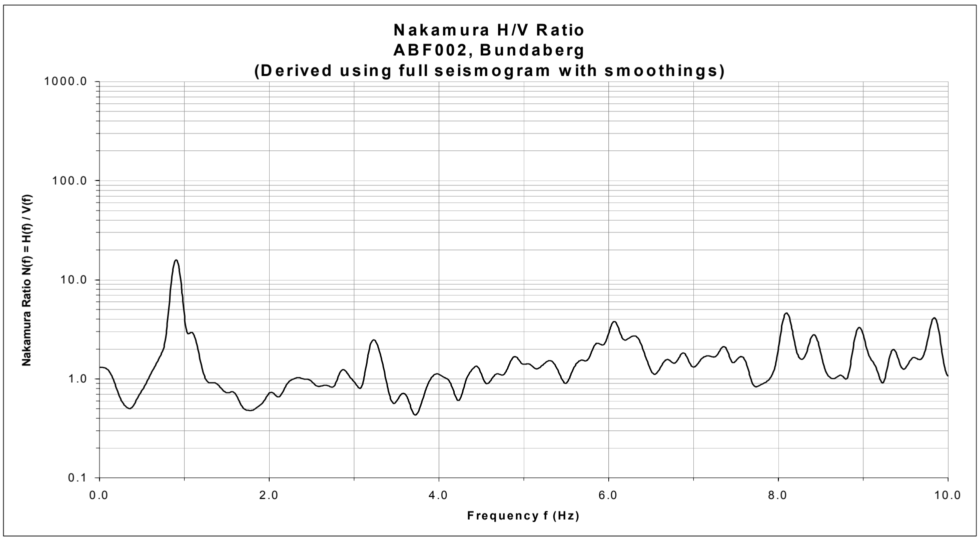

Figure 6.2 **A typical amplification versus frequency spectrum.**

Figures 6.2 and 6.3 are examples of frequency and period amplification spectra for the same site, presented here to demonstrate typical spectra presentation formats. The measure of amplification used in the spectra was derived using a horizontal to vertical ratio method (Nakamura, 1989). The spectra display a prominent amplification peak at 0.92 Hz (1.08 s). This peak may be an amplification resonance peak, or it may be caused by a periodic seismic energy source. It should be noted that, although Figure 6.2 seems to indicate that useful gains can be obtained down to 0Hz. This perception is an artifact of the software application used to produce the graph and is not obtainable in practice. The useful lower frequency depends on the characteristics of the instrumentation used to obtain the source data.

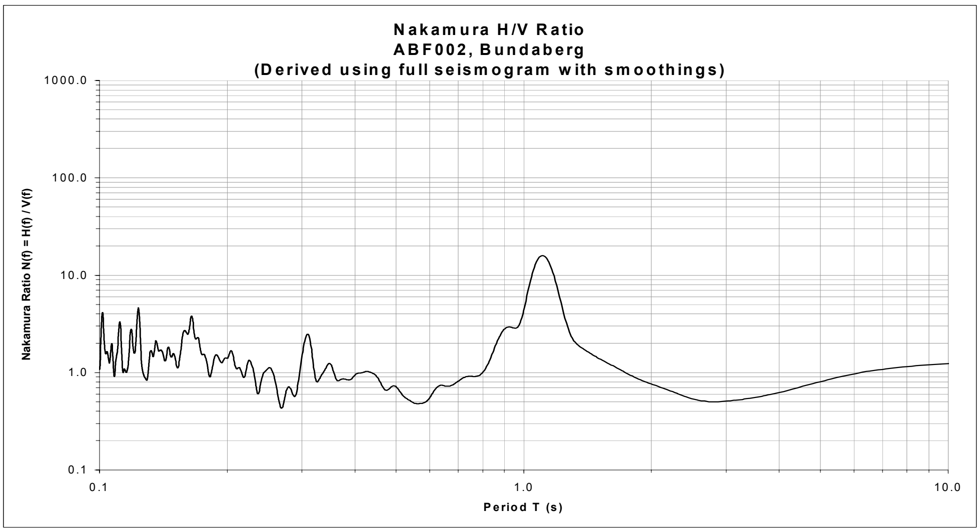

Figure 6.3 **A typical amplification versus period spectrum.**

Other causes of ground movement amplification

Thus far only the effect of anisotropic ground motion caused by the passage of surface waves has been mentioned. Little has been said of possible additional effects on ground motion caused by such things as superposition of waves of different types, period and amplitude, variations in surface geology, surface and basement topography, and confinement of seismic energy due to reflection of waves at high contrast impedance boundaries. It is obvious from the heuristic consideration of simple surface waves that a general treatment of ground motion theory is beyond the scope of this thesis.

In practice, however, there are techniques available which allow the effect of ground motion to be measured in situ. These techniques obviate the need for theoretical knowledge of the causative mechanisms, to a great extent, and permit the process of characterisation and quantification to proceed in an applied, pragmatic manner. In applying these techniques it is often more appropriate to refer to the overall *reactive response* of the site of interest to seismic waves, rather than the rather simplistic ground amplification. Consequently, in this thesis, the term *site response* will be used to refer to the reaction of a site to the application of seismic energy, including the contributions of ground amplification and other effects.

CHAPTER 7 SPECTRAL RATIO METHODS OF DETERMINING SITE RESPONSE

Introduction

There are two broad categories of methods used in characterising the response of a particular site to incident seismic energy. In one method basic physical theory and knowledge of the site conditions (geology, topography and boundary conditions) are used to create a mathematical model of the site. The solution(s) to these mathematical models require extensive computational capability and expert knowledge. The mathematical model is typically encoded as a computer program and solved by numerical methods. Models of one, two and three dimensions have been produced (c.f. Coutel, 1998). This is probably the more useful of the two categories in that the site response is dynamically depicted by means of animated video displays, and, once encoded, the site response parameters and energy source parameters can be easily manipulated to study variations within the model. Two and three-dimensional models, in particular, are heavily dependent on the computational power of digital computers, require extensive specialist knowledge in the practitioner, and depend on detailed physical knowledge of the site of interest. Such detailed knowledge is rarely available, so assumptions have to be made which reduce confidence in the modelled results. The formulation and solution of the model is time consuming and expensive.

The other category of site response characterisation methods relies on direct measurement of ground movement amplification within the area of interest. The ground movement at a matrix of sites within the area is measured and the results are used to produce a static map depicting the relative risk present at adjacent sites. Two methods that fit into this category will be briefly described.

Two site spectral ratio method

This method relies on the presence, within the area of interest, of a reference site that has the response characteristics of basement bedrock. Such a reference site may be obtained by boring a hole down to the bedrock and installing an instrument at the bottom of the hole; or, preferably, by locating an instrument on a nearby outcrop of solid basement rock. The quality of results obtained using this method is dependent on the characteristics of the reference site and considerable care must be taken in choosing a suitable reference site (Steidl et al, 1996).

During the measurement period two instruments are deployed, one at the site of interest and one at the reference site. The instruments are triggered simultaneously, or within an overlapping time period, to measure ground movement at both sites stimulated by a common seismic energy source. The horizontal time series data from each site is converted by Fourier transform techniques to an amplitude or power spectrum and the ratio of the site spectrum to the reference spectrum is produced. The site to reference ratio is a direct measure of the ground movement amplification at the site of interest.

If the reference site is the actual basement bedrock under the measurement site then the ratio is equivalent to the basement to surface layer, frequency dependent horizontal transfer function $T_{BS}(f)$.

$$T_{BS}(f) = H_S(f) \,/\, H_B(f) \qquad \ldots \qquad \text{Eq. 7.1}$$

This method has been employed using various seismic energy sources; including earthquake S waves (c.f., Chavez-Garcia et al, 1997; Coutel & Mora 1997; Wen et al, 1995a; Wen et al, 1995b), P waves (c.f. Lachet et al, 1996), earthquake coda (c.f. Field, 1996), ambient seismic noise (c.f. Seht & Wohlenberg, 1999; Konno & Ohmachi, 1998; Coutel & Mora 1997; Lachet et al, 1996; Chavez-Garcia et al, 1996; McCue & Boreham, 1996b; Field, 1996; Ferritto, 1996; Seekins et al, 1996; Clithero & Taber, 1995; Field & Jacob, 1995; Somerville et al, 1993; Kagami et al, 1986) and high explosive blasts (c.f. Malagnini et al, 1996).

There has been considerable interest in using this method employing ambient seismic noise as the source. This technique has the obvious advantage that the instrumentation does not need to be put in place over long periods to observe actual earthquake events. All that is needed is for the reference instrument to be deployed and the site instrument to be transported from station to station in order to collect matching pairs of ambient noise recordings. If numerous sites are to be occupied, however, there is still considerable time involved. There is also the logistic difficulty of simultaneous triggering of the instruments to be considered.

The method has been used extensively in site response characterisation where relatively few sites are occupied. It has been used in a limited capacity for microzonation where relatively few sites have been used (c.f. Lachet et al, 1996; McCue & Boreham, 1996b; Clithero & Taber, 1995; Sommerville et al, 1993; Darragh & Shakal, 1991); but has had limited application in large-scale high-resolution microzonation except for one notable exception in Perth, Western Australia (Gaull et al, 1995). In this latter study six instruments were used simultaneously; five at basin stations, and one at the reference site. The five basin stations were deployed to take late night simultaneous readings over two nights. Over 100 sites were occupied using 3 km grid spacing, implying that the data collection would have taken more than 40 days.

The method has the disadvantage that the presence of noise generated by localised social movement (cars, trucks, trains pedestrians etc.), which does not equally effect the site and reference instrument, tends to produce results which are not characteristic of the site of interest, but are characteristic of the energy source. Consequently the periods during which the technique can be employed are limited to those times of the day when social noise is at a minimum (usually in the hours between midnight and dawn). It also has the disadvantage that it cannot be employed in areas where a suitable reference site is not available.

Single site spectral ratio method

It was stated in the previous chapter of this thesis that if it could be shown that the vertical ground motion at a site of interest was characteristic of the basement bedrock motion at that site, then the horizontal to vertical ground motion ratio corresponded to the site/reference measure of horizontal ground motion amplification. The single site spectral ratio method of characterising site response relies on this condition. In this method the simultaneous horizontal and vertical ground motion is measured using a single multi-axis instrument. The amplitude or power spectrum of the horizontal and the vertical data are determined using standard Fourier transform techniques, and the ratio of the horizontal to vertical spectra is produced. This method is generally referred to as the Horizontal-to-Vertical Spectrum Ratio (HVSR) method.

The Nakamura method

In 1989 Yutaka Nakamura used the single site method to study responses at socially noisy sites, using ambient seismic noise sources, and found that the results resembled the transfer functions for horizontal motion in the surface layers. Nakamura showed that, for a relatively wide frequency range, localised noise sources consisting of mainly Rayleigh waves were cancelled out during the horizontal to vertical ratio process. His reasoning was as follows.

The basement to surface layer, frequency dependent horizontal transfer function $T_{BS}(f)$ is defined as:

$$T_{BS}(f) = H_S(f) / H_B(f) \qquad \ldots \qquad \text{Eq. 7.2 (Eq 7.1 repeated for convenience)}$$

Where $H_S(f)$ is the horizontal spectrum at the surface layer and $H_B(f)$ is the horizontal spectrum at the basement layer.

It was noted that $H_S(f)$ is readily affected by locally generated social noise, which mainly consists of Rayleigh waves. It was also noted that the vertical spectrum at the surface layer $V_S(f)$ should include the local Raleigh wave contribution, but the basement vertical spectrum $V_B(f)$ should not.

Assuming that the surface layer does not amplify the vertical ground motion, the effect of the local Rayleigh waves on the incident microtremor motion, within the surface layer, can be represented as:

$$\varepsilon_S(f) = V_S(f) / V_B(f) \qquad \ldots \qquad \text{Eq 7.3}$$

Where there is a Rayleigh wave contribution $\varepsilon_S(f)$ will be greater than unity, and this will converge to unity as the contribution of the local Rayleigh wave decreases; therefore $\varepsilon_S(f)$ is greater than or equal to unity at all frequencies.

Assuming that the effect of the local Rayleigh wave on the horizontal and vertical incident motion is equal (i.e. its ellipticity is unity), a modified surface layer horizontal transfer function $T_{BSM}(f)$ may be defined as:

$$T_{BSM}(f) = T_{BS}(f) / \varepsilon_S(f) \qquad \ldots \qquad \text{Eq 7.4}$$

We also define the following ratios:

$$R_S(f) = H_S(f) / V_S(f) \qquad \ldots \qquad \text{Eq 7.5}$$

$$R_B(f) = H_B(f) / V_B(f) \qquad \ldots \qquad \text{Eq 7.6}$$

Which allows $T_{BSM}(f)$ to be expressed as:

$$T_{BSM}(f) = R_S(f) / R_B(f) \qquad \ldots \qquad \text{Eq 7.7}$$

Nakamura was able to show that the 24 hour averaged horizontal to vertical basement ratio $R_B(f)$, for three different measurement sites, was approximately unity over a frequency range from 0.1 Hz to 20 Hz.

Under the condition that $R_B(f) \approx 1$ (i.e. the ellipticity of the incident waves in the basement material is approximately unity), Eq 7.7 reduces to

$$R_N(f) = T_{BSM}(f) \approx R_S(f) = H_S(f) / V_S(f) \qquad \ldots \qquad \text{Eq 7.8}$$

Where $R_N(f)$ is referred to as the Nakamura spectral ratio.

It can be seen that the Nakamura spectral ratio is the basement to surface layer, frequency dependent horizontal transfer function $T_{BS}(f)$, modified to allow for the possible presence of a Rayleigh wave generated locally within the surface layer. Under the assumption that the ellipticity of the local Rayleigh wave is unity, the effect of the local Rayleigh wave is cancelled out of the modified horizontal transfer function.

In reality ideal cancellation does not occur and the modified horizontal transfer function does not reproduce the original horizontal transfer function faithfully. Spectra produced using the Nakamura ratio, are similar but demonstrably different from those produced using the horizontal transfer function. This may be due to several factors some of which are suggested below.

- The locally generated noise may not be purely Rayleigh waves.
- The ellipticity of the local noise waves in the surface layer may not be unity.
- The ellipticity of the incident waves in the basement layer may not be (indeed probably would not be) unity.
- The ellipticity of the local noise and the incident waves may vary over time and space depending on the nature of the local noise and the incident waves.

The Nakamura method is a special application of the HVSR method. It has the particular advantage of providing an efficient and cheap means of collecting data from numerous sites, within a short space of time, at any time during the day. Support for the assumption that $R_B(f) \approx 1$, or at least that the average over the frequency range of interest is approximately unity, has been reported by later researchers (c.f. Somerville et al, 1993; Lermo & Chavez-Garcia, 1993 & 1994).

Over the past decade the Nakamura method has been used in numerous site response characterisation and microzonation studies (c.f. Clithero & Taber, 1995; Lachet et al, 1996; Milana et al, 1996; Seekins, 1996; Field, 1996; Konno & Ohmachi, 1998; Jones et al, 1998; Cuthbertson et al, 1998; Michael-Leiba & Jensen, c.1999).

Several studies have been carried out to compare the results of the Nakamura method with those obtained by other methods, including the general HVSR and reference site methods. Some studies have reported adverse findings (c.f. Malagnini et al, 1996), while others indicate that the Nakamura method is valid within certain constraints (c.f. Dimitriu et al, 1998; Chavez-Garcia et al, 1997; Chavez-Garcia et al, 1996; Lachet et al, 1996; Coutel & Mora, 1997; Field, 1996; Seekins et al, 1996, Dravinski et al, 1996; Theodulidis et al, 1996; Clithero & Taber, 1995; Field & Jacob, 1995; Lermo & Chavez-Garcia, 1994 and 1993; Field & Jacob, 1993). It is generally recognised that the Nakamura method adequately identifies the fundamental resonance peak of a site within reasonable error bounds, but is incapable of identifying higher orders of resonance. Similarly, whilst the spectra produced using the method can be used to quantify relative hazard between adjacent sites, they are incapable of indicating the absolute ground motion amplification of a given site.

Recent investigations have employed the Nakamura method to successfully determine the thickness of soft sediments (Seht & Wohlenberg, 1999). This indicates that a comparison of actual sedimentary depths with depths determined from Nakamura spectra can be used to validate the quality of the spectra.

Elsewhere in this thesis the author reports the use of the Nakamura method to obtain site response spectra at a number of sites in the Bundaberg City area. These spectra were used to conduct a microzonation of the area concerned. A comparison of sedimentary depths calculated from the fundamental resonance peaks of the spectra, against sedimentary depths measures in test boreholes, indicated a positive correlation; thus both confirming the ability to estimate sedimentary depths from Nakamura spectra, and supporting the use of the spectra for microzonation purposes.

CHAPTER 8 A METHODOLOGY FOR DERIVING NAKAMURA SPECTRA FROM MICROSEISMOGRAMS

Introduction

As was explained in the previous chapter, a Nakamura spectrum is derived from the ratio of the horizontal and vertical ground movement spectra obtained by Fourier transform conversion of time series data measured at the site of interest. Expressed in that simplistic form it would then not appear to be difficult to do. However, it is not all that straight forward. There are a number of considerations that need to be addressed in order to produce clear and meaningful spectral ratios from the raw field data.

The field data tend to contain a good deal of extraneous noise superimposed on the underlying information. Filtering and smoothing techniques need to be applied in order to isolate the wanted information from the unwanted noise.

The horizontal data are collected as two orthogonal data sets from the tri-axial seismic sensor. How the two horizontal data sets are to be combined has to be decided. Should they be combined in the time domain or in the frequency domain? Should they be combined geometrically or arithmetically?

There are a variety of ways that the frequency domain data can be derived from the time domain data. The time domain data set can be treated as a single data set or subdivided into a number of subsets. The latter method may be statistically more desirable, but it takes more computation, and does it add any additional worth to the results?

These and other factors need to be considered in formulating a methodical approach to data collection and processing.

Length of data collection

Although Yutaka Nakamura (1989) continuously monitored each site for up to 30 hours, only data sets of 2048 points, or about 20 seconds of data were used for analysis purposes. Kagami et al (1986) monitored each site for 15 minutes, but only sections of 1024 datum points were used for analysis. In carrying out their microtremor study of Newcastle, Somerville et al (1993) took six series of 33-second readings at 125 samples per second at each site. From these recordings subsets of 2000 data were used for analysis.

For data collection at sites used in microzonation of Bundaberg city the author chose to record for 2 to 2.5 minutes at a sampling rate of 100 samples per second. This provided a total of from 12000 to 15000 data points from each site for analysis purposes.

Size and conditioning of analysis data set

The size and numbers of the data sets used by past investigators vary considerably. Similarly, the conditioning techniques sometimes applied to the time series data prior to performing the Fourier transform on it varied considerably.

Michael Winter, a post-graduate student studying at the Queensland University Advanced Centre for Earthquake Studies (QUAKES), has made available to me the C source code for numerous analysis routines that he used over an approximate three year period to perform single and double site spectral analysis of field data collected for microzonation within the greater Brisbane metropolitan area. He has employed a variety of time series data conditioning techniques including

- cosine tapering,
- linear tapering,
- overlapping of data windows,
- demeaning and detrending,
- high and low pass filtering, and
- zero filling of incomplete data sets.

From comments included in his source code and from personal conversations I have had with him, Michael informed me that, in his experience, preconditioning of the time series data has little or no effect on the appearance of the resulting spectral ratios. This has also been my personal experience. As long as the size of the data set is sufficient, preconditioning the time series data by means of any of the above techniques seems to produce no appreciable difference to the resultant spectral ratios.

The use of multiple windows, from the one time series data set, allows the calculation of the mean and standard deviation for further analysis purposes and to ensure the reproducibility of the data. A suitable minimum size for the time series data set is considered to be 1024. It would seem that, for microzonation purposes, a single raw data window of sufficient size *may* be suitable; however, it must be pointed out that the results obtained from a single data window will not be reproducible, and the use of multiple time series windows is a superior method.

Smoothing

Conditioning techniques applied to the frequency spectra after performing the Fourier transformation produces by far the most noticeable visual effect on the appearance of spectral ratios displayed as graphs. The spectra obtained from the raw time series data contain considerable extraneous and apparently random noise, superimposed on the underlying spectral information.

Figure 8.1 shows an unconditioned Nakamura spectral ratio obtained from a single data set of size about 15000 with zero fill to make it up to 16384. In Figure 8.1 the shape of the underlying spectral line is masked by the presence of superimposed extraneous fluctuations.

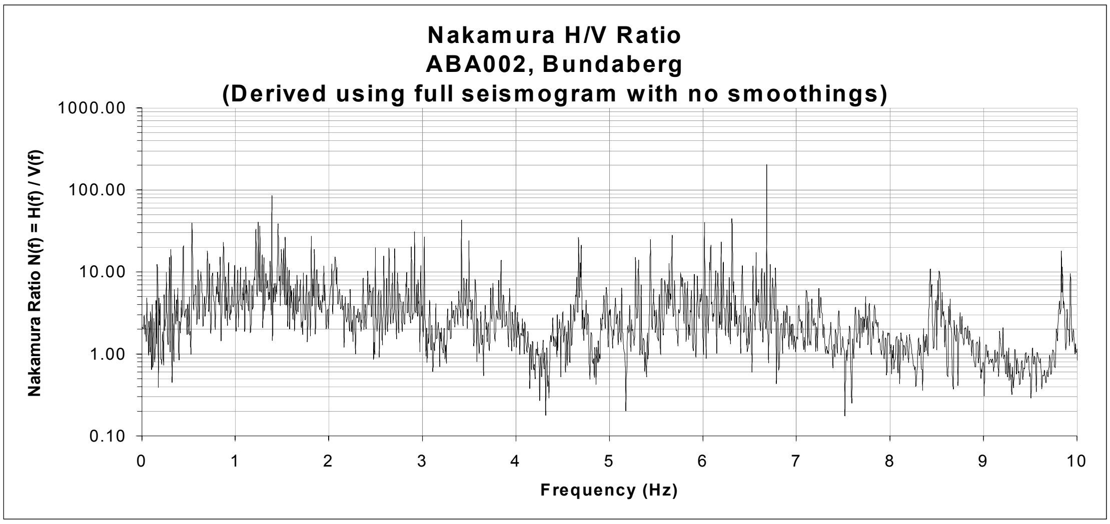

Figure 8.1 **<u>Unconditioned Nakamura spectral ratio.</u>**

These unwanted fluctuations could be removed using a simple moving average technique, sometimes referred to as a *boxcar* smoothing filter. The technique gets its name from the analogy to a box containing the sub-set of the data being averaged, moving over the data set from one end to the other. At either end of the data set the target datum in the sub-set is duplicated to fill up the boxcar.

It should be noted that, although Figure 8.1, and other figures in this chapter, seems to indicate that useful gains can be obtained down to 0Hz. This perception is an artifact of the software application used to produce the graph and is not obtainable in practice. The useful lower frequency depends on the characteristics of the instrumentation used to obtain the source data.

```
// Traverse half the boxcar length either side of the ith datum.
for(j = i - hw; j < i + hw + 1; ++j)
{
   if( j < 1 || j > length -1)
   {
      sum += temp[i]; // Accumulate the centre datum.
   }
   else
   {
      sum += temp[j]; // Accumulate the actual datum.
   }
}
++num; // Count the number of data in the boxcar.
} // End of boxcar traversal.
// Replace the datum with the mean of the boxcar set.
data[i] = sum / (float)num;
```

(Original source code was supplied by Michael Winter and modified by the author.)

Figure 8.2 <u>Boxcar filter source code fragment</u>

The C++ source code fragment provided in Figure 8.2 indicates the computational algorithm used to implement the boxcar filter technique. The width of the boxcar (i.e. the number of data used for the moving average) can be varied to suit, and the filter can be applied to the same data set as many times as required.

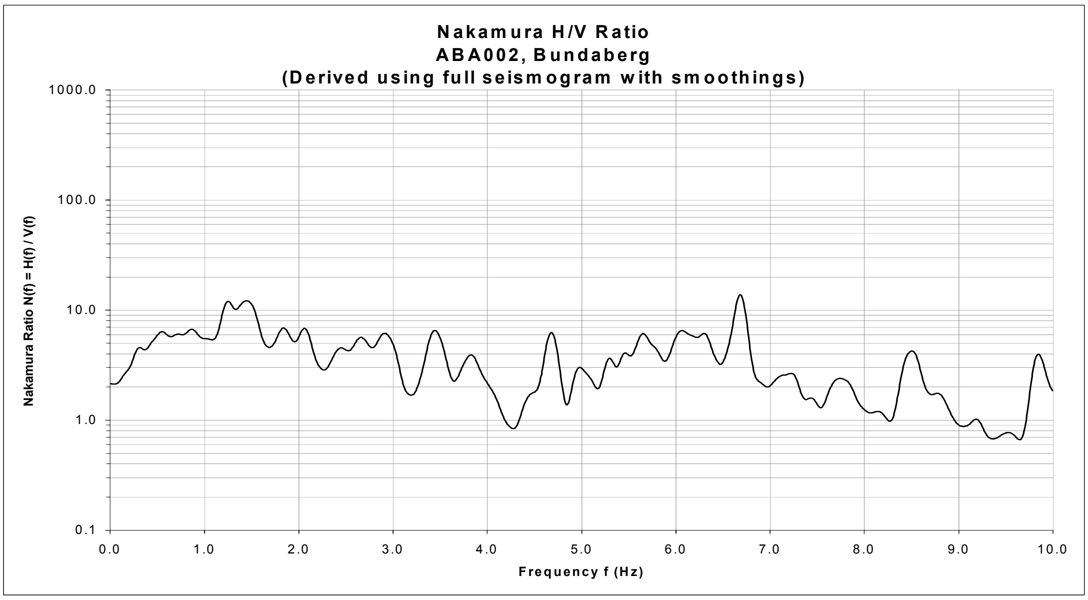

Figure 8.3 **Smoothed Nakamura spectral ratio.**

The Nakamura spectral ratio shown in Figure 8.3 was obtained by conditioning the spectral data displayed in Figure 8.1 by applying a boxcar smoothing filter of width 9 using 10 passes.

It should be noted that, in relation to the method later used to analyse the spectral ratios for microzonation purposes, it does not matter whether the smoothing is applied or not. This is because the microzonation analysis that will be used performs averaging over chosen frequency ranges of the spectrum (See Figure 9.3). The average of the smoothed spectrum over any chosen frequency range will be the same as the average of the raw spectrum over the same frequency range. Consequently the application of smoothing is performed for cosmetic purposes when displaying the spectra as graphs.

Boxcar smoothing software

A console based DOS application program has been written in C++ by the author to assist in the microzonation analysis of site response spectra. The application is named SMOOTH. DOS files containing the C++ source code and the DOS executable file are contained on the CD ROM that accompanies this thesis.

The SMOOTH application is designed to execute from a DOS command line. It will process any number of TAB delimited text files containing site response spectral information in the format shown in Figure 8.4.

```
<frequency value1><TAB><gain value1><EOL>
<frequency value2><TAB><gain value2><EOL>
<frequency value3><TAB><gain value3><EOL>
.
.
.
<frequency valueN><TAB><gain valueN><EOL>
<EOF>
```

Figure 8.4 **TAB delimited spectra text file format suitable for the SMOOTH application.**

The syntax for executing the SMOOTH application is as shown in Figure 8.5. Before being invoked the SMOOTH executable file must be present in the current default directory, or the path to its subdirectory must be added to the DOS PATH environmental string. For instance, to smooth a set of site response spectra with the file names of the form `AAA001.NSR, AAA002.NSR, … , ZZZ999.NSR`, using a boxcar half width of 4 data with 10 passes, storing the results in files with extensions .RSM, the following command would be issued.

SMOOTH –w 4 –n 10 –r 0 RSM *.NSR

Upon successful completion the SMOOTH application will create a set of TAB delimited text files, named as requested, in the current default directory. The contents of those files will be in the same format as the files from which the data was sourced.

```
Syntax: smooth [[-?] [-w <n>] [-n <m>] [-r <b> [<e>]]] <filePattern>
-?     Display this usage information.

-w <n> Use <n> number of data in the boxcar half-width.
   <n> Must be an integer value. (Default 5)

-n <m> Apply the smoothing <m> times.
   <m> Must be an integer value. (Default 1)

-r 1   Reuse the source file as the target file.
       Default is -r 0 mmm

-r 0 <e> Do not reuse the source file as the target file.
     <e> Is the three character file extension to use for
         the target file. The target file will have the
         same filename as the source.
         Default: Target file has same filename as the source
                  with the extension "mmm"
         Warning: If you choose to override the default
                  setting with the -r 0 switch you MUST
                  also provide the file extension.

<filePattern> A valid DOS path and file pattern in 8.3 format.
              Wildcards are permitted
```

Figure 8.5 **Syntax for the SMOOTH application.**

Multiple Windowing

Figures 8.6 and 8.7 each show comparisons of three ground motion spectra calculated from single window time series data sets obtained from the same sites at different times. Figure 8.6 shows spectra obtained from the site designated AAB001 during three separate data collection episodes, designated BBGA, BBGC and BBGD. Figure 8.7 shows spectra obtained from a different site designated ABA001 during three separate data collection episodes, designated BBGB, BBGC and BBGD.

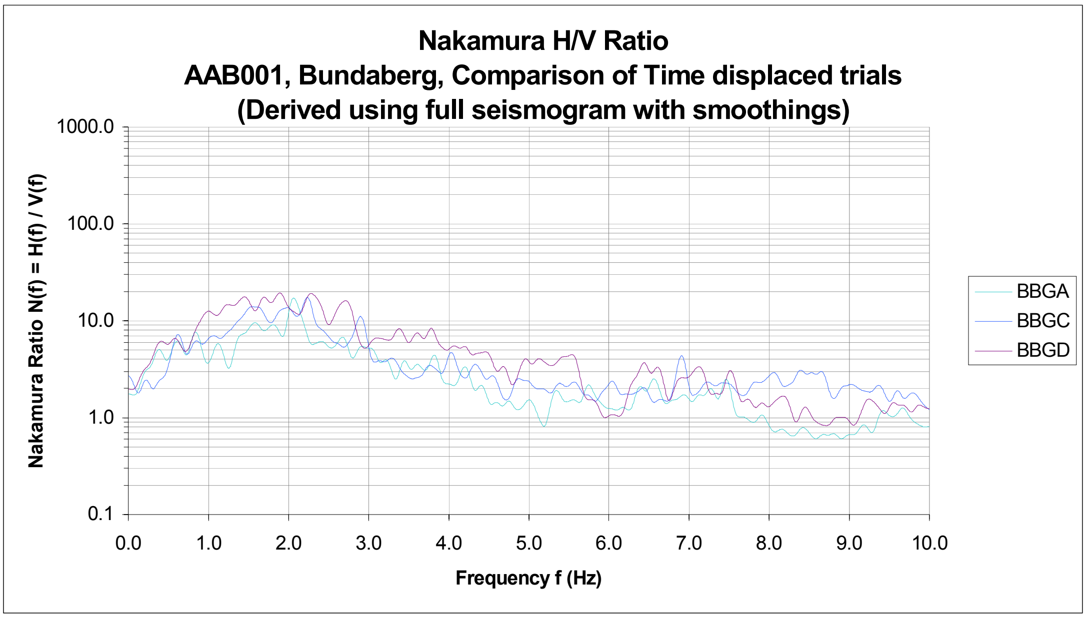

Figure 8.6 <u>**Spectra for site AAB001 derived from time-displaced data sets.**</u>

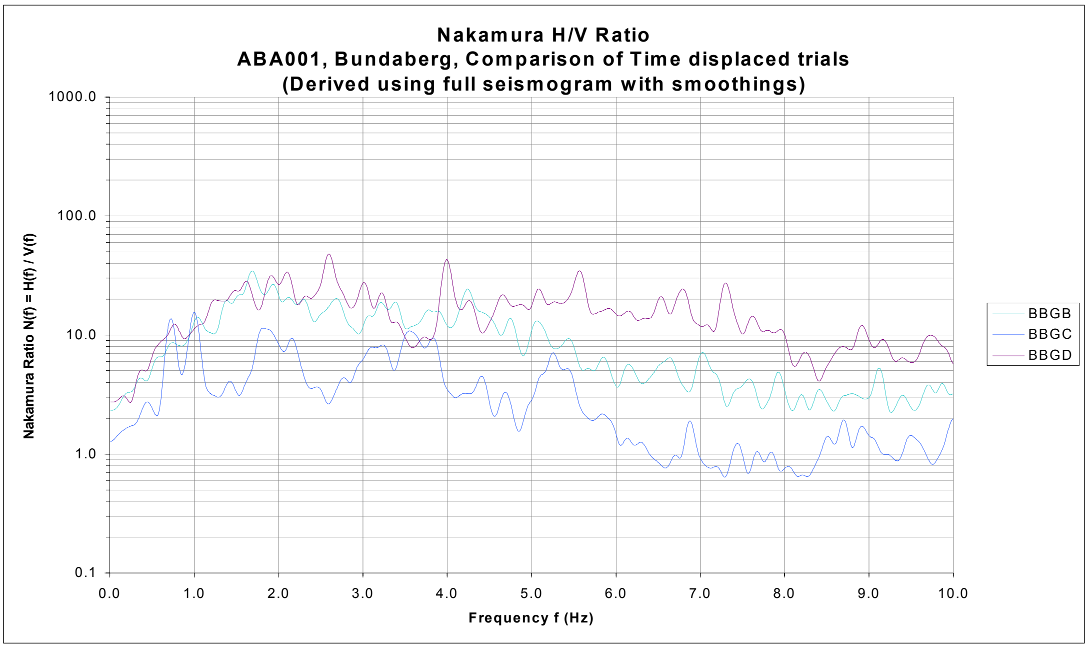

Figure 8.7 <u>**Spectra for site ABA001 derived from time-displaced data sets.**</u>

Inspection of the spectra in the above figures reveals that, whilst the various spectra obtained for the same site at different times are *similar*, they contain an obvious degree of difference, due to the natural variability of the microtremor seismic energy sources over time. As a consequence of the variability in the individual spectra it would be undesirable to use any one spectrum for microzonation purposes. The results of that process would, in general, be irreproducible by analysis of data collected at future times and could not be used to monitor for possible changes in the microzonation results over time.

A more statistically valid method would be to combine several spectra obtained at different times by averaging the data points and calculating the standard deviation. This could be done either by collecting time series data by means of several field trips over an extended period of time, or by collecting a single time series reading of sufficient length to provide a number of mutually exclusive contiguous data sets (data windows) of size 1024.

Both of the above methods are equivalent. The only difference is the time lag between the sequential windows of contiguous data. In the former case the time difference may be days or months. In the latter case the time difference is seconds or fractions of a second.

Figure 8.8 depicts a ground amplification spectrum derived by using multiple data windows extracted from a single seismogram. The original data set used to derive the spectrum in Figure 8.8 is the same data set used to derive the spectrum labelled BBGB in Figure 8.7. However, whilst the individual spectra in Figure 8.7 are, in general, irreproducible from data obtained at different times, the spectrum in Figure 8.8 can be reproduced, within the calculated statistical bounds, from time series data collected at the site at any time.

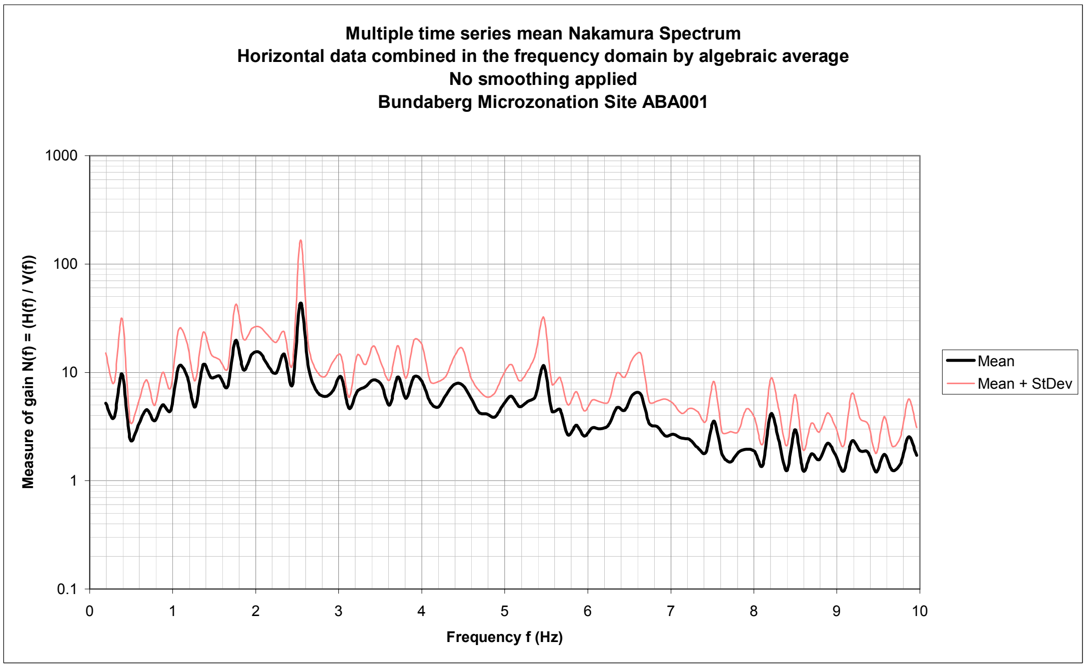

Figure 8.8 **Spectrum derived from multiple data windows.**

Multiple Windowing Software

A MicroSoft® Windows® based DOS application program has been written in C++ by the author to assist in ground amplification spectral analysis of Kelunji seismograms. The application is named MNAKRAT. DOS files containing the C++ source code and the MicroSoft® Windows® executable file are contained on the CD ROM that accompanies this thesis. Sections of the code used to calculate the Fourier Transformations of the time series data were based on numerical routines described by Press et al (1992). Parts of the code used to extract the time series data from Kelunji files use definitions of the Kelunji data storage format supplied by Vaughan Wesson (Personal communications, 1998) and C code made available by Mike Winter (Personal communications, 2000) suggested some coding ideas to the author.

The MNAKRAT application is designed to execute within the MicroSoft® Windows® environment. It will process any number of Kelunji Classic seismograms. Before being invoked the MNAKRAT executable file must be present in the current default directory where the seismograms are all stored, or the path to its subdirectory must be added to the DOS PATH environmental string.

Upon successful completion the MNAKRAT application will create a series of TAB delimited text files with the same file name as the Kelunji seismograms and the extension .NSR in the current default directory. The contents of those files will be in the format shown in Figure 8.9.

```
<SiteName><EOL>
<FrequencyValue1><TAB><AverageGain1><TAB><StdDev1><EOL>
<FrequencyValue2><TAB><AverageGain2><TAB><StdDev2><EOL>
<FrequencyValue3><TAB><AverageGain3><TAB><StdDev3><EOL>
.
.
.
<FrequencyValueN><TAB><AverageGainN><TAB><StdDevN><EOL>
<EOF>
```

Figure 8.9 **TAB delimited microzonation data file.**

The frequency values will be in the range from 0.1 Hz to 10 Hz.

When the application is executed the user will be prompted as to whether the horizontal data is to be combined in the time domain or the frequency domain, and whether the combination is to be carried out using a geometric average or an arithmetic average.

Combining the horizontal data sets

There are a number of different ways that the horizontal data sets can be combined. They can be combined in the time domain or the frequency domain, and in either case a number of combinational algorithms can be used. The data could be averaged, either by simple arithmetic average, by geometric average, by using the square root of the mean of the squared values (i.e. the RMS or Root Mean Squared value) or by some other more obscure method.

The following series of four figures shows ground amplification spectra obtained from the same time series data set, and with the horizontal components combined by various methods.

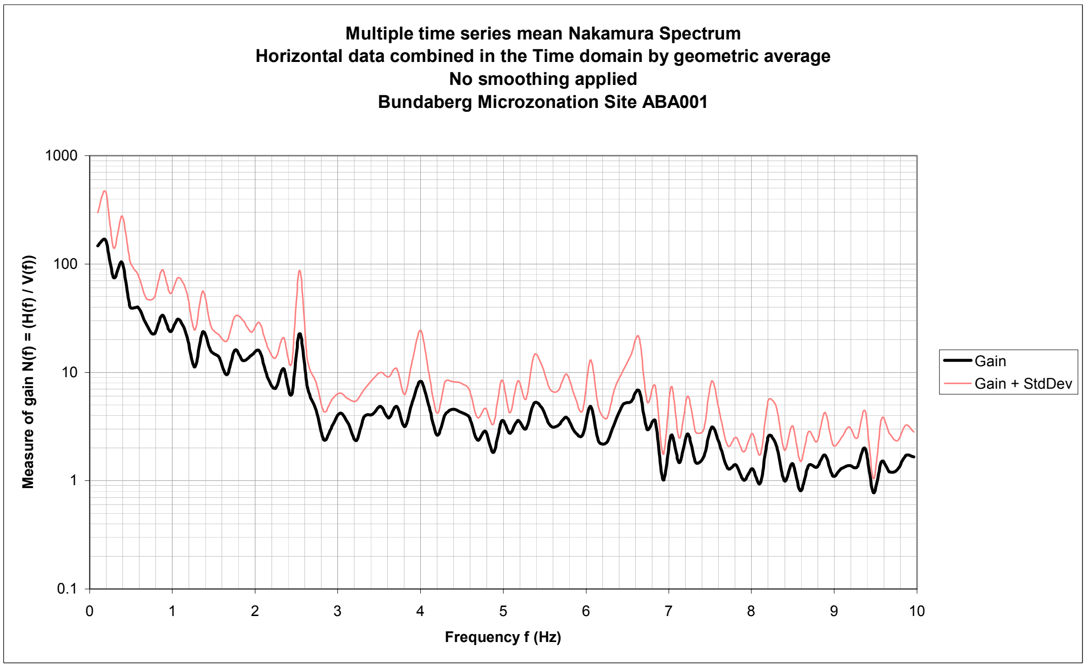

Figure 8.10 **Horizontal combined in Time Domain by Geometric mean**

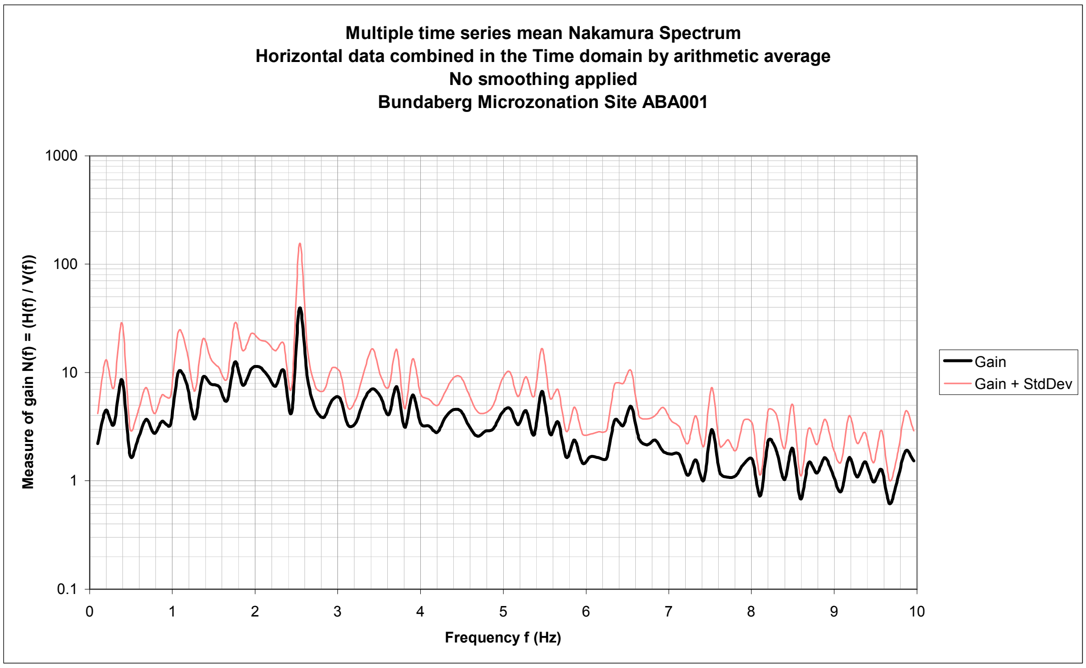

Figure 8.11 **Horizontal combined in Time Domain by Arithmetic mean**

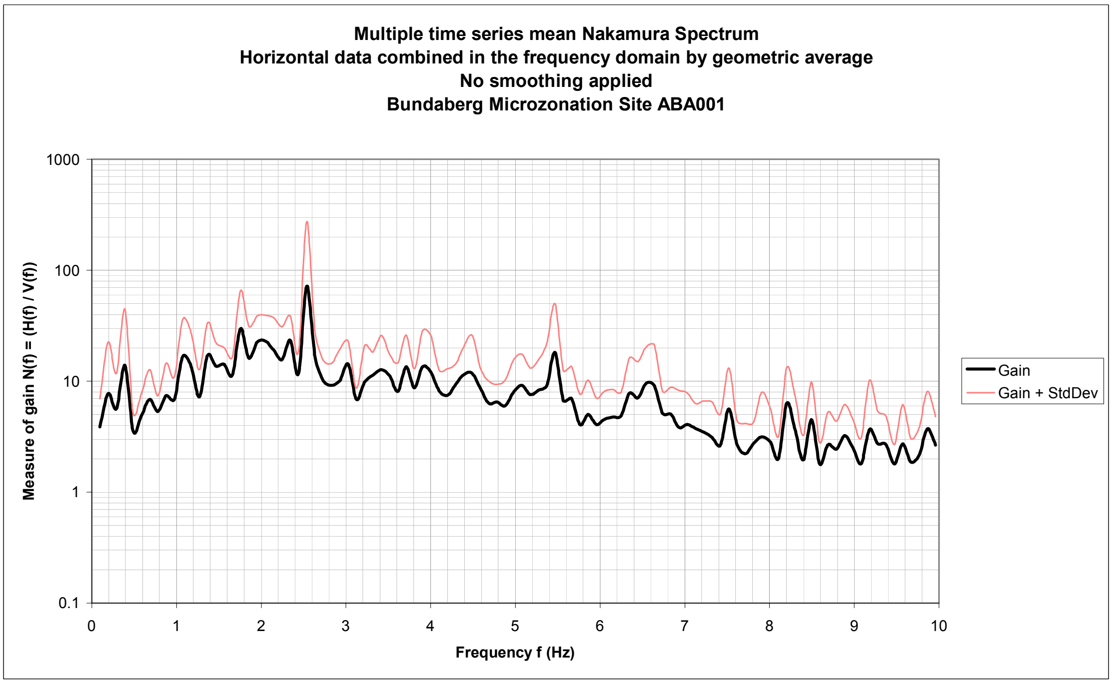

Figure 8.12 **Horizontal combined in Frequency Domain by Geometric mean**

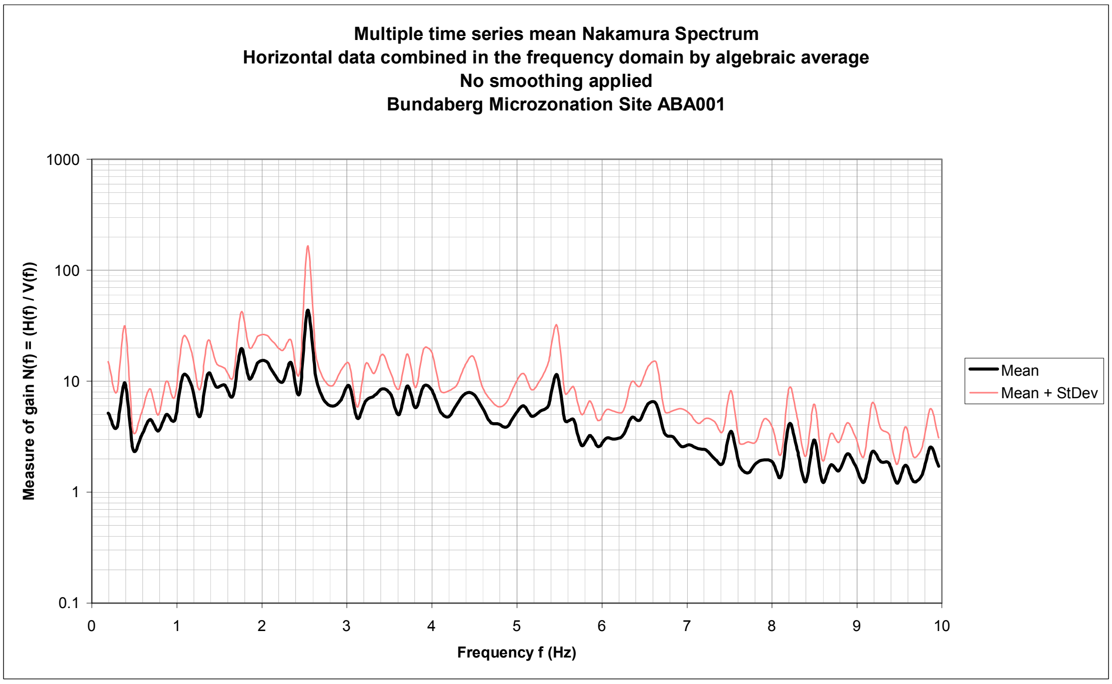

Figure 8.13 **Horizontal combined in Frequency Domain by Arithmetic mean**

Inspection of Figure 8.10, and comparison with Figures 8.11, 12 and 13, reveals that geometric combination of the horizontal components in the time domain produces a spectrum that is substantially different from the other three methods. This is because, in the time domain, the geometric averaging process is equivalent to vector addition. The horizontal time series data sets are derived from orthogonal orientated sensors. If the motion was being stimulated by a point energy source, then the horizontal signals could be regarded as vector signals and used to determine the azimuth of the source. However, the microtremor sources that produce the ground motion are diffused and variable – tending to be random in nature. Therefore the horizontal signals cannot be interpreted as a primary indication of the vector direction from which the motional force is coming. The geometric averaging process is equivalent to vector addition of the two horizontal signals. Consequently, geometric averaging is inappropriate for combining the horizontal components.

Inspection of Figures 8.11, 12 and 13 shows them to be very similar in appearance. Whilst there are some subtle differences between Figure 8.11 and the other two, those differences are fairly minor. Figure 8.12 is identical in form to Figure 8.13 except for a vertical displacement of the trace. This is because the geometric average is accentuating the horizontal motion in comparison to the arithmetic average.

For the purposes of the microzonation analysis carried out in this thesis it was decided to combine the horizontal data in the frequency domain using an arithmetic average.

CHAPTER 9 A MICROZONATION METHODOLOGY

Introduction

In 1976 Esteva (Lomnitz & Rosenbleuth, 1976a, p 221) stated that, “Most of the efforts of microzoning has been devoted to study of the influences of local soil stratigraphy on the intensity and frequency content of earthquakes”. He also comments, in the same article, that the analytical models being used at his time of writing produced results that “ … ranged from satisfactory to poor … “ and that the “ … rational formulation of microzoning for seismic risk is still in its infancy … “.

Studying the local soil stratification with a view to quantifying the local effect of earthquake intensity would appear to be a tedious and time-intensive task. The risk of damage to surface structures is, to a large extent, determined by the degree and nature of surface ground movement within the meizoseismal region, and the physical properties of the structures themselves. Thus a more direct approach to microzonation for seismic risk at a site would be to characterise the ground movement response to seismic energy by direct measurement and compare that response with the shaking resonance of structures that may be built on that site.

The method to be used for microzonation in this thesis will be described below.

Macrozonation for engineering purposes

National structural engineering codes (c.f. SAA, 1979; SAA, 1993a & b) provide information that can be used by engineers to design structures to minimise potential damage from natural occurrences such as earthquakes. The codes provide two basic types of information:

- Locational information that allows the engineer to choose those sites that are more conducive to minimisation of damaging forces and avoid those sites that present a greater hazard.
- Loading information that allows the engineer to employ structural design techniques that are appropriate for the hazard expected at the chosen site.

The national codes provide locational information on a broad regional basis. They do not provide information related to the microstructure of individual towns, cities or residential areas. In this respect national codes may be regarded as providing *macrozonational* information.

Figure 9.1 is a portion of the Seismic Zone Map of Australia used to provide locational information for Queensland in AS2121-1979 (SAA, 1979). It can be seen that only two relatively small zones of Queensland were allocated a significant earthquake hazard rating in that building code.

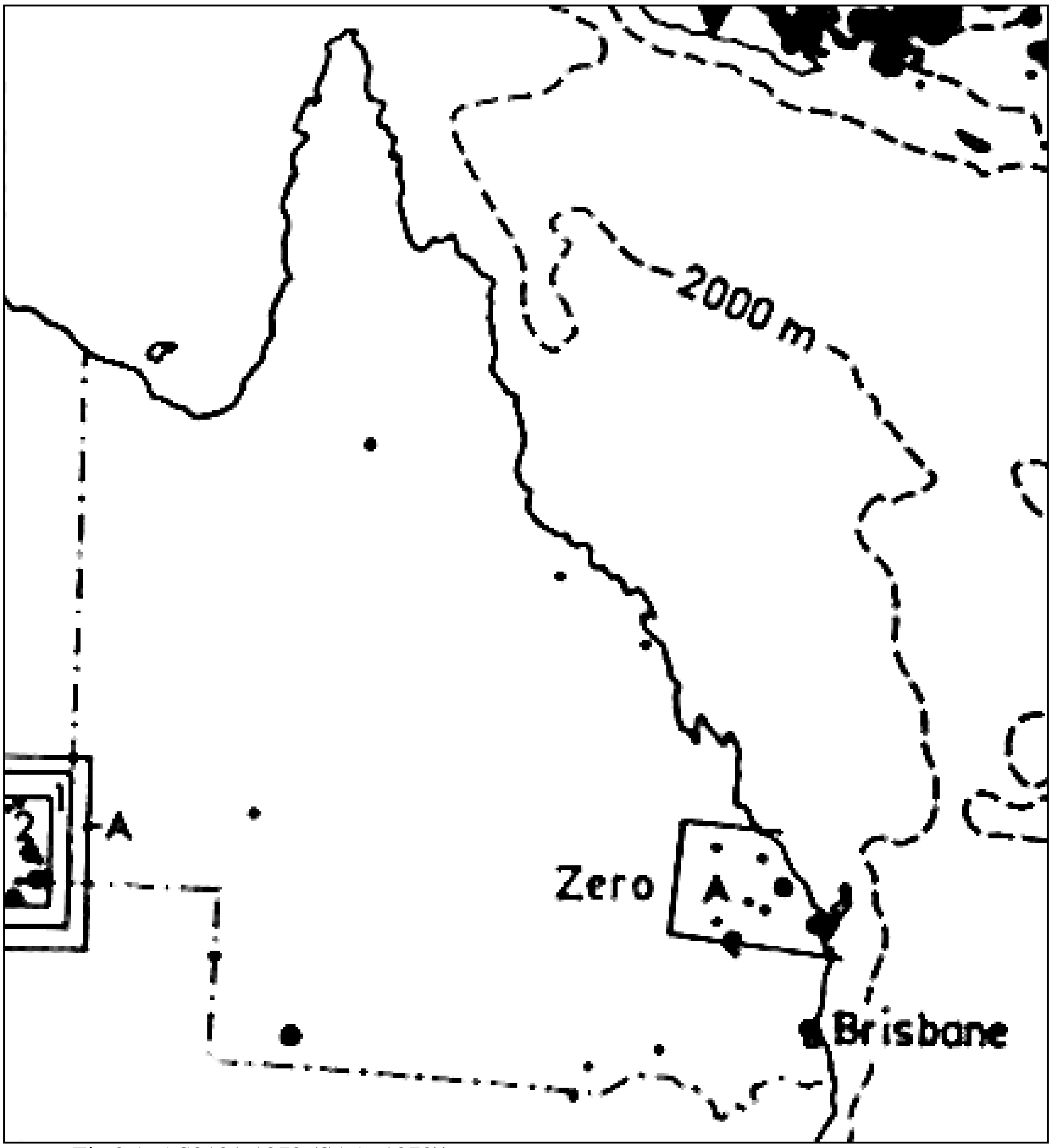

(Source: Fig 3.1, AS2121-1979 (SAA, 1979))

Figure 9.1 **AS2121-1979 Seismic Macrozonation of Queensland.**

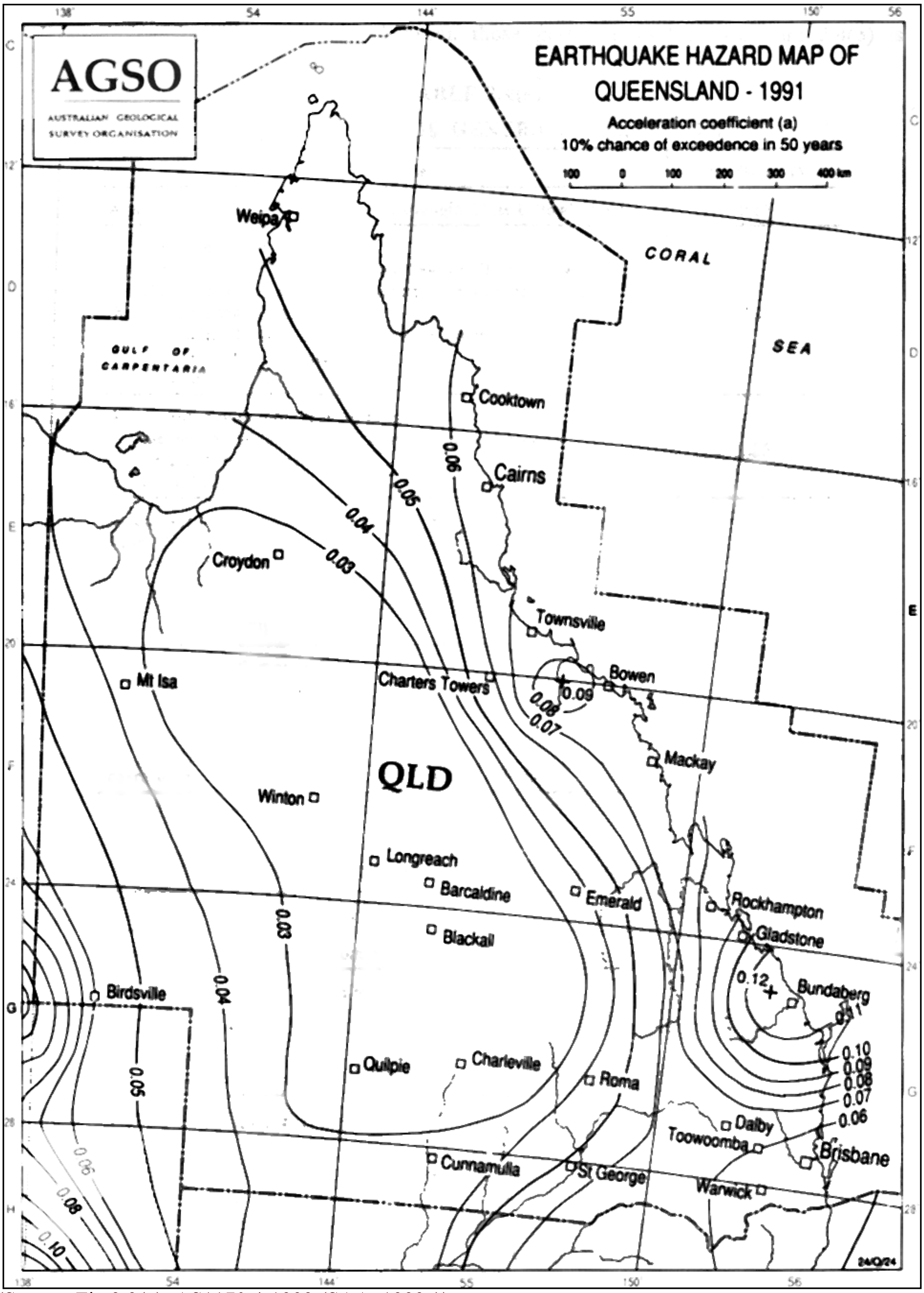

(Source: Fig 2.3(g), AS1170.4-1993 (SAA, 1993a))

Figure 9.2 **AS1170.4-1993 Seismic Macrozonation of Queensland.**

Figure 9.2 is a view of the Earthquake Hazard Map of Queensland used to provide locational information for Queensland, in AS1170.4 – 1993 (SAA, 1993a).

Comparison of Figures 9.1 and 9.2 shows that different methodologies were used to derive the regional earthquake hazard information in the two maps. The method used in Figure 9.2, while essentially retaining the information contained in Figure 9.2, provides considerably more detail for most of Queensland. However, despite the increased engineering usefulness of the information contained in the latter map, the microzonal relative risk details within large urban areas such as Brisbane and Bundaberg are still not revealed. Whilst it is evident from both building codes that Bundaberg is located within a relatively high earthquake hazard zone, no information is provided as to the translation of that hazard to the risks within the confines of the city itself. Indeed, the regional hazard information is incapable of providing that degree of resolution.

In order to derive microzonal seismic risk maps high-resolution seismic surveys, which use spatial differences of less than 10 Km, and assess the relative vulnerability of each site, are required. Such surveys allow the ambient seismic hazard within an area to be discriminated into zones of relative risk. Typically, spacings of about 3 km are considered adequate (Gaul et al, 1995). It should be noted that this process does not define the ambient hazard in the area any better than already known from the regional data.

Microzonation for engineering purposes

Within an area that is subject to a common ambient earthquake hazard, it is known that, in general, zones of differing vulnerability exist. This means that, on a microzonal scale, earthquake risk (from the same earthquake hazard) is, in general, different from place to place. The aim of a microzonation survey is to quantify the relative risk within a small regional area.

The relative vulnerability of different classes of buildings, due to their construction techniques and materials, their shape and size, is acknowledged in the building codes. The building codes also allocate earthquake site loading factors (S) based on soil types at the site of interest. Apart from the construction attributes of a building (which can be optimised by engineering design) it is the degree to which the shaking of the ground is transferred to the buildings that determines the relative vulnerability between adjacent sites. It is almost a trivial observation that a building that is more likely to be shaken during an earthquake is at more risk to damage than one that is not. What is not so trivial is devising survey techniques that will quantify the predisposition of a building of a certain class to shake in response to ground movement caused by an earthquake.

Any method of microzonation should provide an indication of the degree to which seismic energy is transferred from the foundations of a building to the building structure. Building code AS1170.4 – 1993 specifies a range of site loading factors (*S*) varying from 0.67 for rock foundations to 2.0 for the deepest, softest soils. This scale of site factors recognises the propensity for deeper, softer soils to exhibit greater ground movement than shallower, denser materials. However the code makes no allowance for resonant ground movement amplification observed in some areas.

Microzonation using site response spectra

All building structures have a natural shaking frequency. If a building is subjected to seismic shaking which corresponds with its natural shaking frequency then it will absorb more energy, and will shake more violently, than if the seismic energy was concentrated at some other frequency.

For the purposes of microzonation in this thesis it is assumed that the generalised natural shaking frequency (f_N), of a building with N stories, is approximated by the following formula (c.f. Michael-Leiba, 1999).

$$f_N \text{ [Hz]} \approx 10 / N \qquad \ldots \qquad \text{Eq 9.1}$$

Three classes of building will be considered in this study; low-rise (1 to 3 storeys), medium-rise (4 to 9 storeys), and high-rise (10 or more storeys). Table 9.1 lists the range of shaking frequencies relevant to the proposed building classes.

Building Class	Range of number of storeys	Calculated frequency range	Frequency range used for analysis
Low-rise	1 to 3	10 Hz to 3.3 Hz	2.9 ≤ Hz ≤ 10
Medium-rise	4 to 9	2.5 Hz to 1.1 Hz	1.1 ≤ Hz < 2.9
High-rise	10+	≤ 1.0 Hz	0.5 ≤ Hz < 1.1

Table 9.1 **Shaking frequency ranges for building classes.**

Analysis of a site's seismic response spectrum can provide an indication of the relative distribution of seismic energy within the ranges of frequency indicated in Table 9.1. The lower frequency range for high-rise buildings was set at 0.5 Hz because that corresponds to a 20-storey building, which was considered sufficient for the purposes of this study, there being no buildings over 20 storeys in Bundaberg. Figure 9.3 displays a typical site response spectrum and the associated frequency ranges of interest.

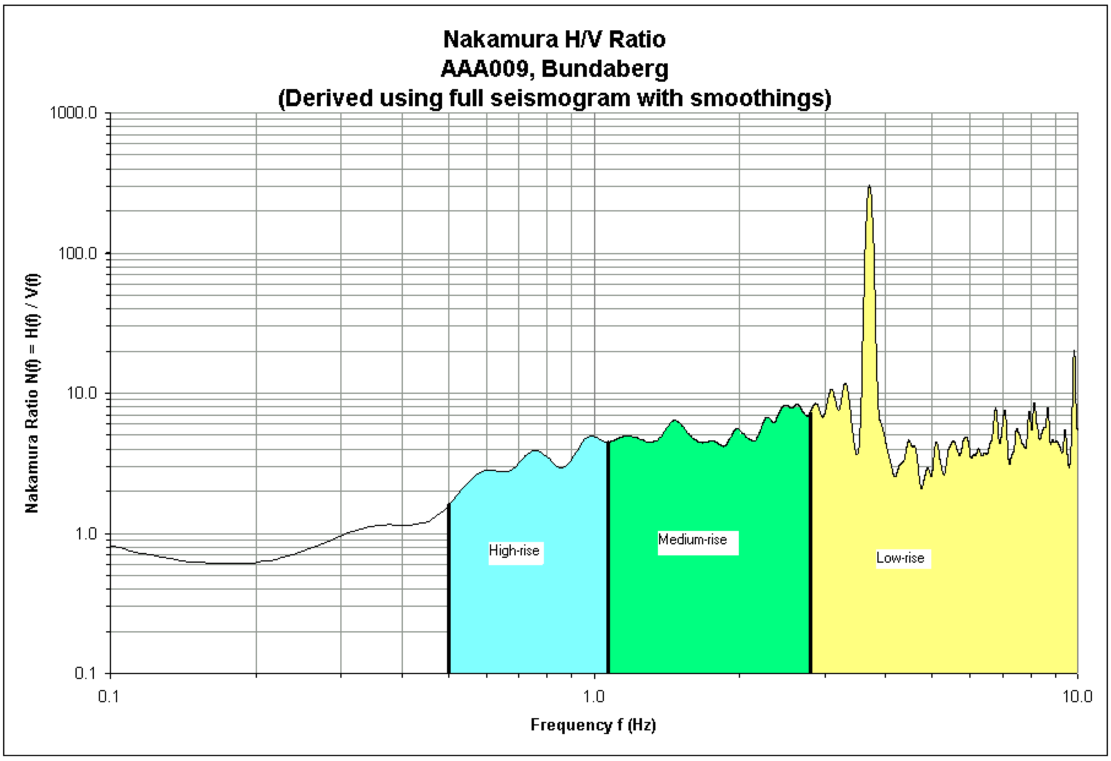

Figure 9.3 **Shaking frequency ranges for building classes.**

In determining the relative energy content in any particular frequency range, from one site response spectrum to the next, it is sufficient to use the average amplitude of the measure of ground movement amplification (the gain). Within any given set of site response spectra, the average gain of each frequency range will vary from some minimum value to some maximum value. The site that exhibits the maximum average gain within a particular frequency range will present the greatest seismic risk to buildings of the associated class within the data collection area.

AS1170.4 – 1993 allocates five earthquake site loading factors depending on the foundation soil type. Table 9.2 paraphrases the soil types used as a basis of the site factor allocations.

Soil Profile	Site factor (*S*)
Rock with low or better strength.	0.67
Rock with very low or extremely low strength or not more than 30 m of stiff or hard unconsolidated materials.	1.00
More than 30 m of stiff or hard unconsolidated materials.	1.25
20 m or more stiff or hard unconsolidated material containing 6 to 12 m of soft or loose materials.	1.50
More than 12 m of soft or loose materials.	2.00

Table 9.2 **Summary of AS1170.4 – 1993 Site Factor allocations.**

In conformity with the AS1170.4 – 1993 site factor allocations (*S*), and following analysis of the site response spectra for each building category, the author has devised an empirical formula for allocation of a microzonation site factors (S_M), based on a partitioning of the average gain ($\mathbb{G}$) at each site in relation to the maximum average gain ($\mathbb{G}_{Max}$) of all sites within the microzonation area. The microzonation site factors (S_M) determined by this method are listed in Table 9.3, and will be used in this microzonation study.

Relationship of the average gain ($\mathbb{G}$) within the frequency range of interest at a particular site, to the maximum average gain ($\mathbb{G}_{Max}$) within the same frequency range at all sites.	Microzonation Site factor (S_M)
$\mathbb{G} < 1.0$	0.67
$1.0 \leq \mathbb{G} < (\mathbb{G}_{Max} * 0.25)$	1.00
$(\mathbb{G}_{Max} * 0.25) \leq \mathbb{G} < (\mathbb{G}_{Max} * 0.50)$	1.25
$(\mathbb{G}_{Max} * 0.50) \leq \mathbb{G} < (\mathbb{G}_{Max} * 0.75)$	1.50
$(\mathbb{G}_{Max} * 0.75) \leq \mathbb{G} \leq \mathbb{G}_{Max}$	2.00

Table 9.3 **Microzonation Site Factor allocations.**

It should be noted that the microzonation site factors (S_M) are not intended to over-ride the AS1170.4 – 1993 site factors (*S*). A conservative approach should be maintained in using the microzonation site factors to supplement the building code. The microzonation information should always be used in conjunction with the building code, and not in isolation. In all instances the higher of the site factors obtained from the joint application of the building code and the microzonation results should be used.

Microzonation analysis software

A console based DOS application program has been written in C++ by the author to assist in the microzonation analysis of site response spectra. The application is named MICROZON. DOS files containing the C++ source code and the DOS executable file are contained on the CD ROM that accompanies this thesis.

```
<site name><EOL>

<frequency value1><TAB><gain value1><EOL>

<frequency value2><TAB><gain value2><EOL>

<frequency value3><TAB><gain value3><EOL>

.

.

.

<frequency valueN><TAB><gain valueN><EOL>

<EOF>
```

Figure 9.4 **TAB delimited spectra text file format suitable as source for MICROZON application.**

The MICROZON application is designed to execute from a DOS command line. It will process any number of TAB delimited text files containing site response spectral information in the format shown in Figure 9.4.

The syntax for executing the MICROZON application is:

```
MICROZON <source file pattern>
```

Where `<source file pattern>` is any valid DOS file name pattern including a directory path and wildcards. Before being invoked the MICROZON executable file must be present in the current default directory, or the path to its subdirectory must be added to the DOS PATH environmental string.

For instance, to analyse a set of site response spectra with the file names of the form `AAA001.RSM`, `AAA002.RSM, … , ZZZ999.RSM`, the following command would be issued.

```
MICROZON *.RSM
```

Upon successful completion the MICROZON application will create a TAB delimited text file named MICROZON.TXT in the current default directory. The contents of that file will be in the format shown in Figure 9.5.

```
SiteName<TAB>LoRiseMeanBased<TAB>MedRiseMeanBased<TAB>HiRiseMeanBased<EOL>
AAA001<TAB><LoRiseSiteFactor><TAB><MedRiseSiteFactor><TAB><HiRiseSiteFactor><EOL>
AAA001<TAB><LoRiseSiteFactor><TAB><MedRiseSiteFactor><TAB><HiRiseSiteFactor><EOL>
AAA001<TAB><LoRiseSiteFactor><TAB><MedRiseSiteFactor><TAB><HiRiseSiteFactor><EOL>
.
.
.
ZZZ999<TAB><LoRiseSiteFactor><TAB><MedRiseSiteFactor><TAB><HiRiseSiteFactor><EOL>
<EOF>
```

Figure 9.5 **TAB delimited microzonation data file.**

The TAB delimited microzonation data file, with the heading line removed, can be imported directly into the ArcView Geographical Information System (GIS) for association with other GIS tables containing a common site name column.

CHAPTER 10 MICROZONATION OF BUNDABERG CITY

Introduction

The current Australian earthquake loading code, AS1170.4 – 1993, places all of Bundaberg City within the highest earthquake hazard region of Queensland. Research into the earthquake hazard existing in the Bundaberg area (See Chapter 5) suggests that the crustal stress gradient is such as to result in a relatively high risk, within Australia, of the recurrence of potentially damaging earthquakes, of relatively large magnitude; and, whilst it is probably true that all of Bundaberg is subject to the same regional hazard from earthquake occurrence, it can be demonstrated that similar structures in different parts of the city are not subject to the same relative risk to damage from the same earthquake event.

Macroseismic data collected subsequent to earthquakes that occurred within 120 km of Bundaberg in 1918 and in 1997 indicates that the surface foundation, on which Bundaberg is sited, has a tendency to amplify ground movement to varying degrees. This variability of ground motion amplification can be attributed to differences in the nature and structure of the surface foundation layers. High amplification is associated with deep soils and unconsolidated materials. Amplification is also affected by the nature and structure of basement materials. Material interfaces that present a sharp gradient in shear wave propagation velocity can, dependent on the interface geometry, reflect a considerable proportion of seismic energy (cf Field, 1996; Dravinski et al, 1996). Under conditions where the basement geometry is suitable, considerable seismic energy resulting from reflected basin-edge-induced waves could conceivably be confined within a basin for extended time, after the initial waves have passed (Field, 1996).

Previous research has supported the use of microseismic field measurements in quantifying ground movement amplification at individual sites. It has been shown that the results of microseismic studies can be used as an indicator of expected macroseismic motion. Two methods of measurement have been employed.

One of these methods, the so-called *reference site* method, requires the use of two instruments. One instrument is deployed at the site of interest. The other instrument is deployed at a nearby reference site that is characteristic of basement bedrock. This method relies on the two instruments being triggered simultaneously to measure the response to the same source of seismic energy. In practice the condition of a common energy source can rarely be achieved. The spatial disparity of the two sites generally results in the energy source at each site being different. This is mainly due to locally generated social noise. Consequently the data collection is usually conducted at odd times during the night hours. The method also relies on the availability of a suitable reference site. Where such a site is unavailable the method cannot be used.

A second method, the method described by Nakamura (1989), uses a single measuring instrument and does not require a reference site. It has been shown to be mostly insensitive to locally generated social noise, and suitable for the characterisation of horizontal ground movement amplification.

The Nakamura method has been used to conduct a study into the distribution of horizontal ground movement amplification in the Bundaberg City area. The results of this study have provided microzonation data that can be used to supplement Australian earthquake loading codes, such as AS1170.4 – 1993, providing refinement of the codes within Bundaberg.

Data collection sites

The field measurements were conducted in two separate episodes. The first episode, in 1998, was designated BBGA. The second episode, in 2000, was designated BBGB. The data collection logs for both BBGA and BBGB are contained in a Microsoft® Excel® spreadsheet file on the CD ROM that accompanies this thesis. The microseismograms recorded at each site are also contained on the same CD ROM.

During January of 1998, 112 BBGA sites were occupied in the residential zone south of the Bundaberg TAFE College. Viable data was collected from 95 of the sites. The remaining sites were not viable due to operation abnormalities, such as non-levelling of the sensor or failing to realise that the recorder memory was full. The sites were chosen on street intersections or about 100 m apart. Figure 10.1 is a map depicting the viable sites occupied during the BBGA data collection episode.

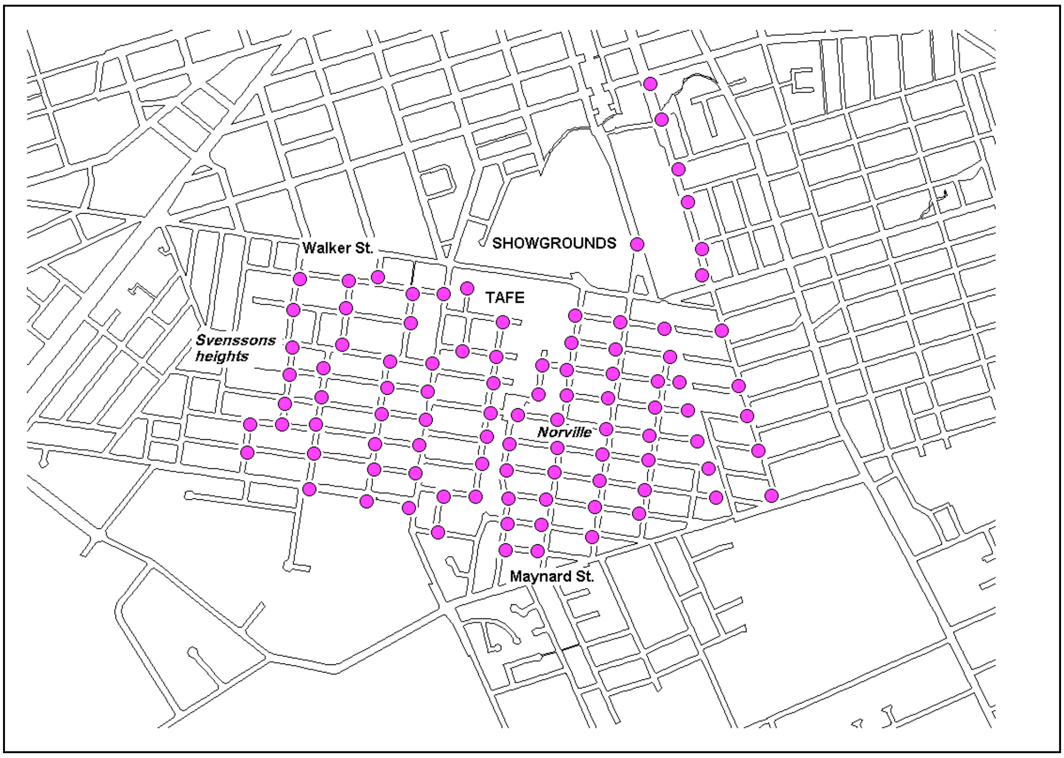

Figure 10.1 **BBGA data collection sites.**

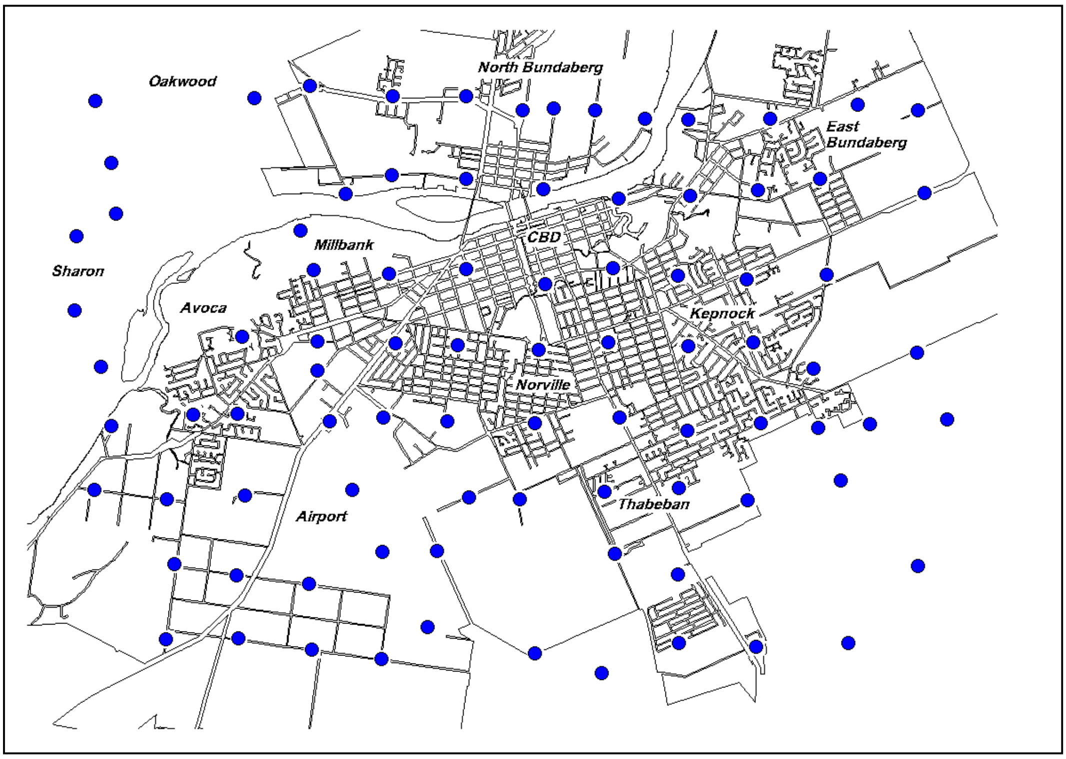

Figure 10.2 **BBGB data collection sites.**

Subsequent to the collection of the BBGA field data it was realized that coverage of the whole of the Bundaberg area at that resolution was impractical. Previous investigators (c.f. Gaul et al, 1995) have indicated that grid spacing in the order of 3 km was sufficient for the purposes of microzonation. Other investigators (McCue & Love, 1997) have demonstrated that irregular spacings of 1 km or less are sufficient to produce microzonation by means of mapped relative risk contours. As it is the intention of this current investigation to produce contoured risk maps of the area under investigation, it was decided to use a grid spacing of 1 km.

During January of 2000, 88 viable BBGB sites were occupied, covering most of the Bundaberg City local government area. The sites were chosen as near as possible to the intersection of the 1000 m grid lines on the Hema Bundaberg street map (Hema, 1997). Those potential sites already occupied during the BBGA episode were not reoccupied. Figure 10.2 is a map depicting the viable sites occupied during the BBGB data collection episode, and includes those BBGA sites that were suitable for inclusion in the BBGB data set.

Instrumentation

All data collection was done using a combination of Kelunji Classic seismograph and Sprengnether S6000 triaxial seismometer. The instrumentation configurations used for the two data collection episodes are detailed in Figures 10.3 and 10.4.

Kelunji #195, GURIA V4.10A
KA2 #44, SKA2 V1.03A
KC1 V2 #170
KI1 #165, board 1, 1024kB
KI1 #164, board 2, 1024kB
KP1 V2 #172
Sampling at 100 samples/second
S6000 #10471

Figure 10.3 **<u>Instrumentation for 1998 BBGA data collection</u>**

Kelunji #164, GURIA V4.12A
KA1M #110
KC1 V2 #128
KI1 #118, board 1, 1024kB
KP1 V2 #138
Sampling at 100 samples/second
S6000 #10471

Figure 10.4 **Instrumentation for 2000 BBGB data collection.**

Both the KA1 and KA2 analogue data processing boards in the Kelunji instruments used for data collection employ direct current coupling and are capable of recording signals in the range from 0Hz up to 25Hz (KA1) or 50Hz (KA2), with a dynamic range in excess of 130dB for the KA1 and 90dB for the KA2 (Pers. Com. Adam Pascale, Seismic Research Centre, 26 March 2001. See also Appendix D.)

The natural period of each pendulum, in the Sprengnether S6000 triaxial seismometer used in this research, is nominally 0.54s (1.85Hz), and the sensor provides a nominal output signal of 120 volts per ms^{-1}. (Pers. Com. Adam Pascale, Seismic Research Centre, 26 March 2001.) The output characteristic specification sheet for the S6000 (See Appendix E) indicates that this sensor provides a usable signal of 5 volts per ms^{-1} at 0.4Hz. This represents a reduction of 13.8dB of voltage below the nominal level; well within the dynamic ranges of the KA1 and KA2 analogue to digital features.

In performing the microzonation analysis the ratio of spectra derived from the seismograms is employed. This being the case, and considering that the seismograph will provide adequate signal down to at least 0.4Hz, the proposed lower frequency of 0.5Hz indicated in Figure 9.3 can be achieved using this instrumentation.

During data collection the instrumentation was conveyed in the back of a vehicle. The vehicle's battery was used to power all instrumentation. A Garmin GPS 12XL was used to determine the geographical location of each site in terms of its longitude and latitude. A Suunto MC-1 compass, corrected for 10º easterly deviation of magnetic north from true north, was used to orientate the sensor at each site. The Springnether S6000 triaxial seismic sensor is designed with an orientation arrow molded into the housing. The manufacturers recommend that the instrument be installed with the arrow pointing due west, so as to ensure correct polarity of the horizontal sensors. At each site the arrow of the sensor was orientated to the west, except in cases where leveling of the sensor could not be achieved. Since the results of the microzonation were not dependent on the correct polarity of the horizontal sensors, in those rare instances the arrow was orientated to the east.

The data from the Kelunji Classic seismograph was downloaded to a Toshiba 220CDS laptop running the Microsoft® Windows95® V4.00.950 B operating system, using Telix® V3.51 communications software for DOS V3.1 or higher.

Data analysis

The microseismograms recorded at each of the data collection sites were analyzed in accordance with the microzonation methodology explained in Chapter 9. This resulted in allocating each site with three microzonation earthquake loading Site factors (S_M), for low-rise, medium-rise and high-rise buildings, depending on the relative horizontal ground movement amplification exhibited at that site.

Subsequent to microzonation analysis the information was imported into an ArcView GIS system and displayed on a map of the Bundaberg City area as site markers of different colours that correspond to the S_M value determined for each site. These colour-coded markers were used to manually draw contour lines by interpolation. Figures 10.5, 6 and 7 on the following pages depict the microzonation results for the three different building categories.

Commentary on common features of the maps

The maps contained in Figures 10.5, 10.6 and 10.7 display colour coded earthquake site loading factor zones. The colours blue, green, yellow, orange and red correspond to S_M = 0.67, 1.0, 1.25, 1.5 and 2.0 respectively. Commentary will be presented in terms of the zone factor values alone, without repeated mention of *site factor* or the use of redundant equations such as "S_M = 1.25".

All three maps display well-defined zones of S_M values superimposed on a background of 1.25. In the center of the low-rise and the high-rise maps is a large 1.0 zone extending east to west from Kepnock to Millbank, and north to south from North Bundaberg to Thabeban. This *central zone* is intersected NNE to SSW by a *central corridor* of higher value. The *central zone* is recognizable in the medium-rise map as two 1.0 zones in the Kepnock and Millbank areas, with a wide separation of 1.25 between them. The NNE to SSW *central corridor* of high values has apparent extensions in the areas of the Airport and the eastern part of North Bundaberg. These extensions appear on all three maps. There are five high value zones at the boundaries of the measurement area to the north, west and south that have counterparts identifiable on all three maps: Avoca/Sharon; the Airport; South Thabeban; East Bundaberg; and the east section of North Bundaberg.

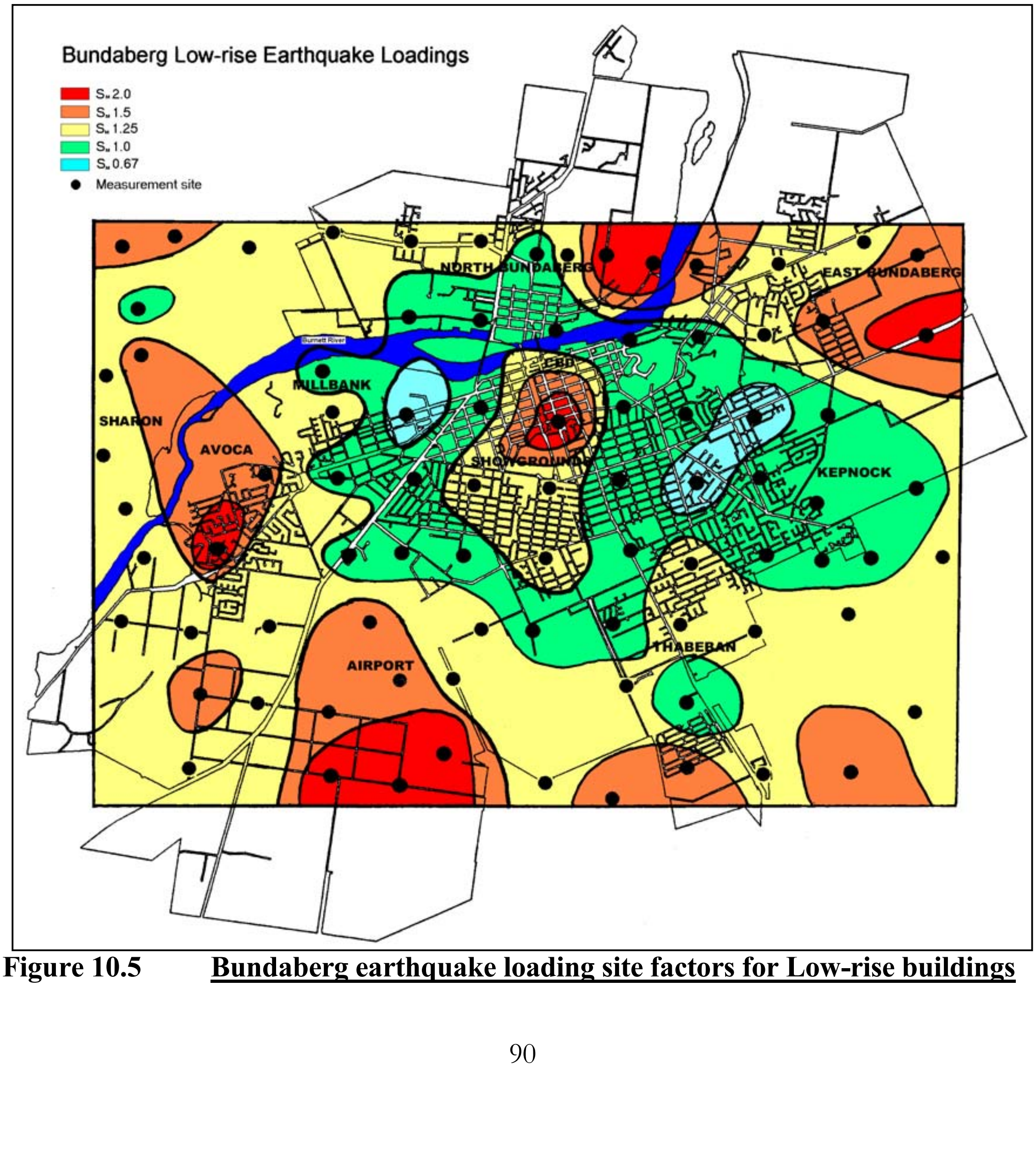

Figure 10.5 **<u>Bundaberg earthquake loading site factors for Low-rise buildings</u>**

Commentary on features of the Low-rise map

The map shown in Figure 10.5 displays several well-defined zones of S_M values superimposed on a background of 1.25. In the center is a large 1.0 zone extending east to west from Kepnock to Millbank, and north to south from North Bundaberg to Thabeban. This *central zone* encloses an oblong *central island* of higher values that separates two zones of 0.67 to the east and west. The *central island* contains a 2.0 core centered on the area just south of the central business district (CBD). The oblong *central island* of high values has apparent extensions in the areas of the Airport and the eastern part of North Bundaberg. The *central zone* is framed by a series of high value zones to the north, west and south. The high value zones in the areas of Avoca/Sharon, the Airport, East Bundaberg and the east section of North Bundaberg exhibit core values of 2.0.

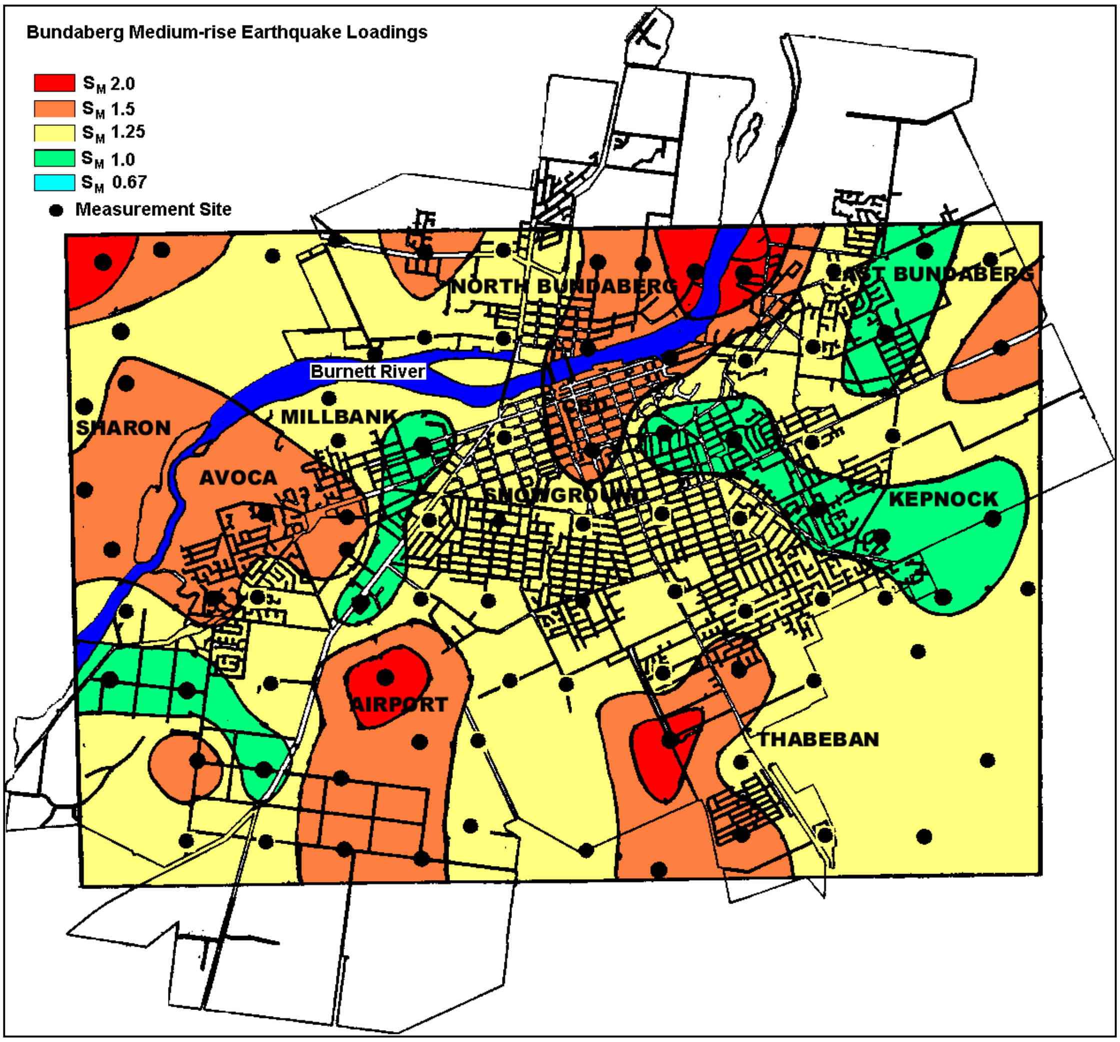

Figure 10.6 **Bundaberg earthquake loading site factors for Medium-rise buildings**

Commentary on features of the Medium-rise map

The map shown in Figure 10.6 displays several well-defined zones of S_M values superimposed on a background of 1.25. Distinctive features are the two high value zones thrusting into the central area of the map from the NNE and SSW. In the center is a broad background area that separates one oblong 1.0 zone (from Kepnock through almost to the CBD) in the east from another (from Millbank down to Sugarlands) in the west. The perimeter is flanked by a series of high value zones to the north, west and south. The high value zones in the areas of the Airport, south Thabeban, the east section of North Bundaberg and north Sharon exhibit core values of 2.0.

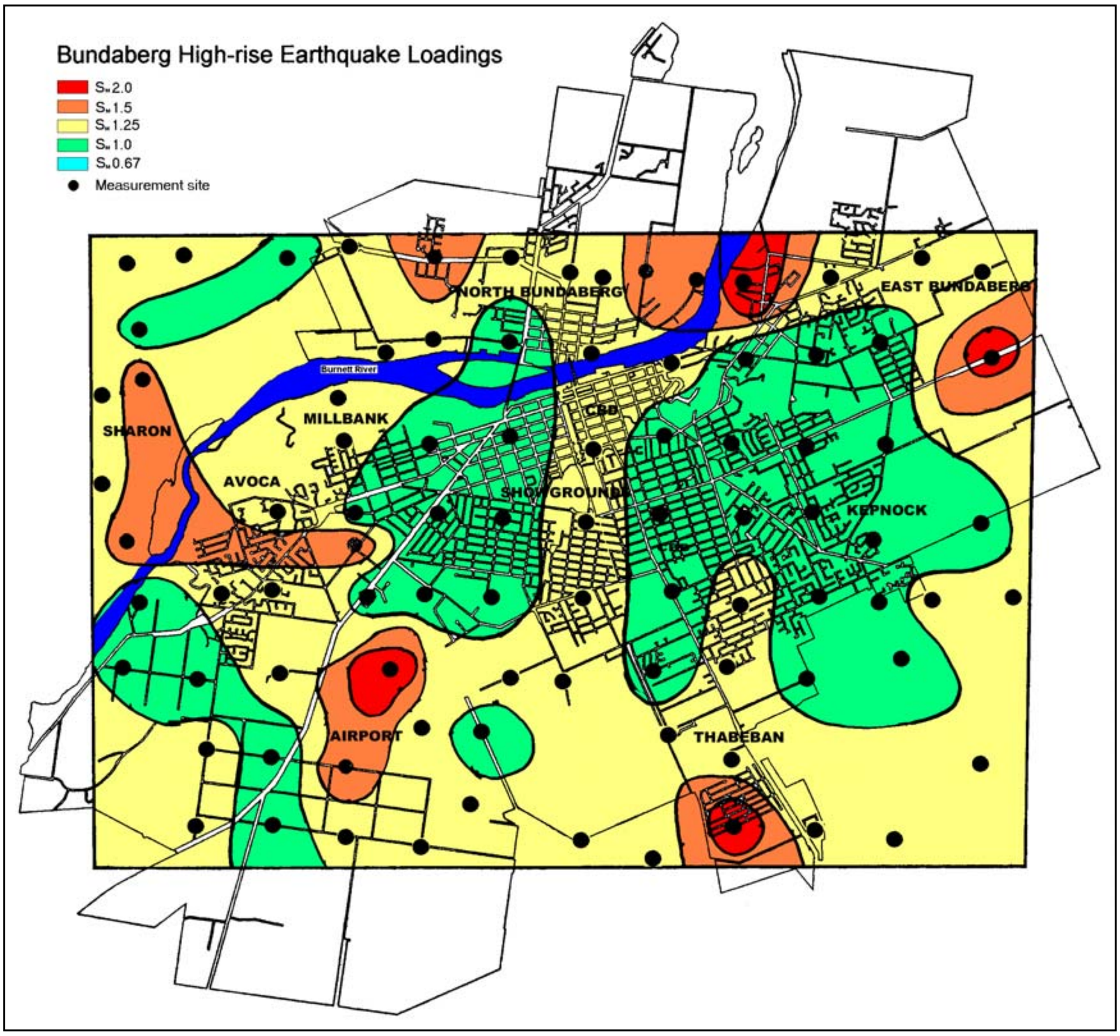

Figure 10.7 <u>**Bundaberg earthquake loading site factors for High-rise buildings**</u>

Commentary on features of the High-rise map

The map shown in Figure 10.7 displays several well-defined zones of *S* values superimposed on a background of 1.25. In the center are two 1.0 *central zones* extending east to west from Kepnock to Millbank, and north to south from North Bundaberg to Thabeban separated by a background *central corridor*. The *central zones* are framed by a series of high value zones to the north, west and south. The high value zones in the areas of the Airport, south Thabeban, East Bundaberg and the east section of North Bundaberg exhibit core values of 2.0.

Recommended qualitative descriptions.

The boundaries between adjacent risk zones depicted in Figures 10.5, 10.6 and 10.7 are approximate only, and may vary from the actual positions depicted. For explanatory purposes the qualitative descriptions listed in Table 10.1 are recommended.

Seismic microzonation loading factor (S_M).	Qualitative description of relative seismic risk.
0.67	Low to Moderately Low.
1.00	Moderately low to moderate.
1.25	Moderate
1.50	Moderate to moderately high
2.00	Moderately high to high

Table 10.1 **Qualitative description of relative risk.**

In using these descriptions it must be kept in mind that, whilst the relative risk zones depicted in the microzonation maps are internally consistent within the source data set (that is, they are applicable within the Bundaberg City area), they cannot be used to compare the Bundaberg risk zones with risk zones derived for other areas, using a different spectral data set.

CHAPTER 11 INDIRECT DETERMINATION OF SEDIMENT DEPTH IN BUNDABERG CITY.

Introduction

A test of the validity of results obtained from any analysis is the ability for those results, or the data used to produce those results, to predict other, related and verifiable, information about the system being investigated. Recent investigators (Seht & Wohlenberg, 1999) have shown that Nakamura spectra can, in some cases, be used to indirectly determine the depth of the sediment at the sites where the microseismograms were collected. In the case of the Nakamura spectra used in the microzonation of Bundaberg City, sufficient directly measured sedimentary depths are available to compare with those calculated using the Nakamura spectra. A positive outcome from this comparison is an indication of the reliability of the microzonation results.

Bundaberg City surface geology

Figure 11.1 shows the surface geology of the Bundaberg district, including the major waterways and structural elements. The approximate area of the microzonation is depicted as a rectangular line in the Bundaberg city area.

Bundaberg is situated on the Burnett River, about 20 to 30 km from its mouth, in sedimentary deposits confined in a basin formed by outcropping of bedrock consisting chiefly of the Burrum Coal Measures. The basin is filled primarily with Tertiary fluvial deposits of the Elliott Formation. Within the area of microzonation two other units overlay the Elliott Formation. To the south of the Burnett River, between the Bundaberg city area and the coast, the Hummock Basalts were extruded onto the Elliott Formation during the late Pleistocene. The Moore Park landform extends from the Burnett River to the mouth of the Kolan River and lies between the Bundaberg city area and the coast. The Elliott Scarp defines the western limit of the Formation. This was the coastal boundary during the late Pleistocene (Robertson, 1979). The Moore Park landform is composed of extensive Holocene mangrove flats and accretion ridges.

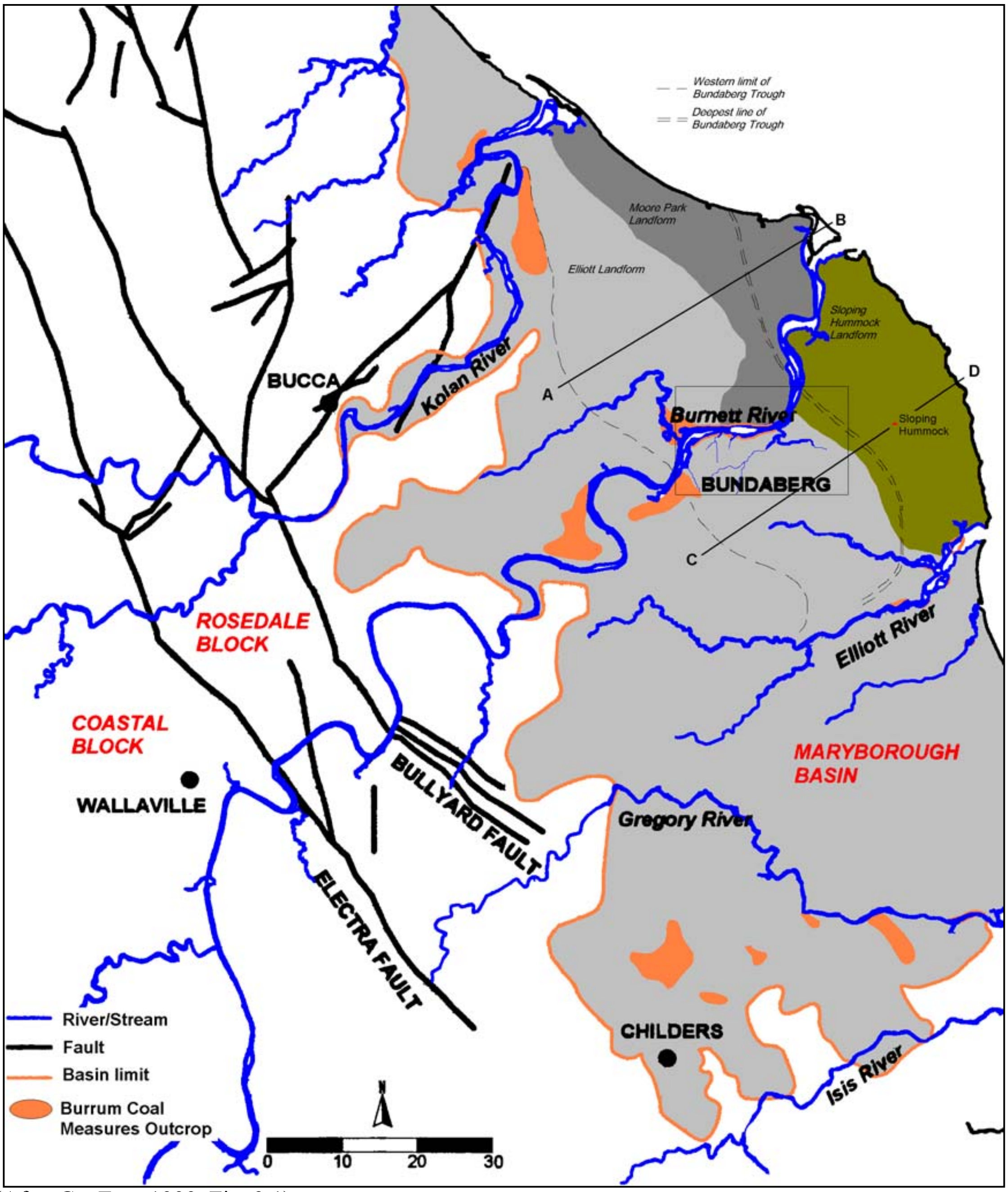

(After GeoEng, 1999, Fig. 3.1)

Figure 11.1 **Surface geology of the Bundaberg region**

The Elliott Formation unconformably overlies the Burrum Coal Measures and conformably overlies the Fairymead Beds in the Bundaberg Trough (c.f. Figure 11.2).

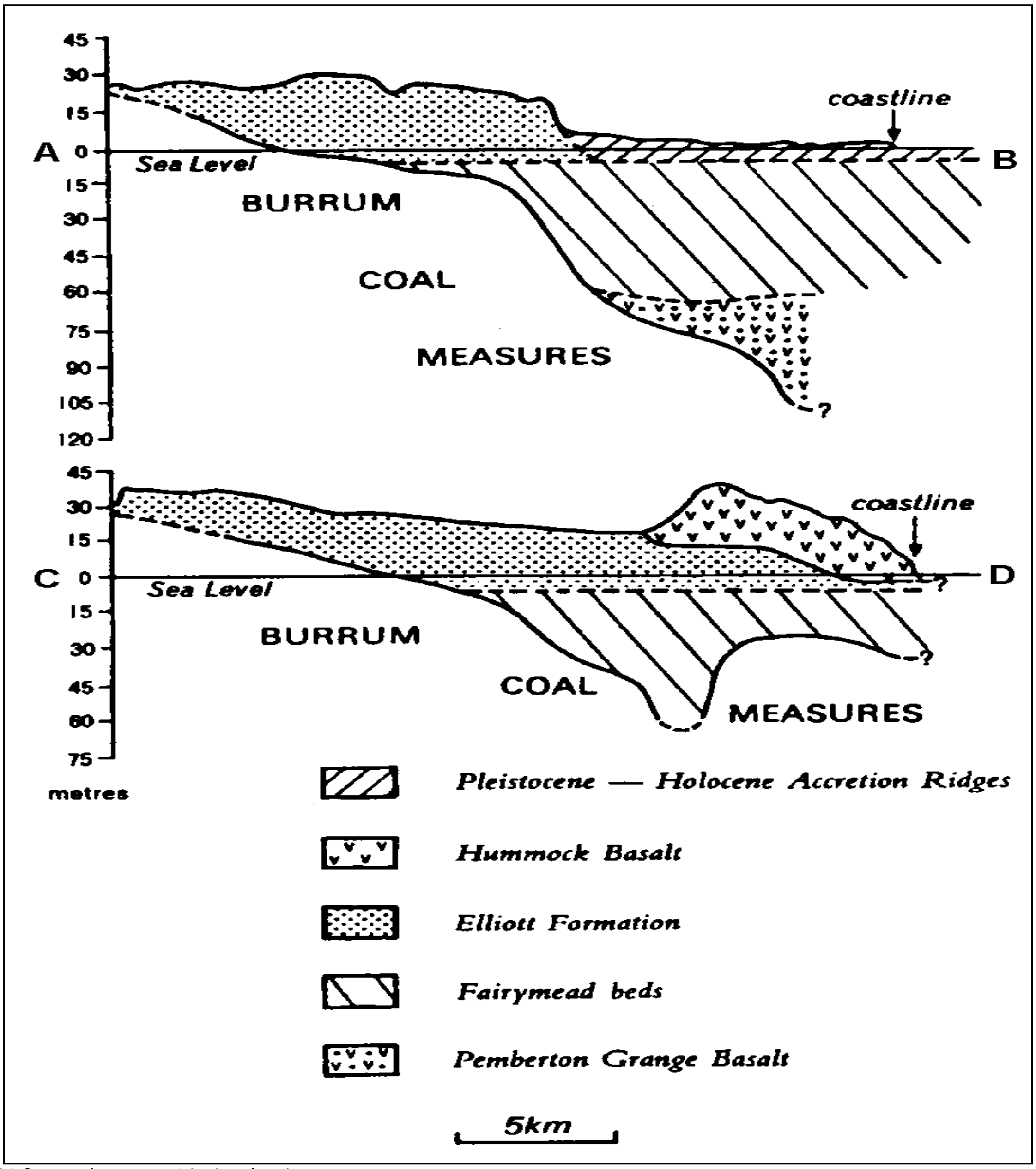

(After Robertson, 1979, Fig.5)

Figure 11.2 **Cross-sections of the Bundaberg Trough**

The Bundaberg city area lies almost completely on sediments within a section of a longitudinal depression in the underlying Burrum Coal Measures referred to informally as the Bundaberg Trough. This depression is filled with Late Eocene (Robertson, 1979) Fairymead Beds sediments, which are in turn overlain by the Elliott Formation. The base of this trough has a shallow dip to the east under the Bundaberg city area and has a maximum depth in the Bundaberg city area of about 50 m in the northwest corner of the city. Figure 11.2 shows two typical cross-sections (After Robertson, 1979) of the trough in the Bundaberg district. The surface lines of the cross-sections are shown in Figure 11.1.

At the western limits of Bundaberg city, extending east along the line of Splitters Creek and the Burnett River, there is a zone of outcropping of weathered forms of the Burrum Coal Measures. There is a similar zone of outcropping in the southwest corner of the city limits.

Standard Penetration Tests (SPT)

The proprietor of C.M. Testing Services at Bundaberg, Mr. Ian Ferris, has made available shallow borehole log data from five test holes drilled in the Bundaberg CBD. These five test holes were drilled at two locations, two on the corner of Quay and Barolin Streets (QB1 and QB2), and the other three at Wide Bay Capricorn House in Barolin Street (WB1, WB2 and WB3), about 150 m south of the previous site (see Figure 11.3). The QB holes were drilled to a depth of 3 m and the WB holes were drilled to 8.5 m.

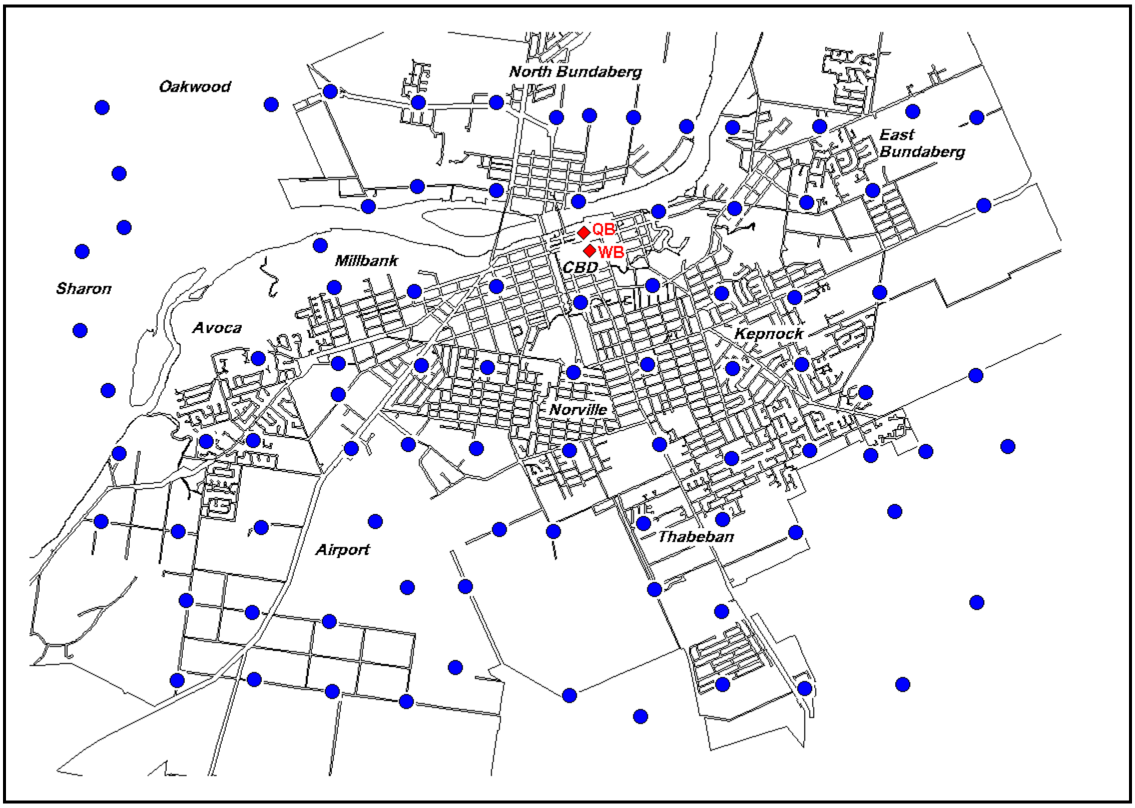

Figure 11.3 <u>Data collection area showing SPT borehole siles</u>

In addition to the stratigraphic information the logs also provide several Standard Penetration Tests (SPT) from which shear wave velocities (v_s) can be estimated. The method of performing the SPT is provided in AS1289.6.3.1-1993 (SAA, 1993).

By its nature the results derived from a Standard Penetration Test are subject to considerable variation. The SPT result is the number of blows from a 63.5 kg hammer required to drive a standard shaped test tool through two sets of 150 mm of the soil being tested, after it has already been driven through an initial 150 mm of the soil (SAA, 1993). In other words, the test tool has to be driven through 450 mm of the soil for a full test to be performed. Often a full test cannot be completed due to the nature of the soil, inclusions in the soil, or for other reasons. In such cases it is said that the test is unrepresentative, insufficient, or has been refused because the soil was too hard.

The results of a completed SPT are recorded in the following manner (c.f. examples in SAA, 1993, p2).

(A) For full penetration, the number of blows for each 150 mm penetration and the N value (the number of blows for the second and third 150 mm added together), e.g. for successive blow counts of 4, 7, and 11 for each 150 mm penetration

4, 7, 11
N = 18;

(B) For a result of 4 blows for the first 150 mm, 18 blows for the next 150 mm and 30 blows for the next 15 mm

4, 18, 30/15 mm

(C) For a result of 30 blows for the first 80 mm penetration

30/80 mm

In the above examples only example (A) is a complete test. The other two examples do not provide sufficient information for an SPT to be completed.

The velocity of shear wave propagation within soil can be determined from the SPT. The shear wave velocity can in turn be used in conjunction with the ground amplification spectra to estimate the sediment depth of a site (Seht & Wohlenberg, 1999).

Relationship between SPT and Shear Wave Velocity

In a recent report on the analysis of a Japanese bridge to earthquake response (Ganev et al, 2000) a set of measured SPT with associated measured shear wave velocities is given. These data are reproduced in Table 11.1.

SPT N Value	Shear Wave Velocity (m/s)
10	160.0
15	290.0
20	290.0
17	320.0
43	370.0
29	240.0
50	340.0
18	210.0
50	410.0

(Source Ganev et al, 2000)

Table 11.1 <u>Cross-sections of the Bundaberg Trough</u>

It is assumed that the SPTs carried out by the investigators in Japan were done in compliance with the published standards that specify the test procedure. In effect the SPT is a measure of the shear modulus of the material. It was assumed that soil in the Bundaberg area, that presents the same SPT values as those in Japan, would have the same shear modulus and hence shear wave velocity. Under that assumption, linear regression of the data in Table 11.1 may be used to derive a relationship between SPT values and the shear wave velocity.

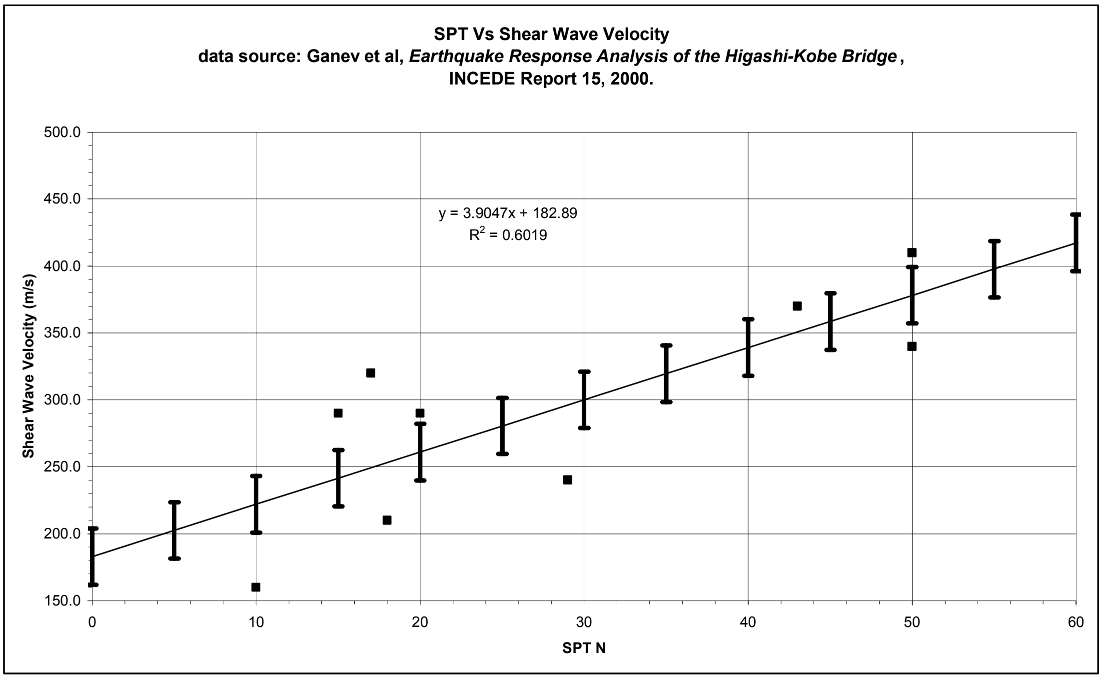

Figure 11.4 **Correlation between SPT and Shear Wave Velocity**

From the linear regression of the data in Table 11.1, depicted in Figure 11.4, the following approximate relationship between SPT and v_s can be derived.

$$v_s\,[ms^{-1}] \approx 3.9SPT + 182.9 \quad \ldots \quad \text{Eq. 11.1}$$

The standard error of the predicted shear wave velocity value (the y value) for each SPT value (the x value) in the regression is a measure of the amount of error in the prediction of the shear wave velocity for an individual SPT value.

The equation used for calculation of the standard error of the predicted shear wave velocity values is:

$$S_{y \cdot x} = \sqrt{\left[\frac{1}{n(n-2)}\right]\left[n\sum y^2 - \left(\sum y\right)^2 - \frac{\left[n\sum xy - \left(\sum x\right)\left(\sum y\right)\right]^2}{n\sum x^2 - \left(\sum x\right)^2}\right]}$$

This indicates a standard error of ±70ms^{-1} in the predicted shear wave velocity values.

From the borehole data provided by of C.M. Testing Services three viable SPTs obtained at the WB sites can be used to determine shear wave velocities using Eq. 11.1. These are shown in Table 11.2.

Site and depth	Measured SPT N (Source C.M. Testing Services, Bundaberg)	Calculated Shear Wave Velocity V_s (ms^{-1})
WB1 (6 m)	32	308±70
WB2 (7.7 m)	34	316±70
WB3 (8.55 m)	26	284±70
	Average velocity	303±40

Table 11.2 **Shear wave velocities in Bundaberg CBD**

The three individual results have been combined to determine an average shear wave velocity for the sediments in the Bundaberg CBD. From the known distribution and nature of the sediments in the Bundaberg city area this value will be assumed for all sedimentary sites.

Estimation of Bundaberg City sediment depth from Spectral results

In a simple two layer model it can be shown (c.f. Seht & Wohlenberg, 1999) that the relationship between fundamental resonant frequency (f_r), shear wave velocity (v_s) and sediment depth (d) is given by the following equation.

$$f_r\ [\mathrm{Hz}] = v_s / 4d \qquad \ldots \qquad \text{Eq. 11.2}$$

If the fundamental frequency and the shear wave velocity are known then the sediment depth can be calculated.

The fundamental resonant frequency peaks of the ground amplification spectra used for the Bundaberg microzonation have been estimated by visual inspection of the spectra. Using the previously estimated average shear wave velocity for the Bundaberg city area (303±40ms^{-1}), the sediment depth at the measurement sites has been estimated. The results of this estimation are shown in Table 11.3.

Site ID	Fundamental resonance frequency (Hz)	Depth calculated from Shear Wave Velocity (m)	Site ID	Fundamental resonance frequency (Hz)	Depth calculated from Shear Wave Velocity (m)
AAA007	3.0	25	ABE004	2.5	30
AAB013	1.9	41	ABE005	2.3	34
AAG015	1.9	41	ABE006	2.3	32
ABA001	2.5	30	ABE007	1.2	65
ABA002	1.3	60	ABE008	2.1	37
ABA003	2.0	39	ABE009	1.2	65
ABA004	1.6	49	ABE010	1.9	41
ABA005	1.7	46	ABE011	1.6	49
ABA006	1.6	49	ABE012	1.9	41
ABA007	1.3	60	ABE013	1.5	52
ABA008	1.6	49	ABF001	3.9	19
ABA009	1.3	60	ABF002	5.4	14
ABA010	1.5	52	ABF003	1.6	49
ABA011	1.2	65	ABF004	0.9	86
ABA012	2.4	31	ABF005	1.5	52
ABA013	1.2	65	ABF006	2.4	31
ABA014	1.2	65	ABF007	2.1	37
ABB001	1.1	71	ABF008	2.1	37
ABB002	1.4	55	ABF009	1.8	43
ABB003	2.1	37	ABG001	1.4	55
ABB004	1.5	52	ABG002	1.8	43
ABB005	2.0	39	ABG003	2.1	37
ABB006	1.9	41	ABG004	2.4	31
ABB007	2.2	35	ABG005	2.1	37
ABB008	2.1	37	ABG007	1.3	60
ABB009	2.0	39	ABG008	4.0	19
ABC001	1.8	43	ABH001	0.8	97
ABC002	1.7	46	ABH002	3.2	24
ABC003	2.0	39	ABH003	1.8	43
ABC004	2.2	35	ABH004	2.0	39
ABC005	1.6	49	ABH005	3.5	22
ABC006	3.2	24	ABH006	2.2	35
ABC007	1.9	41	ABH007	1.7	46
ABC008	2.1	37	ABH008	3.1	24
ABD001	1.0	77	ABH009	2.4	31
ABD002	1.4	55	ABH010	1.3	60
ABD003	1.6	49	ABH011	1.9	41
ABD004	2.1	37	ABH012	1.4	55
ABD005	2.0	39	ABI001	1.5	52
ABD006	1.8	43	ABI002	1.9	41
ABD007	1.5	52	ABJ001	1.9	41
ABD008	2.1	37	ABJ002	2.7	28
ABE001	1.9	41	ABJ003	2.6	29
ABE002	2.3	34	ABJ005	1.5	52
ABE003	1.2	65			

Table 11.3 **<u>Bundaberg city sediment depths</u>**

A statistical summary of the sediment depths is provided in Table 11.4.

Average sediment depth (m)	44
Maximum sediment depth (m)	97
Minimum sediment depth (m)	14
Sample Standard Deviation of sediment depth (m)	14

Table 11.4 **<u>Statistical summary of sediment depths</u>**

The calculated sediment depths shown in Table 11.4 agree fairly well with those proposed by Robertson (1979) as depicted in Figure 11.2.

Comparison of estimated depths to measured depths

During the Bundaberg groundwater investigation project 1998/99 (GeoEng, 1999) a spreadsheet database of test boreholes was produced. Warwick Wood of GeoEng, Bundaberg, has made this database available to the author. Those boreholes located within the limits of the microzonation boundary were isolated, and those that intersected the Burrum Coal Measures were identified from comments in the borehole log (see Figure 11.5).

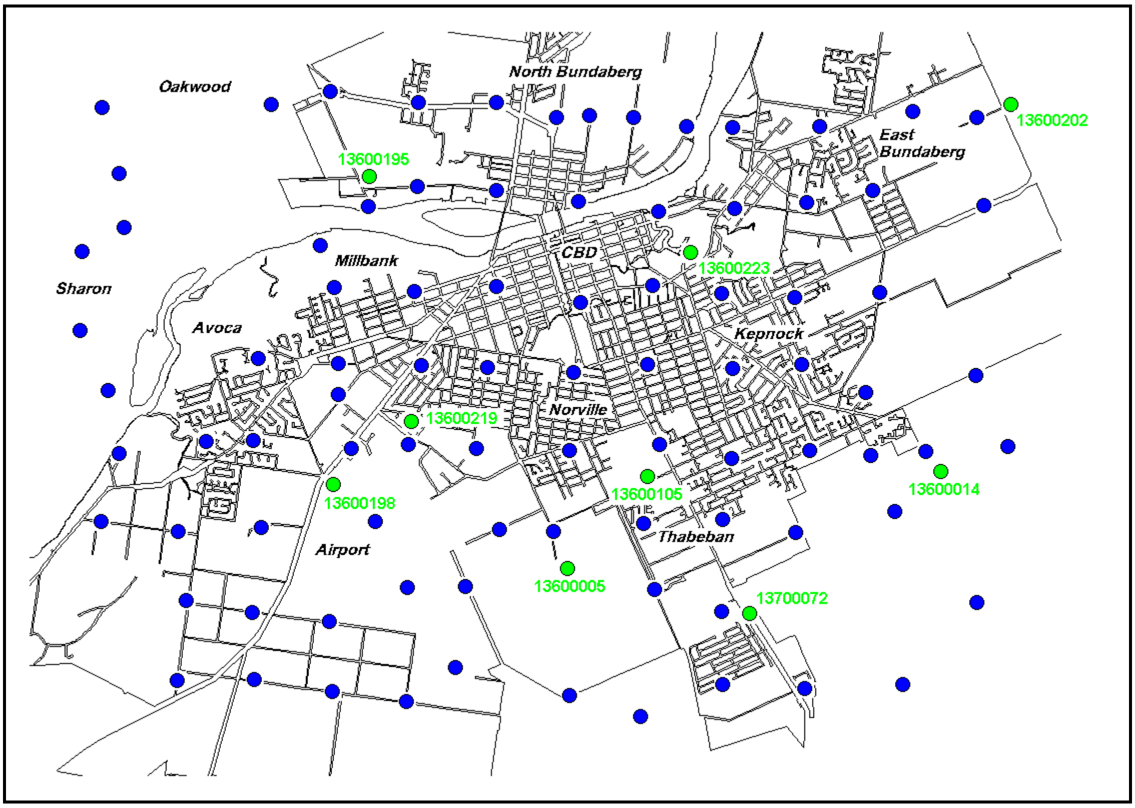

Figure 11.5 <u>Data collection area showing selected deep borehole sites</u>

The microzonation measurement sites adjacent to the identified boreholes were then selected, and the sediment depths as listed in Table 11.2 were calculated.

In selecting the boreholes to use for comparison purposes, only those that had comments in the log to indicate that coal or hard carbonaceous material had been intersected were used. This identified nine boreholes (as depicted in Figure 11.5), adjacent to microzonation measurement sites, from which the depth from the surface to the top of the Burrum Coal Measures could be obtained. For comparison purposes, where the borehole was approximately equidistant from more than one adjacent microzonation site, the calculated sediment depths for those adjacent sites were averaged. If the borehole was significantly closer to one particular microzonation site, the calculated sediment depth for that site alone was used.

Table 11.5 details the comparison of the borehole depths and the calculated depths.

GeoEng Borehole ID	Depth to Burrum Coal Measures (m)	Comment in borehole log	Average calculated sediment depth of adjacent microzone sites (m)	Adjacent Microzonation Site IDs
13600005	41.15	GREY CLAY AND COAL SEAMS	40	ABF005, ABF006, ABG003
13600014	67.06	SANDSTONE GETTING HARDER (COAL OIL SCUM)	46.25	ABE011, ABE012, ABE013, ABF009
13600105	38.1	GREY SHALE & CARBON	34	ABE008, ABF006
13600195	26.3	YELLOW CARBONACEOUS GREY & PINK WEATHERED SILTSTONE	39	ABB009
13600198	24	LIGHT & DARK GREY CARBONACEOUS SILTSTONE	58	ABE004, ABF004
13600202	71.5	LIGHT & DARK GREY CARBONACEOUS SILTY CLAY & SOME SILTSTONE FRAGMENTS	65	ABA014
13600219	31.09	DARK BROWN FIRM CLAY (WITH SHALE) WITH NARROW PEAT BAND	34	ABE005
13600223	41.5	LIGHT GREY CLAY WITH WEATHERED COAL PIECES, SILTSTONE AND SANDSTONE	41	ABB004, ABB005, ABC005, ABC006
13700072	35.05	DARK GREY CLAY WITH COAL OIL SCUM	43	ABG002

Table 11.5 **Comparison of GeoEng depths and calculated depths**

Figure 11.6 displays a graphical comparison of the measured and calculated sediment depths. In Figure 11.6 the black diagonal line represents the position of data points that have ideal coincidence. Any data point for which the calculated depth is over-estimated will lie under the black line. Any calculated data points that under-estimate the actual depth will lay above the black line. The red lines indicate the extremities of the spread of the estimations from the ideal. The blue line is the line of best fit calculated from linear regression of the data points, forced through the origin. Whilst the correlation coefficient for the best-fit line is very low (0.2), its proximity to the ideal line and the well-defined nature of the data spread indicates a positive result for the comparison.

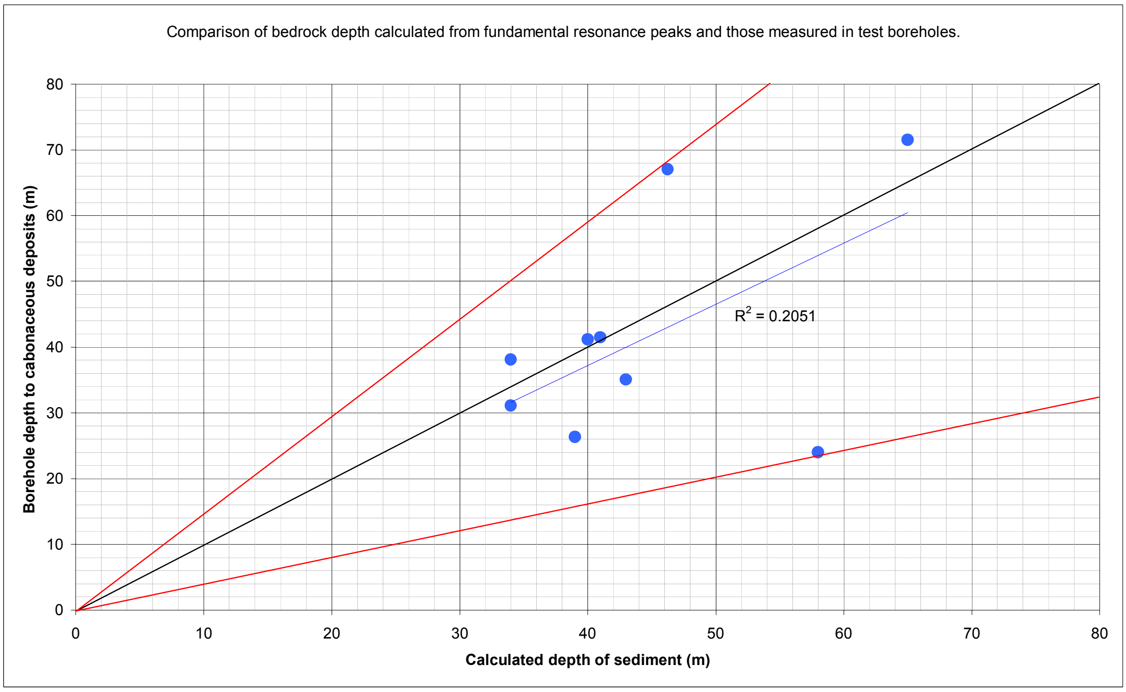

Figure 11.6 **Comparison of GeoEng depths and calculated depths for 9 sites.**

This comparison indicates that, while the spectral method of calculating the sediment depth is potentially capable of achieving excellent results, there is also the tendency for it to produce some results that are unrepresentative of the actual depths. Consequently, while the method shows good potential for calculating average and typical sediment depths for a limited region, the depths calculated for particular sites within that region should not be treated as actual depths without supporting evidence from other sources. However, the fact that the comparisons of measured and calculated sediment depths shows positive statistical correlation is an indication that the spectra used to calculate the depths and to conduct the microzonation are valid.

CHAPTER 12 SIGNIFICANCE OF WORK DONE IN THIS THESIS

Isoseismal map of Bundaberg 1997 earthquake

In carrying out investigations into earthquake risk, it is important to have information about the distribution of the shaking effects of past earthquakes within the area under investigation. Isoseismal maps show the distribution of the perceived shaking effects of earthquakes as reported by witnesses.

Previous investigators have published isoseismal maps of the main shock (Everingham, et al, 1982) and two aftershocks (Rynn et al, 1987) of the 1918 Bundaberg earthquake, and the main shock of the 1935 Gayndah earthquake (Bryan&Whitehouse, 1938). The isoseismal map of the 1997 Bundaberg, presented in this thesis, adds to the body of knowledge available for determining the actual radius of perception of earthquakes occurring in the Bundaberg area. Comparison of this knowledge with the calculated (i.e. the expected) radius of perception has confirmed that horizontal amplification of ground motion caused by seismic waves is occurring in the Bundaberg area.

Earthquake hazard analysis for the Bundaberg area

The work carried out in this thesis has shown that Gumbel Type I analysis of extreme events can be used to obtain verifiable statistics that describe the earthquake history of the Bundaberg area over the past century. These statistics have been used to forecast, with any given confidence, recurrence periods, in the Bundaberg area, for earthquakes of any given magnitude. Conversely, the statistics have been used to estimate the probability of any number of given magnitude earthquakes occurring within any given time period. They have also been used to estimate the historical *b* value for seismicity in the Bundaberg area.

Methodology for deriving Nakamura spectra from microseismograms

Numerous papers are extant relating to the use of spectra, derived by various means, in the analysis of ground motion. Despite this abundance of literature the author found none that provided a description of the methodology, used to derive those spectra, that was sufficiently detailed to replicate the results produced in those papers using the same methodology. The methodology used in this thesis to derive

Nakamura spectra is explained in sufficient detail for other investigators to faithfully replicate the work presented here. Computer programs are provided to automate the process.

Methodology for performing seismic risk microzonation

A search of the literature relating to microzonation indicated that no standard methodology for that process is being used. Each investigator provides a different approach to the task, and presents the results in a variety of ways.

The methodology used in this thesis produces results that are internally consistent within the area of microzonation, and complementary to the Australian building code. The methodology can be applied in a consistent and unambiguous manner using computer programs that are provided to automate the process. The microzonation area can be extended in a step-wise fashion by collecting data over time, and over an extended area, and incorporating the new data into the existing database. The results produced by the computer program are stored in files that can be imported into a Geographic Information System (GIS) that can produce relative seismic risk contouring of the microzonation area.

Microzonation of Bundaberg City

The microzonation of Bundaberg City, presented in this thesis, provides important earthquake risk mitigation information and civil engineering data that was previously unavailable.

The results of the microzonation provide important policy planning information for governments at all levels – particularly for local government bodies and disaster action organisations. Such knowledge provides a basis for effective town planning. It facilitates sensible placement of structures such as hospitals, schools and major utility facilities. It enables disaster plans to be put in place that have a higher chance of success than might otherwise be the case. In conjunction with the Australian building code the microzonation results will allow engineers to refine structure designs, in the Bundaberg area, with a view to minimising vulnerability to damage from earthquakes.

Use of Nakamura spectra as a reliable indicator of sediment depth

The successful use of the Nakamura spectra to estimate the depth of sediments within the Bundaberg area served two notable purposes. Firstly, it validated the use of the spectra in carrying out the microzonation by demonstrating that the spectra could be used to predict independently verifiable information. Secondly, it lends support to the use of Nakamura spectra as a tool for indirectly estimating sediment depths in the absence of any direct measurements.

BIBLIOGRAPHY

Abers G.A., Beavan J., Horton S., Jaume S. and Triep E., *Large Accelerations and Tectonic Setting of the May 1993 Shumagin Islands Earthquake Sequence*, Bulletin of the Seismological Society of America, Vol. 85, No61, pp 1730-1738, December 1995.

Aki K., *Local site effects on strong ground motion*, Unknown source, unknown date (seems to be a precursor to his 1993 paper).

Aki K., Local site effects on weak and strong ground motion, Tectonophysics, 218, pp. 93-111, 1993.

Anderson J.G., Bodin P., Prince J., Singh S.K., Quass R. and Onate M., *Strong ground motion from the Michoacan, Mexico, earthquake*, Science, Vol 233, pp1043-1049, 1986.

Andrews D.J. (U.S. Geological Survey, Menlo Park, California 94025), *Objective Determination of Source Parameters and Similarity of Earthquakes of Different Size*, pp. 259-267, No Journal ref on paper.

Bard P-Y., *Effects of surface geology on ground motion: Recent results and remaining issues*, 10th European Conference on Earthquake Engineering, Duma (ed.), 1995. ISBN 90-5410-528-3.

Benjamin Jack R. and Cornell Carl Allin, *Probability, Statistics and Decision for Civil Engineers*, McGraw Hill, 1970. ISBN 07-004549-6

Beresnev I.A and Wen K-L., *The Accuracy of Soil Response Estimates Using Soil-to-Rock Spectral Ratios*, Bulletin of the Seismological Society of America, Vol. 86, No. 2, pp. 519-523, April 1996.

Beresnev I.A. and Wen K-L., *Review: Nonlinear Soil Response – A Reality?*, Bulletin of the Seismological Society of America, Vol. 86, No 6, pp 1964-1978, December 1996.

Boatwright J., Seekins L.C., Fumal T.E., Lui H.P. and Mueller C.S, *Ground motion amplification in the Marina district*, Bulletin of the Seismological Society of America, Vol. 81, pp 1980-1997, 1991.

Bobée B. and Rasmussen P., *Recent advances in flood frequency analysis,* Rev. Geophys. Vol. 33 Suppl., 1995, in the *U.S. National Report to International Union of Geodesy and Geophysics 1991-1994,* available on line at http://www.agu.org/revgeophys/bobee01/bobee01.html, April 15, 1998 at 12:09 Australian Eastern Time.

Bolt B.A., *Earthquakes*, W.H.Freeman and Company, Revised ed. 1978.

Bonilla L.F., Steidl J.H., Lindley G.T., Tumarkin A.G. and Archuleta R.J., *Site Amplification in the San Fernando Valley, California: Variability of Site-Effect Estimation Using the S-Wave, Coda, and H/V Methods*, Bulletin of the Seismological Society of America, Vol. 87, No 3, pp 710-730, June 1997.

Borcherdt R.D., *Effects of Local Geology on Ground Motion Near San Francisco Bay*, Bulletin of the Seismological Society of America, Vol. 60, No 1, pp 29-61, February 1970.

Borcherdt R.D., Glassmoyer G., Der Kiureghian A. and Cranswick E., *Results and data from seismologic studies following earthquakes of December 7, 1988 near Spitak, Armenia, S.S.R.*, U.S. Geological Survey, Open-File Report, pp89-163A, 1989.

Borcherdt R.D. and Glassmoyer G., *On the characteristics of local geology and their influence on ground motions generated by the Loma Prieta earthquake in the San Fransiscoi Bay region, California*, Bulletin of the Seismological Society of America, Vol. 82, pp 603-641, 1992.

Boreham B.W., *Hazard Analysis Methodology for Calculance of recurrance relationships*, personal notes, 1996.

Boreham B.W., McKavanagh B., McCue K.F., Zammit R., Muller C. and Bugden C., *Comparison of Methodologies Used in the Microzonation of Earthquake Risk Assessment for the Central Queensland Regional Centres of Rockhampton and Mackay*, paper S51B02, American Geophysical Union Western Pacific Geophysics Meeting, Brisbane, July 23-27, 1996, EOS Transactions, AGU, Vol. 77, No. 22, p W88, 1996.

Bryan W.H. and Whitehouse F.W., *The Gayndah Earthquake of 1935*, The proceedings of the Royal Society of Queensland, Vol. XLIX, No. 10, pp106-119, June 1938. (Also in University of Queensland Papers, Dept. of Geology, Vol. 1, 1938, Nos. 5 & 6.)

Bullen K.E & Bolt B.A., *An introduction to the theory of seismology*, Fourth Ed., Cambridge University Press, 1985.

Burridge R., Mainardi F. and Servizi G., *Soil Amplification of Plane Seismic Waves*, Physics of the Earth and Planetary Interiors, 22(1980) pp 122-136, Elsevier, Amsterdam, Netherlands.

Burton, *Perceptible Earthquakes in the United Kingdom*, Geophys J R ast Soc 54, 475-479, 1978.

Burton P., *Seismic Risk in Southern Europe through to India examined using Gumbel's third distribution of extreme values*, Geophys J R astr Soc. 59. pp 249 – 280, 1979.

Castro R.R., Munguia L. and Brune J.N., *Source Spectra and Site Response from P and S Waves of Local Earthquakes in the Oaxaca, Mexico, Subduction Zone*, Bulletin of the Seismological Society of America, Vol. 85, No 3, pp 923-936, June 1995.

Chavez-Garcia F.J., Sanchez L.R. and Hatzfeld D., *Topographic Site Effects and HVSR. A Comparison Between Observations and Theory*, Bulletin of the Seismological Society of America, Vol. 86, No 5, pp 1559-1573, October 1996.

Chavez-Garcia F.J., Rodriguez M., Field E.H. and Hatzfeld D., *Topographic Site Effects, A Comparison of Two Nonreference Methods*, Bulletin of the Seismological Society of America, Vol. 87, No 6, pp 1667-1673, December 1997.

Clitheroe G.M., and Taber J.J., *Assessing earthquake site response using Microtremors: A case study in Wellington City, New Zealand*, Pacific Conference on Earthquake Engineering, Australia, 20-22 November, 1995.

Cornell C.A., *Engineering Seismic Risk Analysis*, Bulletin of the Seismological Society of America Vol. 58, No. 5, pp1583-1606, October, 1968.

Cornell C.Allin., and Vanmarcke Erik.H., *The major influences on seismic risk*, in Proceedings 4th World Conference on Earthquake Engineering, Santiago, Chile, pp 69-83, 1969.

Cornell C.A. and Winterstein S.R., *Temporal and magnitude dependence in earthquake recurrence models*, Bullelin Seismological Society of America, 78 (4), pp 1522-1537, 1988.

Coutel F. and Mora P., *Simulation Based Comparison of Four Site-Response Estimations Techniques*, Submiytted to Bulletin of the Seismological Society of America, Revised manuscript of September 18, 1997.

Coutel F., L*arge scale 3D modelling of seismic waves: studies of site effects for estimating earthquake risk*, Submitted in fulfilment of the requirements for the degree of Doctor of Philosophy in the Department of Earth Sciences, QUAKES, The University of Queensland, May 26, 1998.

Crone A.J., Machette M.N., and Bowman J.R, *Episodic nature of earthquake activity in stable continental regions revealed by palaeoseismicity studies of Australia and North American Quaternary faults*, Australian Journal of earth Sciences 44, pp 203 – 214, 1997.

Cuthbertson R.J. and Jaume S.C, *Earthquake Hazard in Queensland*, Queensland University Advanced Centre for Earthquake Studies, QUAKES Report #1, May 1996.

Cuthbertson R., Winter M., and Jaume S., *Preliminary results of Brisbane microtremor survey*, Australian Earthquake Engineering Society, Proceedings of the 1998 Conference, Perth, Western Australia, Paper 12, 1998. ISBN 0-7340-1442-2 (Also presented at the 2nd Annual AGSO Cities Project Workshop, Townsville 8 July 1998.)

Darragh R.B. and Shakal A.F., *The Site Response of Two Rock and Soil Station Pairs to String and Weak Ground Motion*, Bulletin of the Seismological Society of America, Vol. 81, No 5, pp 1885 - 1899, October 1991.

Dimitriu P.P., Papaioannou Ch.A. and Theodulidis N.P., *EURO-SEISTEST Strong-Motion Array near Thessaloniki, Northern Greece: A Study of Site Effects*, Bulletin of the Seismological Society of America, Vol. 88, No 3, pp 862 - 873, June 1998.

Donovan N.C., *Earthquake hazards for buildings*, Dames & Moore, Engineering Bulletin, 46, 19??.

Dowrick D.J., *The Modified Mercalli Earthquake Intensity Scale – Revisions Arising from Recent Studies of New Zealand earthquakes*, Bulletin of the New Zealand National Society for Earthquake Engineering, Vol. 29, No. 2, pp 92-106, June 1996.

Doyle H. & Underwood R., *Seismological Stations in Australia*, Aust. J. Sci., Vol. 28, No. 2, pp 40-43, 1965.

Dravinski M., Ding G., and Wen K.-L., *Analysis of Spectral Ratios for Estimating Ground Motion in Deep Basins*, Bulletin of the Seismological Society of America, Vol. 86, No. 3, pp 646-654, June 1996.

Eiby G.A., *The Modified Mercalli scale of earthquake intensities and its use in New Zealand*, New Zealand Journal of Geology and Geophysics, 9(1/2), pp122-124, 1966

Ellis P.L and Whitaker W.G., *Geology of the Bundaberg 1:250 000 Sheet Area*, Report No. 90, Geological Survey of Queensland, 1976.

Esteva L., *Seismicity*, Seismic Risk and Engineering Decisions (Developments in geotechnical Engineering 15), Elsevier Scientific Publishing Company, 1976, Chapter 6. 1976.

Everingham I.B. McEwin A.J. & Denham D., *Atlas of Isoseismal Maps of Australian Earthquakes*, Australian Department of National Development & Energy, Bureau of Mineral resources, Geology and Geophysics, Bulletin 214, Canberra, 1982.

Ferritto J.M., *Repeatability of Microseism Measurements in Port Hueneme Case Study*, Bulletin of the Seismological Society of America, Vol. 86, No. 2, pp. 428-435, April 1996.

Field E. and Jacob K., *The Theoretical Response of Sedimentary Layers to Ambient Seismic Noise*, Geophysical Research Letters, Vol. 20, No. 24, PP. 2925-2928, December 23, 1993.

Field E. and Jacob K., *A Comparison and Test of Various Site-Response Estimation Techniques, Including Three That Are Not Reference-Site Dependent*, Bulletin of the Seismological Society of America, Vol. 85, No. 4, pp. 1127-1143, August 1995.

Field E.H., *Spectral Amplification in a Sedimen-Filled Valley Exhibiting Clear Basin-Edge-Induced Waves*, Bulletin of the Seismological Society of America, Vol. 86, No. 4, pp. 991-1005, August 1996.

Furumura M., Sasatani T. and Furumura T., *Generation of Basin-Induced Surface Waves Observed in the Tokachi Basin, Hokkaido, Japan*, J. Phys. Earth, 45, pp. 287-305, 1997.

Ganev T., Yamazaki F., Ishizaki H. and Kitazawa M., *Earthquake Response of the Higashi-Kobe Bridge*, INCEDE Report 15, 2000.

Gao S., Lui H., Davis P.M. and Knopoff L., *Localized Amplification of Seismic Waves and Correlation with Damage due to the Northridge Earthquake: Evidence for Focusing in Santa Monica*, Bulletin of the Seismological Society of America, Vol. 86, No 1B, pp S209-S230, February 1996.

Gaull B.A. Michael-Leiba M.O. & Rynn J.M.W., *Probabilistic earthquake risk maps of Australia*, Australian Journal of Earth Sciences 37, pp 169-187, 1990.

Gaull B.A, Kagami H. and Taniguchi H., *The Microzonation of Perth, Western Australia, Using Microtremor Spectral Ratios*, Earthquake Spectra, Vol. 11, No. 2, May 1995.

Geo-Eng Australia Pty. Ltd., *Bundaberg groundwater investigation project 1998/99, Phase 1&2 draft final report*, Report to Department of Natural Resources, Bundaberg, Queensland, 15 March 1999 (unpublished).

Geological Survey of Queensland, *Bundaberg sheet SG 56-2: Australia 1:250 000 Geological Series*, 1st Ed., 1974

Greenhalgh S.A., Denham D., McDougall R. and Rynn J.M., *Magnitude-Intensity Relations for Australian Earthquakes*, Bulletin of the Seismological Society of America, Vol. 78, No 1, pp 374-379,, February 1988.

Gumbel E.J., *Statistical Theory of Extreme Values and Some Practical Applications*, U. S. National Bureau of Standards Applied Mathematics Series, No. 33, Washington D. C., 1954.

Gumbel E.J., *Statistics of Extreme values*, Columbia University Press, New York, 1958.

Haan Charles T., *Statistical Methods in Hydrology*, The Iowa State University Press, 1977.

Hamill T.M. and Colucci S.J., *Verification of Eta/RSM Short-Range Ensemble Forcasts,* Department of Soil, Crop and Atmospheric Sciences, Cornell University, Ithica, New York, 30 July 1996, available on line at http://ensemble.cit.cornell.edu/sref.htm, April 15, 1998 at 11:35 Australian Eastern Time.

Hamill T.M. and Colucci S.J., *Evaluation of Eta/RSM Ensemble Probabilistic Precipitation Forcasts,* Department of Soil, Crop and Atmospheric Sciences, Cornell University, Ithica, New York, 22 February 1997, available on line at http://ensemble.cit.cornell.edu/sref2v2.htm, April 15, 1998 at 11:18 Australian Eastern Time.

Hanks T.C and Krawinkler H., *The 1989 Loma Prieta earthquake and its effects: introduction to the special issue*, Bulletin of the Seismological Society of America, Vol. 81, pp. 1783-1812, 1991.

Harrington H.J., *Earthquake prediction and greater Sydney*, Australian Geologist (Letters to the Editor), March 31 1997.

Hedley C., *The Queensland Earthquake of 1918*, Transactions of the Royal Geological Society of Australasia (Queensland), Reports of the Great Barrier Reef Committee, Vol. 1, 13 July 1925.

Hema Maps Pty. Ltd., *Bundaberg including Bargara, Elliott Heads, Burnett Heads and Moore Park*, Edition 3, 1997.

Holmes W.T., *Recent Developments in Earthquake Mitigation in the United States*, Bulletin of the New Zealand National Society for Earthquake Engineering, Vol. 29, No. 2, June 1996.

Hough S.F, Borcgerdt R.D, Friberg P.A., Busby R., Field F.H. and Jacob K.H., *The role of sediment-induced amplification in the collapse of the Nimitz freeway during the October 17, 1989 Loma Prieta earthquake,* Nature Vol 344, pp 853-855, 1990.

Jackson D.D., and Kagan Y.Y, *Testable Earthquake Forecasts for 1999*, Seismological Research Letters, Vol. 70, No. 4, pp 393-403, July/August 1999.

Jaume S.C., Jones T., Winter M. and Coutel F., *Earthquake Site Amplification in the Cairns Region Estimated From Microtremor Recordings*, Cities Project Workshop, Townsville, 1997

Jaume S., Winter M. and Cuthbertson R., *Using long distance earthquakes to study local site amplification*, Australian Earthquake Engineering Society, Proceedings of the 1998 Conference, Perth, Western Australia, Paper 13, 1998. ISBN 0-7340-1442-2 (also in QUAKES Report #3, October 1998)

Johnson R.W. (Ed), *Intraplate Volcanism in Eastern Australia and New Zealand*, Cambridge University Press in association with the Australian Acadamy of Science, 1989.

Jones T.D., Gibson G., McCue K.F., Denham D., Gregson P.J. and Bowman J.R., *Three large intraplate earthquakes near Tennant Creek, Northern Territory, Australia on 22 January 1988*, Bureau of Mineral Resources Journal of Australian Geology and Geophysics, 1992.

Jones T., Granger K. and Scott G., *Towards best practice in Australian earthquake risk assessment*, Australian Earthquake Engineering Society, Proceedings of the 1998 Conference, Perth, Western Australia, Paper 10, 1998. ISBN 0-7340-1442-2

Jones T., Laume S., Granger K., Scott G. and Cuthbertson R., *Earthquake risk in Cairns: A pilot study*, Australian Earthquake Engineering Society, Proceedings of the 1998 Conference, Perth, Western Australia, Paper 11, 1998. ISBN 0-7340-1442-2. (Also in QUAKES Report #3, October 1998.)

Kagami H., Okada S., Shiono K., Oner M., Dravinski M and Mal A.K., *Observation of 1- to 5-second Mocrotremors and their Application to Earthquake Engineering. Part III. A Two-Dimensional Study of Stie Effects in the San Fernando Valley*, Bulletin of the Seismological Society of America, Vol. 76, No 6, pp 1801-1812, December 1986.

Kato K., Keiiti A. and Takemura M., *Site Amplification from Coda Waves: Validation and Application to S-Wave Site Response*, Bulletin of the Seismological Society of America, Vol. 85, No 2, pp 467-477, April 1995.

Konno K. and Ohmachi T., *Ground-Motion Characteristics Estimated from Spectral Ratio between Horizontal and Vertical Components of Microtremor*, Bulletin of the Seismological Society of America, Vol. 88, No 1, pp 228-241, February 1998.

Khan A., *Possible effect of a dam reservoir on the seismicity of the area*, Australian Earthquake Engineering Society, Proceedings of the 1998 Conference, Perth, Western Australia, Paper 22, 1998. ISBN 0-7340-1442-2

Lachet C., Hatzfeld D., Bard P-Y., Theodulidis N., Papaioannou C and Savvaidis A., *Site Effects and Microzonation in the City of Thessaloniki (Greece) Comparison of Different Approaches*, Bulletin of the Seismological Society of America, Vol. 86, No. 6, pp. 1692-1703, December 1996.

Lam N., Wilson J., Edwards M., and Hutchinson G., *A displacement based prediction of the seismic hazard for Australia*, Australian Earthquake Engineering Society, Proceedings of the 1998 Conference, Perth, Western Australia, Paper 20, 1998. ISBN 0-7340-1442-2

Lermo J. and Chavez-Garcia F.J., *Are Microtremors Useful in Site Response Evaluation?*, Bulletin of the Seismological Society of America, Vol. 84, No 5, pp 1350-1364, October 1994.

Lermo J. and Chavez-Garcia F.J., *Site Effect Evaluation Using Spectral Ratios With Only One Station*, Bulletin of the Seismological Society of America, Vol. 83, No 5, pp 1574-1594, October 1993.

Lewis Ajita, Project Manager, Newcastle Earthquake Database Newcastle Region Library, *The Newcastle Earthquake*, http://www.newcastle.infohunt.nsw.gov.au/library/eqdb/earthq.htm, available online 14:30AET 16 August, 1999.

Lomnitz C., *Global Tectonics and Earthquake Risk*, in Developments in Geotectonics 5, Elsevier Scientific Publishing Company, Amsterdam – London – New York, 1974.

Lomnitz Cinna, and Rosenblueth Emilio, (Editors), *Seismic Risk and Engineering Decisions (Developments in Geotechnical Engineering 15)*, Elsevier Scientific Publishing Company, 1976a.

Lomnitz Cinna, and Singh S.K., *Earthquakes and Earthquake Prediction*, Seismic Risk and Engineering Decisions (Developments in geotechnical Engineering 15), Elsevier Scientific Publishing Company, 1976, Chapter 2. 1976b.

Louie J., *What is Richter Magnitude?*, Available online at http://www.seismo.unr.edu/ftp/pub/louie/class/100/magnitude.html, 11:55am 13 March 2001.

Malagnini L., Tricarico P., Rovelli A., Herrmann R.B., Opice S., Biella G. and Franco R.de., *Explosion, Earthquake, and Ambient Noise Recordings in a Pliocene Sediment-Filled Valley: Inferences on Seismic Response Properties by Reference- and Non-Reference-Site Techniques*, Bulletin of the Seismological Society of America, Vol. 86, No. 3, pp. 670-682, April 1996.

McCue K., *Seismicity and Earthquake Hazard in Australia*, in Proceedings of the seminar: Earthquake Engineering and Disaster Reduction pp 9-14, (Eds J Wilson & C van Doorn), Australian Earthquake Engineering Society, Melbourne University, 25 October, 1993a.

McCue K. (Compiler), Gibson G., Michael-Leiba M., Love D., Cuthbertson R., and Horoschun G., *Earthquake Hazard Map of Australia 1991*, 1993b.

McCue K*, Atlas of Isoseismal Maps of Australian Earthquakes Part 3*, Australian Department of Primary Industries and Energy, Australian Geological Survey Organisation, AGSO Record 1995/44, Canberra, 1996a.

McCue K. F. and Boreham B. W., *Microzonation for an earthquake risk assessment at Rockhampton Queensland and implications for AS1170.4*, Australian Cival/Structural Engineering Transactions, Volume CE39, No. 1, September 1996b.

McCue K and Love D., *Microtremor Survey of Adelaide*, Australian Earthquake Engineering Society, Proceedings of the 1997 Conference, Brisbane, Queensland, Paper 19, 1997. ISBN 0-7325-1072-4.

McCue K., Somerville M. and Sinadinovski C., *GSHAP and the proposed Australian Earthquake Hazard Map*, Australian Earthquake Engineering Society, Proceedings of the 1998 Conference, Perth, Western Australia, Paper 18, 1998. ISBN 0-7340-1442-2

McCue K, *Seismic Hazard Mapping in Australia, The Southwest Pacific and Southeast Asia*, Report on Region 10, Global Seismic Hazard Assessment Program, A Project of IASPEI, available on line at http://seismo.ethz.ch/gshap/swpacific/swpacific.html 17 February 2000.

McEvilly Tomas V., *Seismological Instrumentation*, Seismic Risk and Engineering Decisions (Developments in geotechnical Engineering 15), Elsevier Scientific Publishing Company, 1976, Chapter 10. 1976.

McFadden P., Sinadinovski C., McCue K. and Collins C., *Is Earthquake Risk Uniform Across Australia?*, Draft unpublished paper, 2000.

McGregor P.M. & Ripper I.D., *Notes on Earthquake Magnitude Scales*, Australian Bureau of Mineral Resources, Record 1976/56, 1976.

Melchers R.E., *On Intra-plate Earthquakes and Existing Structures*, Australian Civil Engineering Transactions, Vol CE36, No. 4, pp 265 – 272, November 1994.

Merz H.A. and Cornell C.A., *Seismic risk analysis based on quadratic magnitude-frequency law*, Bulletin of the Seismological Society of America, Vol. 63 No. 6, pp 1999 – 2006, December, 1973.

Michael-Leiba M. and Jensen V., *Seismic Microzonation of Launceston, Tasmania, Australian* Geological Survey brochure, undated circa 1999.

Milana G., Barba S., Del Pezzo E. and Zambonelli E., *Site Response from Ambient Noise Measurements: New Perspectives from an Array Study in Central Italy*, Bulletin of the Seismological Society of America, Vol. 86, No. 2, pp. 320-328, April 1996.

Milne Prof. J., *Earth Movements in Australia*, The Argus, Saturday, October 10, 1885.

Milne J., *Seismology*, 1st Ed., Kegan Paul, Trench, Truber, London, 1898.

Nakamura Y., *A Method for Dynamic Characteristics Estimation of Subsurface using Microtremor on the Ground Surface*, Quarterly Report of Railway Technical Research Institute Vol. 30, No. 1, pp. 25-33, February 1989.

Newmark N. and Rosenblueth E., *Fundamentals of Earthquake Engineering*, Prentice Hall Inc., 1971.

Nordquist J.M., *Theory of Largest Values Applied to Earthquake Magnitudes*, Transactions, American Geophysical Union, Vol. 26, Part I, August 1945.

Papastamatiou D., *Incorporation of crustal deformation to seismic hazard analysis*, Bulletin of the Seismological Society of America, Vol. 70, No. 4, pp 1321 – 1335, August 1980.

Pigot E.F., Riverview College Observatory, Seismological Bulletin, June 1918,

Press W.H., Teukolsky S.A., Vetterling W.T. and Flannery B.P, *Numerical Recipes in C: The Art of Scientific Computing*, 2nd Ed., Cambridge University Press, 1992.

QUAKES (Queensland University Advanced Centre for Earthquake Studies), *Queensland Earthquake Database (QED)*, Excel Spreadsheet, copy obtained February 2000.

Queensland Electricity Commission (QEC), *Stanwell Chimney Seismic Risk Study*, Queensland Power Consultants, January 1986.

Rautian T.G. and Khalturin V.I, *The Use of the Coda for Determination of the Earthquake Source Spectrum*, Bulletin of the Seismological Society of America, Vol. 68, No 4, pp 923-948, August 1978.

Richter C.F., *Elementary Seismology*, W.H.Freeman and Company, 1958.

Robertson A.D., *Revision of the Cainozoic geology between the Kolan and Elliott Rivers*, Queensland Government Mining Journal, pp350-363, July 1979.

Robertson A.D.C., *Geophysical Exploration and Drilling of the Tararan Vent*, Geological Survey of Queensland Record 1993/4, 1993.

Rynn J.M.W., *A Reapraisal of Queensland's Largest Known Earthquake – The "Queensland" Earthquake of 6 June 1918, Magnitude ML 6.2*, private paper, Circa 1985-86.

Rynn J.M.W., *Queensland Seismic Risk Study*, University of Queensland, Department of Geology and Mineralogy, Report QSRS – 4, 1986.

Rynn J.M.W. Denham D. Grenhalgh S. Jones T, Gregson P.J. McCue K. & Smith R.S., *Atlas of Isoseismal Maps of Australian Earthquakes Part 2*, Australian Department of National Development & Energy, Bureau of Mineral resources, Geology and Geophysics, Bulletin 222, Canberra, 1987.

(SAA) Standards Association of Australia, *AS 2121 – 1979, The design of earthquake-resistant buildings (known as the SAA Earthquake Code)*, Standards Australia, 1979 (Withdrawn, superseded by AS 1170.4).

(SAA) Standards Association of Australia, *AS 1170.4 – 1993, Minimum design loads on structures (known as the SAA Loading Code) Part4: Earthquake loads*, Standards Australia, 1993a. ISBN 0-7262-8297-9

(SAA) Standards Association of Australia, *AS 1170.4 Supp1 – 1993, Minimum design loads on structures (known as the SAA Loading Code) Part4: Earthquake loads Commentary (Supplement to AS 1170.4 - 1993*, Standards Australia, 1993b. ISBN 0-7262-8298-7

(SAA) Standards Association of Australia, *AS1289.6.3.1 – 1993, Method 6.3.1: Soil strength and consolidation tests – Determination of penetration resistance of a soil – Standard penetration test (SPT)*, Standards Australia, 1993c. ISBN 0-7262-8117-4

Seekins L.C., Wennerberg L., Margheriti and Liu H-P., *Site Amplification at Five Locations in San Francisco, California: A Comparison of S Waves, Codas, and Microtremors*, Bulletin of the Seismological Society of America, Vol. 86, No. 3, pp 627-635, June, 1996.

Seht M. I-v. and Wohlenberg J., *Microtremor Measurements Used to Map Thickness of Soft Sediments*, Bulletin of the Seismological Society of America, Vol. 89, No. 1, pp 250-259, February, 1999.

Singh S.K., Lermo J., Dominguez T., Ordaz M., Espinosa J.M., Mena E. and Quas R., *The Mexico Earthquake of September 19, 1985 – A study of amplification of seismic waves in the valley of Mexico with respect to a hill zone site*, Earthquake Spectra, Vol 4, pp653-673, 1988.

Somerville M.R., Kagami H. and McCue K.F., *Seismic Amplification Determined from Microtremor Monitoring at Alluvial and Rock Sites in Newcastle*, Bulletin of the New Zealand National Society for Earthquake Engineering, Vol. 26, No. 2, June 1993.

Somerville M., McCue K. and Sinadinovski C., *Response Spectra Recommended for Australia*, Australian Earthquake Engineering Society, Proceedings of the 1998 Conference, Perth, Western Australia, Paper 19, 1998. ISBN 0-7340-1442-2

Spassov E. Kennett B. & Weeks J., *Seismogenic zoning of southeast Australia*, Australian Journal of Earth Sciences 44, pp 527-534, 1997.

Steidl J.H., Tumarkin A.G. and Archuleta R.J., *What is a Reference Site?*, Bulletin of the Seismological Society of America, Vol. 86, No 6, pp 1733-1748, December 1996.

Su F. and Aki K., *Site Amplification factors in Central and Southern California Determined from Coda waves*, Bulletin of the Seismological Society of America, Vol. 85, No 2, pp 452-466, April 1995.

Suter M., Carrillo-Martinez M, and Quintero-Legorreta O., *Macroseismic Study of Shallow Earthquakes in the Central and Eastern Parts of the Trans-Mexican Volcanic Belt, Mexico*, Bulletin of the Seismological Society of America, Vol. 86, No. 2, pp. 1952-1963, December 1996.

Toshinawa T., Taber J.J. and Berrill J.B., *Distribution of Ground-Motion Intensity Inferred from Questionnaire Survey, Earthquake Recordings, and Microtremor Measurements – A Case Study in Christchurch, New Zealand, during the 1994 Arthurs Pass Earthquake*, Bulletin of the Seismological Society of America, Vol. 87, No 2, pp 356-369, April 1997.

Theodulidis N., Bard P.-Y., Archuleta R. and Bouchon M., *Horizontal-to-Vertical Spectral ratio and Geological Conditions: The Case of Garner Valley Downhole Array in Southern California*, Bulletin of the Seismological Society of America, Vol. 86, No. 2, pp. 306-319, June 1996.

Turnbull M.L., *Proposed Earthquake Risk Assessment Map for Bundaberg – A lay perspective,* in *Diverse Dialogues*, O'Brial et al (Eds), Central Queensland University Press, pp253-261, 1997.

Turnbull M.L., *A Direct Comparison of McCue and Boreham's (1996) Return Period Results for Rockhampton and Turnbull and Boreham's (1998) Results for SE Queensland*, April 1998a, (unpublished).

Turnbull M.L. and Boreham B.W., *An estimation of earthquake hazard in southeast Queensland using Lomnitz' extreme value method and Gumbel's Type I probability*, April 1998b, (unpublished).

Turnbull M.L., *A Discussion of the Felt Reports Resulting from the Bundaberg Earthquake, May 29 1997*, Bundaberg: A Regional Perspective, Neuenfeldt et al (Eds.), Centre for Social Science Research, Central Queensland University, ISBN 1-876674-02-4, pp63-78, January 2000.

Turner H.H. (Ed), *International Seismological Summary, 1918*, University Observatory, Oxford, 1923.

Vanmarcke Erik H., *Structural Response to Earthquake*, Seismic Risk and Engineering Decisions (Developments in Geotechnical Engineering 15), Elsevier Scientific Publishing Company, 1976, Ch 8, 1976.

Wen K.-L., Beresnev I.G., and Yeh Y.T., *Investigation of non-Linear Site Amplification at two Downhole Strong Motion Arrays in taiwan*, Earthquake Engineering and Structural Dynamics, Vol. 24, pp 313 – 324, 1995a.

Wen K.-L., Peng H.-Y., Lui L.-F., and Shin T.-C., *Basin Effects Analysis from a Dense Strong Motion Observation Network*, Earthquake Engineering and Structural Dynamics, Vol. 24, pp 1069 - 1083, 1995b.

Yamanaka H., Dravinski M. and Kagami H., *Continuous Measurements of Microtremors on Sediments and Basement in Los Angeles, California*, Bulletin of the Seismological Society of America, Vol. 83, No 5, pp 1595-1609, October 1993.

Yamanaka H., Takemura M., Ishida H. and Niwa M., *Characteristics of Long-Period Microtremors and Their Applications in Exploration of Deep Sedimentary Layers*, Bulletin of the Seismological Society of America, Vol. 84, No 6, pp 1831-1841, Decenber 1994.

Yegulalp T.M. and Kuo J.T., *Application of Extreme Statistics to the Maximum Magnitude Earthquakes*, Transactions, American Geophysical Union, Vol. 47, 1996, p163 (Extract only).

Yegulalp T.M. and Kuo J.T., *Statistical Prediction of the occurrence of maximum magnitude Earthquakes*, Bulletin Seismological Society of America Vol. 64, No. 2, April 1974.

Zammit R., *Seismic Hazard of City of Mackay*, Central Queensland University, Honours Project Report, 1995.

Zeng Y. and Benites R., *Seismic Response of Multi-Layered Basins with Velocity Gradients upon Incidence of Plane Shear Waves*, Earthquake Engineering and Structural Dynamics, Vol. 27, pp. 15-28, 1998.

APPENDIX A – MODIFIED MERCALLI (MM) SCALE OF EARTHQUAKE INTENSITY

(New Zealand version, 1965, after Eiby, 1966)

MM I

Not felt by humans, except in especially favourable circumctances, but birds and animals may be disturbed. Reported mainly from the upper floors of buildings more than ten storeys high. Dizziness or nausea may be experienced. Branches of trees, chandeliers, doors and other suspended systems of long natural period may be seen to move slowly. Water in ponds, lakes, reservoirs, etc., may be set into seiche oscillation.

MM II

Felt by a few persons at rest indoors, especially by those on upper floors or otherwise favourably placed. The long-period effects listed under MM I may be more noticeable.

MM 11I

Felt indoors, but not identified as an earthquake by everyone. Vibrations may be likened to the passing of light traffic. It may be possible to estimate the duration, but not the direction. Hanging objects may swing slightly. Standing motorcars may rock slightly.

MM IV

Generally noticed indoors, but not outside. Very light sleepers may be awakened. Vibration may be likened to the passing of heavy traffic, or to the jolt of a heavy object falling or striking the building. Walls and frame of buildings are heard to creak. Doors and windows rattle. Glassware and crockery rattle. Liquids in open vessels may be slightly disturbed. Standing motorcars may rock, and the shock can be felt by their occupants.

MM V

Generally felt outside, and by almost everyone indoors. Most sleepers awakened. A few people frightened. Direction of motion can be estimated. Small unstable objects are displaced or upset. Some glassware and crockery may be broken. Some windows cracked. A few earthware toilet fixtures cracked. Hanging pictures move. Doors and shutters swing. Pendulum clocks stop, start, or change rate.

MM VI

Felt by all. People and animals alarmed. Many run outside. Difficulty experienced in walking steadily. Slight damage to Masonry D. Some plaster cracks or falls. Isolated cases of chimney damage. Windows, glassware, and crockery broken. Objects fall from shelves, and pictures from walls. Heavy furniture moves. Unstable furniture overturned. Small church and school bells ring. Trees and bushes shake, or are heard to rustle. Loose material may be dislodged from existing slips, talus slopes, or shingle slides.

MM VI

General alarm. Difficulty experience in standing. Noticed by drivers of motorcars. Trees and bushes strongly shaken. Large bells ring. Masonry D cracked and damaged. A few instances of damage to Masonry C. Loose brickwork and tiles dislodged. Unbraced parapets and architectural ornaments may fall. Stone walls cracked. Weak chimneys broken, usually at the roof-line. Domestic water tanks burst. Concrete irrigation ditches damaged. Waves seen on ponds and lakes. Water made turbid by stirred-up mud. Small slips, and caving-in of sand and gravel banks.

MM VIII

Alarm may approach panic. Steering of motorcars affected. Masonry C damaged, with partial collapse. Masonry B damaged in some cases. Masonry A undamaged. Chimneys, factory stacks, monuments, towers, and elevated tanks twisted or brought down. Panel walls thrown out of frame structures. Some brick veneers damaged. Decayed wooden piles broken. Frame houses not secured to the foundation may move. Cracks appear on steep slopes and in wet ground. Landslips in roadside cuttings and unsupported excavations. Some tree branches may be broken off.

MM IX

General panic. Masonry D destroyed. Masonry C heavily damaged, sometimes collapsing completely. Masonry B seriously damaged. Frame structures racked and distorted. Damage to foundations general. Frame houses not secured to the foundations shifted off. Brick veneers fall and expose frames. Cracking of the ground conspicuous. Minor damage to paths and roadways. Sand and mud ejected in alluviated areas, with the formation of earthquake fountains and sand craters. Underground pipes broken. Serious damage to reservoirs.

MM X

Most masonry structures destroyed, together with their foundations. Some well-built wooden buildings and bridges seriously damaged. Dams, dykes, and embankments seriously damaged. Railway lines slightly bent. Cement and asphalt roads and pavements badly cracked or thrown into waves. Large landslides on river banks and steep coasts. Sand and mud on beaches and flat land moved horizontally. Large spectacular sand and mud fountains. Water from rivers, lakes, and canals thrown up on the banks.

MM XI

Wooden frame structures destroyed. Great damage to railway lines. Great damage to underground pipes.

MM XII

Damage virtually total. Practically all works of construction destroyed or greatly damaged. Large rock masses displaced. Lines of sight and level distorted. Visible wave-motion of the ground surface reported. Objects thrown upwards into the air.

Categories of non-wooden construction

Masonry A.

Structures designed to resist lateral forces of about 0.1g, such as those satisfying, the New Zealand Model Building Bylaw, 1955. Typical buildings of this kind are well reinforced by means of steel or ferro-concrete bands, or are wholly of ferro-concrete construction. All mortar is of good quality, and the design and workmanship are good. Few buildings erected prior to 1935 can be regarded as Masonry A.

Masonry B.

Reinforced buildings of good workrnanship and with sound mortar, but not designed in detail to resist lateral forces.

Masonry C.

Buildings of ordinary workmanship, with mortar of average quality. No extreme weakness, such as inadequate bonding of the corners, but neither designed or reinforced to resist lateral forces.

Masonry D.

Building with low standards of workmanship, poor mortar, or constructed of weak materials like mud brick and rarnmed earth. Weak horizontally.

Windows.

Window breakage depends greatly upon the nature of the frame and its orientation with respect to the earthquake source. Windows cracked at MM V are usually either large display windows, or windows tightly fitted to metal frames.

Chimneys.

The 'weak chimneys' listed under MM VII are unreinforced domestic chimneys of brick, concrete block, or poured concrete.

Water tanks.

The 'domestic water tanks' listed under MM VII are of the cylindrical corrugated-iron type common in New Zealand rural areas. If these are only partly full, movement of the water may burst soldered and riveted seams. Hot-water cylinders constrained only by supply and delivery pipes may move sufficiently to break pipes at about the same intensity.

APPENDIX B – CONTENTS OF COMPACT DISK

The Compact Disk (CD) that accompanies this thesis contains all of the raw and derived data used in the microzonation analysis performed in the body of the thesis. It also contains the source code for all computer programs developed to aid the analysis, and the ArcView files used to display the microzonation in an ArcView Geographic Information System (GIS) Version 3.0.

The earthquake databases used for the hazard analysis using Gumbel statistics have not been included on the CD. Access to those databases was provided to the author on the consent of the organisations and personnel who maintain those databases. Similarly, the borehole databases and log sheets used in the comparison of calculated and measured sediment depths were not included on the CD. The original sources for those databases and log sheets are acknowledged in the body of the thesis.

Each of the major sub-directories on the CD contains an HTML *readme* file that is suitable for viewing in any World Wide Web (WWW) browser. These *readme* files are inter-linked via a Table of contents file and a main index file. The initial entry to the *readme* network is via the **index.html** file in the root directory of the CD.

APPENDIX C – ANALYSIS OF GREENHALGH'S RELATIONSHIP

Greenhalgh's relationship (Greenhalgh et al, 1988) between Richter magnitude M_L and Radius of perceptibility R_p is stated as:

$$M_L = 0.33(\log_{10} R_P)^2 + 0.74(\log_{10} R_P) + 1.63$$

Let $\log_{10} R_P = X$

$$M_L = 0.33(X)^2 + 0.74(X) + 1.63$$

$$0 = 0.33(X)^2 + 0.74(X) + (1.63 - M_L)$$

Using the quadratic formula, solve for L:

$$L = (-0.74 \pm (0.74^2 - 1.32(1.63 - M_L))^{½}) / 0.66$$

$$= -1.12 \pm (3.03M_L - 3.68)^{½}$$

Which will produce real solutions for L where:

$$M_L \geq 1.215$$

APPENDIX D – KELUNJI CLASSIC SPECIFICATIONS.

Specifications

The Kelunji Classic consists of a Power and Timing Board (KP1), a Computer Board (KC1), an Analogue Board (KA1 or KA2), and one to three Data Storage Modules (KI1). These are mounted in a double Euro-connector card frame within a powder coated stainless steel case (KF1). A KGB Module can be connected to facilitate GPS reception, phone and modem power regulation, low battery cut-off and external watchdog monitoring.

KF1 - Housing

Dimensions:	280 x 275 x 200 mm
Mass:	typ 7.6kg
Display LED's:	Running, Error, Trigger, Modem, Insert Memory, Memory Half Full, Memory Full & Disarmed.
Connector LED's:	Battery Low, Battery OK, Battery Fuse OK, Charger Fuse OK
Controls:	LED enable, Disarm/Trigger/Restart

KP1 - Power & Timing Board

Operating Voltage:	11 - 15 Volts
Charger Voltage:	12 - 18 Volts
Charger Regulator:	Up to 3A
Power Consumption:	typ. 45mA @ 12V
Crystal Accuracy:	0.2 ppm, 0 - 50°C, others available
Clock Sync.:	To logic level, relay closure or tone
Standby Crystal Acc.:	50 ppm, 0 - 50°C
Standby Battery Life:	typ. 10 years
Auxiliary Input:	0 - 5V, 10 bit precision
Auxiliary Outputs:	0 - 5V, 8 bit precision (std.) 0 - 5V, 12 bit precision (opt.) Relay close for ext. radio or alarm
Analogue Monitoring:	10 bit precision monitoring of voltages, currents, temperature etc.

KC1 - Computer Board

Power Consumption:	typ. 30mA @ 12V
Serial Interfaces:	2 @ 300 - 38400 baud
Alarms:	2 logic level outputs

KI1 - Internal Data Storage Board

Data Capacity:	1 MByte
Type:	Battery backed CMOS
Battery Type:	3V Lithium, 1.8Ah
Battery Life:	300 days (continuous use) to 10 years (if never used)
Battery Monitor:	Usage day counter
Power Consumption:	typ. 1mA @ 12V

KGB Module

Quiescent Current:	typ. 7mA @ 12V
Phone Power:	Max. 1.5A @ 12V
Modem Power:	Max 500mA @ 12V
GPS Power:	140mA @ 12V
Low Voltage Cut-Off:	11.0V ±1%

KA1 - 12 Bit Gain Ranging Analogue Board

No. of Channels:	1 or 3
Anti-alias Filter:	4th order Bessel @ 25Hz (std.) Butterworth filter and other anti-alias frequencies optional
Pre-amp Gain:	x1 (std.) to x10 (H/W selectable)
Coupling:	DC or AC @ 0.2Hz (std.)
Resolution:	12 bit
Active Gain Ranging:	12 stages, x1 to x2048
Dynamic Range:	130+ dB
Sample Rate:	8 to 250sps (S/W selectable)
Power Consumption:	typ. 30mA @ 12V
Transducer Power:	+12V, 250mA and ±15V, 150mA
Input:	Single ended
Calibration:	Step or sine, voltage or current

KA2 - 16 Bit Linear Analogue Board

No. of Channels:	1 to 6
Anti-alias Filter:	7th order Bessel @ 50Hz (std.) Butterworth filter and other anti-alias frequencies optional
Pre-amp Gain:	1, 10 or 100 (H/W selectable) 1, 2, 4 or 8 (S/W selectable)
Coupling:	DC or AC @ 0.1Hz (std.)
Resolution:	16 bit
Dynamic Range:	90+ dB
Sample Rate:	64 to 400 (S/W selectable) (std.) Up to 2000 (opt.)
Power Consumption:	typ. 40mA @ 12V for 3 channel typ. 50mA @ 12V for 6 channel
Transducer Power:	+12V, 250mA and ±15V, 150mA
Input:	Differential
Calibration:	Step, square, sine, swept sine or pseudo-random, voltage or current

9-11-1994

(Source: Seismological Research Centre)

APPENDIX E – S6000 OUTPUT VS FREQUENCY RESPONSE

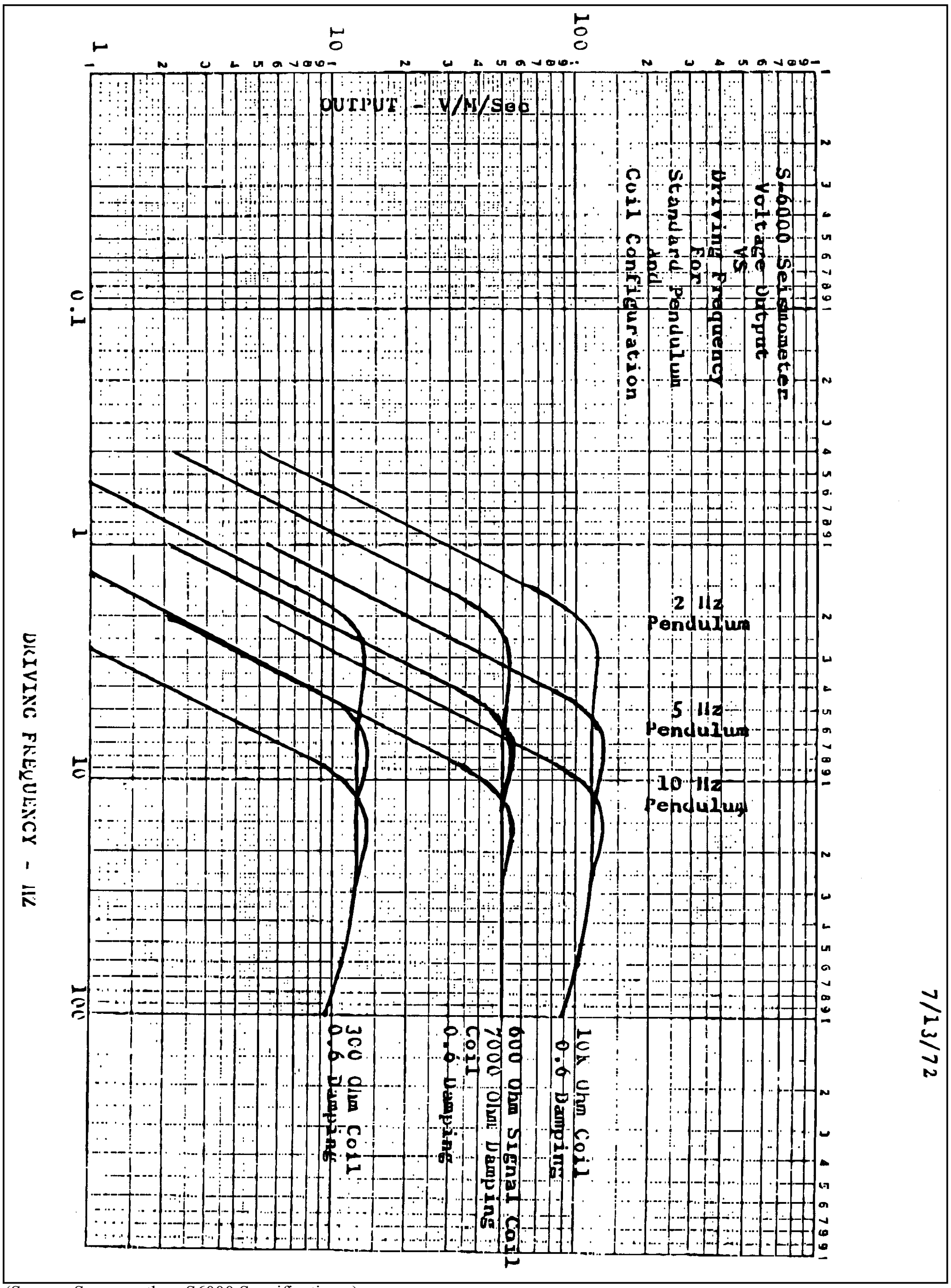

(Source: Sprengnether, S6000 Specifications.)

APPENDIX F – THE GUTTENBERG/RICHTER MAGNITUDE/FREQUENCY RELATIONSHIP

Richter and Guttenberg (Richter, 1958) both demonstrated that the frequency of earthquakes of various magnitudes throughout the world, can be approximated by the equation,

$$\log_{10}N = A + bM \qquad \text{(Eq. 1)}$$

where N is the number of events of magnitude M or greater, per unit time.

An alternative expression for Eq. 1 is,

$$\log_{10}N' = a + bM \qquad \text{(Eq. 2)}$$

where N′ represents the average number of events per unit time for which the magnitude is M, within a given range (Bullen & Bolt, 1985, p 377), and is expressed as

$$N' = -(dN/dM) \qquad \text{(Eq. 3)}$$

and,

$$a = A + \log_{10}(b/q) \qquad \text{(Eq. 4)}$$

where,

$$q = \log_{10}e \qquad \text{(Eq. 5)}$$

Using the then available world event data for events of magnitude 7 and over during the period 1918 to 1955, and events of magnitude 6 to 7 for the period 1935 to 1938, Richter determined the parameters a = 8.56, A = 8.2 and b = 1.0 (Richter, 1958, p 359). Guttenberg, using nearly the same data, but using finer gradations of magnitude range, determined the parameters to be a = 7.72, A = 7.41 and b = 0.90 (Richter, 1958, p 359).

Bullen and Bolt (1985, p 379) state that the b value should not be regarded as constant over time, and that it naturally will exhibit variation within a range. They furthermore point out (Bullen & Bolt, 1985, p 391) that the value of b for a population of foreshocks prior to a major event may be significantly smaller than the average *b* value for the region over a long interval of time. This implies that a relatively small value of the *b* value indicates a relatively high regional stress gradient, whereas a relatively high *b* value suggests a relatively relaxed regional stress gradient.

It has been observed (Bolt, 1978) that the *b* value in most regions varies between 0.7 and 1.0, although values of $b = 0.6$ have been observed (Bolt, 1978, p 147).

INDEX